Channelized Deposits and Regional Parasequence Sets of the Grouse Paleovalley: McMurray Formation, Alberta, Canada

by

Zennon Weleschuk

Bachelor of Science in Geology (Hons.), University of Calgary, 2015

Thesis Submitted in Partial Fulfillment of the
Requirements for the Degree of
Master of Science

in the
Department of Earth Sciences

SIMON FRASER UNIVERSITY
Fall 2017

Approval

Name:	**Zennon Weleschuk**
Degree:	**Master of Science**
Title:	**Channelized Deposits and Regional Parasequence Sets of the Grouse Paleovalley: McMurray Formation, Alberta, Canada**
Examining Committee:	**Chair: Derek Thorkelson** Professor, Department of Earth Sciences
	Shahin Dashtgard Senior Supervisor Professor, Department of Earth Sciences
	James MacEachern Committee Member Professor, Department of Earth Sciences
	Murray Gingras External Examiner Professor, Department of Earth and Atmospheric Sciences University of Alberta
Date Defended/Approved:	September 20th, 2017

Abstract

The Grouse Paleovalley occurs in the south-central portion of the McMurray Sub-Basin. Regionally continuous parasequence sets and associated channel belts, capped by allogenic flooding surfaces were investigated within the McMurray Formation to determine depositional settings and their stratigraphic significance. Core descriptions and wireline data were used to map surfaces and facies associations across the study area. Three stacked parasequence sets were investigated. The two oldest parasequence sets are interpreted to represent deposition of a prograding, sheltered shoreface to bay-margin, punctuated by brackish-water channels in a low accommodation setting. The youngest parasequence set is interpreted to have been deposited in a wave/storm-dominated prograding delta, also in a low accommodation setting. A new stratigraphic model for the upper McMurray is proposed, consisting of transgressive and highstand systems tracts. The progradational successions represent the highstand phases, whereas ravinement and retrogradation constitute the transgressive phases.

Keywords: McMurray Formation; Parasequence; Stratigraphy; Sedimentology; Paleovalley

Acknowledgements

I would like to give a special thanks to Cheryl Hodgson for her helpful insight on facies and stratigraphy. I would like to acknowledge and thank Jonathon Broadbent, Thomas Jean, Bryan Kent, Macy Jones, Nakarí Díaz, and the rest of my colleagues in the ARISE group for their great company and insightful conversations. I would like to thank my supervisor, Shahin Dashtgard and committee member, James MacEachern for their support and guidance during my time at Simon Fraser University. I would also like to thank the external examiner, Murray Gingras, and Derek Thorkelson for chairing the defense. Lastly I would like to thank the McMurray Consortium members at University of Calgary and University of Alberta and the industry representatives for their contributions and input.

Table of Contents

List of Tables

List of Figures

List of Acronyms

SCU	Sub-Cretaceous Unconformity
GPV	Grouse Paleovalley
API	American Petroleum Institute
fU	Upper fine-grained sand
vfL	Lower fine-grained sand
mL	Lower medium-grained sand
IHS	Inclined Heterolithic Stratification
HCS	Hummocky Cross Stratification
BI	Bioturbation Index
PSS	Parasequence set
Fm	Formation

1 Introduction

1.1 Introduction

Several of the largest oil sands deposits in the world are located in the Western Canadian Sedimentary Basin, and of these, the largest deposit is the Athabasca oil sands (Fig. 1.1A; Rahnama et al., 2013). The main bitumen-bearing unit in the Athabasca oil sands is the McMurray Formation. Although significant resources have been invested by the petroleum industry into understanding the geology of the McMurray Formation, the regional depositional context remains poorly constrained. In particular, the stratigraphy of McMurray parasequences between adjacent paleovalleys is not well understood, and a basin-wide stratigraphic framework for the McMurray Fm has yet to be developed. To improve the exploitation of bitumen trapped in the McMurray Formation, it is necessary to develop a comprehensive stratigraphic and depositional model for the entire McMurray Sub-Basin, and to as analyze the distribution and architecture of sedimentary strata across the basin.

1.2 Geologic Overview

The McMurray Formation is part of the Lower Cretaceous (Aptian) Mannville Group, which unconformably overlies Middle to Upper Devonian carbonates of the Beaverhill Lake, Woodbend, and Wabamun Groups (Oldale and Munday, 1994; Switzer et al., 1994). Underlying Devonian strata dips towards the southwest, and the contact between these strata and the McMurray Fm (Sub-Cretaceous Unconformity (SCU)) is an angular unconformity (Carrigy, 1959). The SCU displays significant relief that probably resulted from dissolution of the underlying Prairie Evaporite Fm, and karstification of underlying Devonian carbonates. Dissolution and karstification along the subcrop edge of evaporites and carbonates resulted in the formation of long and wide valleys (Ranger and Pemberton, 1997; Broughton, 2013). Deposition of the oldest McMurray sediments was confined to these valleys.

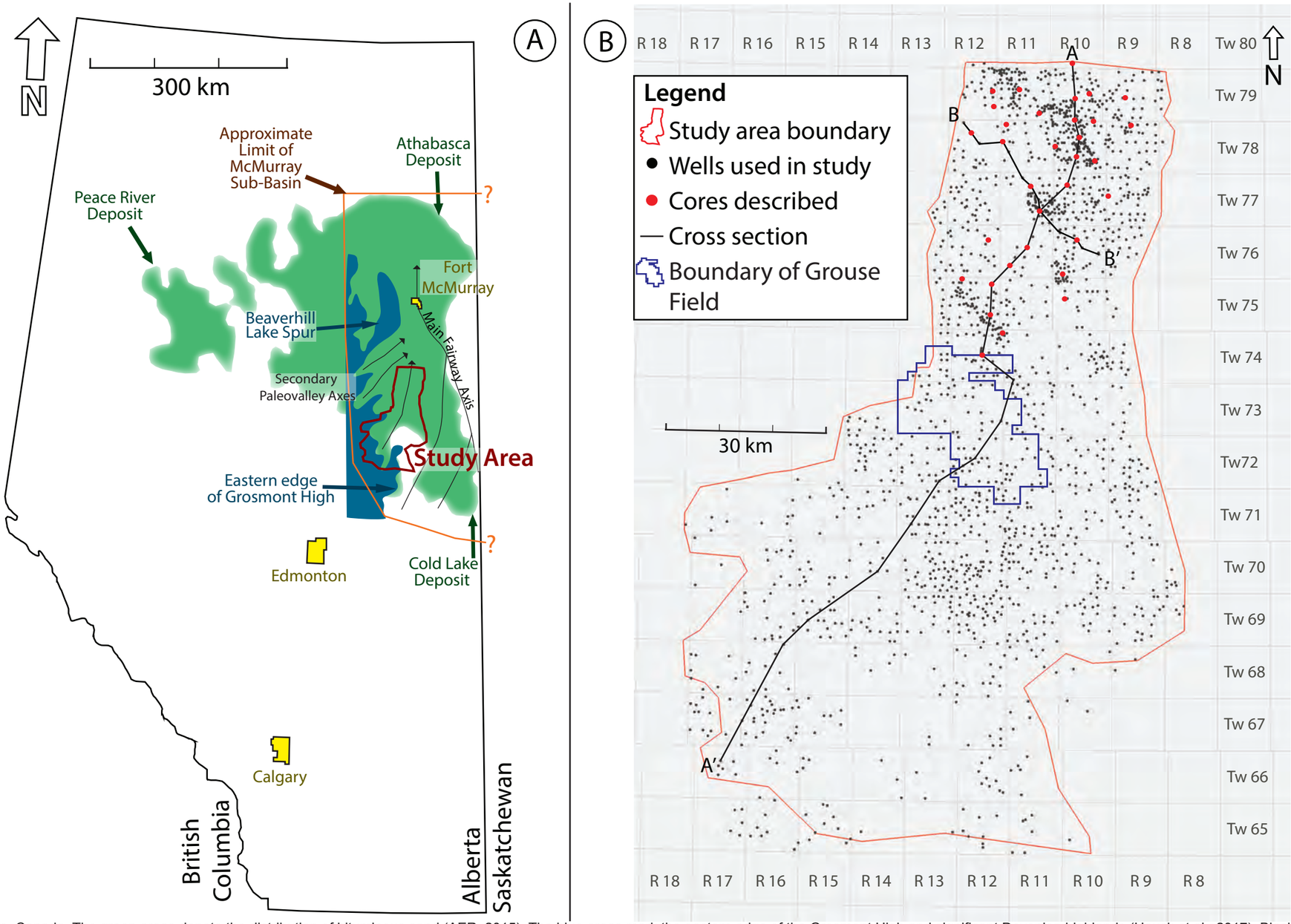

Figure 1.1 - A) Map of Alberta, Canada. The green areas denote the distribution of bituminous sand (AER, 2015). The blue areas mark the eastern edge of the Grosmont High and significant Devonian highlands (Hauck et al., 2017). Black arrows denote the approximate axis of the main fairway. Secondary paleovalley axes are shown trending away from the Grosmont High. The orange polygon denotes the extent of the McMurray Sub-Basin in Alberta, and the red polygon outlines the study area. B) Study area and distribution of wells used for the study. The blue polygon denote the extent of the Grouse Field.

The McMurray Formation encompasses continental to paralic deposits. Sediments consist largely of unlithified sand and lithified and unlithified, silty (50–70% silt) mudstone (Carrigy, 1963; Yale et al., 2010). The McMurray Formation is interpreted to have been deposited in a low accommodation setting, and potentially formed part of a continental-scale drainage system (Hubbard et al., 2011; Benyon et al., 2014; Blum and Pecha, 2014). It is overlain by transgressive, marine glauconitic silty sands of the Wabiskaw Member of the Clearwater Formation (Jeletzky, 1971). The McMurray-Wabiskaw contact has been inferred to represent a transgressive surface of erosion formed during transgression of the Boreal Sea (Ranger and Pemberton, 1997; Hein et al., 2000).

Multiple stratigraphic frameworks have been proposed for the McMurray Formation; however, no scheme has been universally accepted and the topic remains highly contentious (Fig. 1.2; Carrigy, 1959; Ranger and Pemberton, 1997; Hein et al., 2013). Carrigy (1959) subdivided the McMurray Formation into lower, middle, and upper members. The lower member of the McMurray is commonly interpreted as fluvial-dominated, continental deposits distributed in paleotopographic lows on the Sub-Cretaceous Unconformity (Carrigy, 1971; Mossop and Flach, 1983). The middle McMurray is widely regarded as tidally influenced brackish-water deposits, with large-scale packages of inclined heterolithic stratification (IHS) that commonly exhibit meandering river architectures (Mossop and Flach, 1983; Smith et al., 2009). The upper McMurray is typically interpreted to represent regional extensive paralic, estuarine and deltaic deposits, displaying a greater degree of marine influence compared to that of the middle member (Carrigy, 1959; Mossop and Flach, 1983; Flach and Mossop, 1985; Ranger and Pemberton, 1997). Carrigy's (1959) model reflects a general shift from more landward (continental) deposition to more seaward (shallow-marine) environments. The three-fold subdivision of the McMurray Fm is the most widely used framework in the petroleum industry owing to its simplicity. However, it remains an informal lithostratigraphic nomenclature that greatly oversimplifies the complex internal stratigraphy of the McMurray Formation.

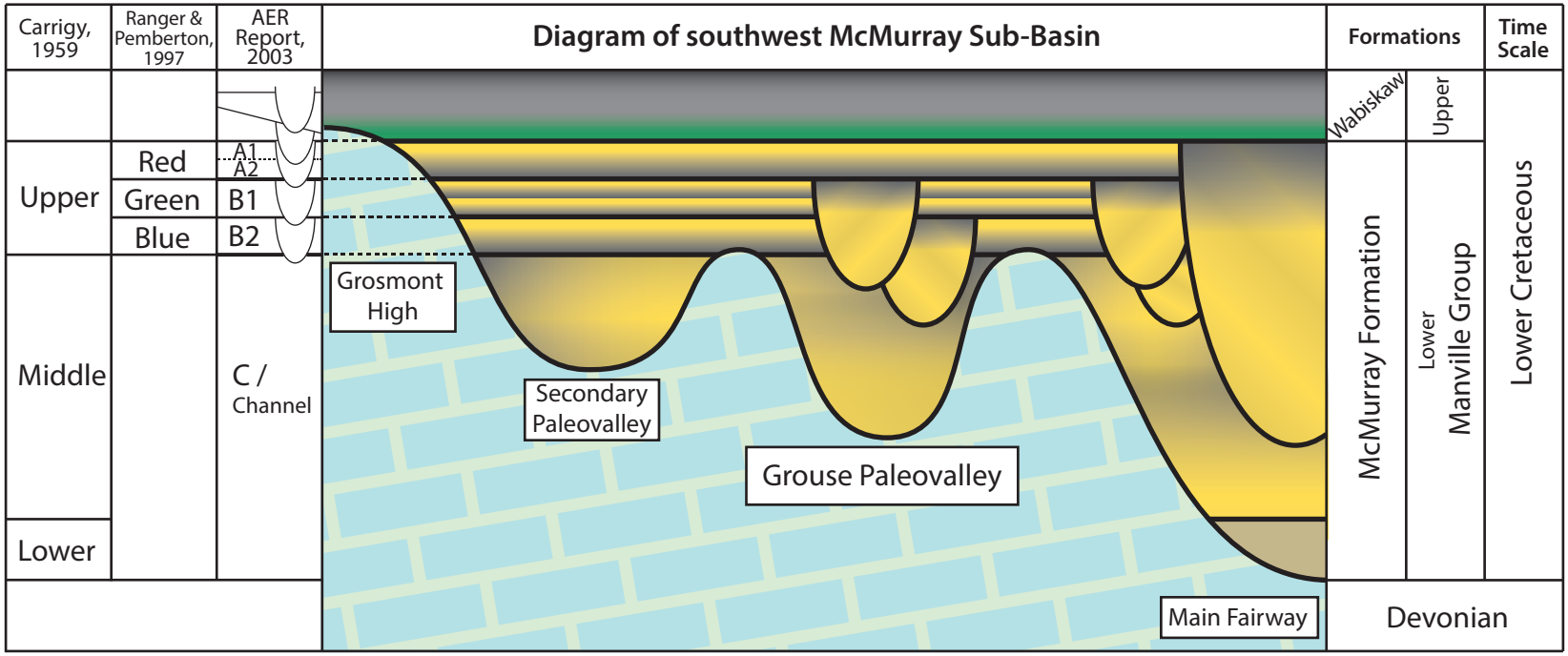

Figure 1.2 – Lithostratigraphic chart and schematic stratigraphy of the Lower Mannville Group in the southwestern portion of the McMurray Sub-Basin.

Ranger and Pemberton (1997) present a sub-regional stratigraphic framework for the upper McMurray Formation. They define 3 “shoreface” parasequences named, from base to top, blue, green, and red (Fig. 1.2). Shoreface parasequences were picked based on wireline signatures, where the red and blue parasequences display an upwards decrease in their API values (interpreted as coarsening upwards signatures),

and the green parasequence has a more complex and irregular gamma-ray signature. The top of the red parasequence coincides with the top of the McMurray Formation and has an erosional upper contact (Ranger and Pemberton, 1997). In general, the younger the parasequence, the better its preservation, implying that older deposits are partly eroded (Ranger and Pemberton, 1997).

Ranger and Pemberton (1997) further proposed that the blue, green, and red shoreface parasequences represent highstand systems tract (HST) deposits. Sea level lowering from falling stage and lowstand systems presumably led to the incision of valleys and erosion in each of the blue, red, and green shoreface successions (Ranger and Pemberton, 1997). As sea level rose, fluvial to progressively more estuarine deposits filled these incised valley complexes. At the top of the red parasequence, the erosive surface between the McMurray Formation and Wabiskaw Member is interpreted to have formed as a result of another significant relative sea level fall before major transgression of the Boreal Sea (Ranger and Pemberton, 1997).

A regional stratigraphic framework was proposed by the Alberta Energy Utilities Board (now Alberta Energy Regulator (AER)) in 2003 (AEUB, 2003A). The AER model was developed in response to a resource dispute between gas producers and bitumen-right holders in the Chard-Leismer Fields. There, the gas and bitumen shared a contact, and questions arose as to the impact of gas production on bitumen extraction using steam-assisted gravity drainage (SAGD; AEUB, 2003B). The AER scheme encompasses the entire McMurray Formation and the Wabiskaw Member, but mainly focuses on Wabiskaw and upper McMurray parasequences with the associated subtending channels. The middle and lower McMurray were bundled into a “C” interval that were not subdivided further (Fig. 1.2). The upper McMurray was divided into “B” and “A” intervals, where B is older than A. The B is subdivided into B2 (older) and B1

parasequences, which are comparable to the blue and green parasequences, respectively, of Ranger and Pemberton (1997). The A interval corresponds to the Ranger and Pemberton (1997) red parasequence, and was further subdivided into A2 (older) and A1 parasequences (Fig. 1.2).

Hein et al. (2013) refined the AEUB stratigraphic model, and interpreted the B2, B1, A2, and A1 parasequences as brackish-bay fills representing HST deposits. They hypothesized that base level drops resulted in channel incision, and transgressive pulses filled the incised valleys with fluvial to tidal fluvial deposits (Hein et al., 2013). In the model proposed by Hein et al. (2013) each parasequence is separated by an unconformity, and more than 5 major unconformities are present.

The three stratigraphic frameworks described above (e.g., Carrigy, 1959; Ranger and Pemberton, 1997; EUB 2003; Hein et al., 2013) all show a shift from more continental, freshwater deposition to more brackish-water to shallow-marine deposition upwards through the McMurray Formation. The observations and descriptions from the aforementioned studies are useful for developing a new stratigraphic framework of the upper McMurray Fm within the Grouse Paleovalley.

1.3 Study Area: Grouse Paleovalley (GPV)

The Grouse Paleovalley (GPV) is a north-south trending paleovalley confined by paleotopographic highs on underlying Devonian carbonates. It is named after the Grouse Field (Fig. 1.1B). Grouse was selected as the name for the paleovalley as the Grouse Field occurs over the deepest portion of the paleovalley. The GPV occurs in the southwest portion of the McMurray Sub-Basin, and its southern limit is defined by the Grosmont High. Separating the GPV from the main fairway to the east is the Wiau Lake carbonate ridge. West of the GPV are other smaller paleovalleys, and north of the GPV is the “confluence” between the GPV and two smaller paleovalleys (Fig. 1.1A). North of the confluence zone is the Beaverhill Lake Spur/Thickwood Hills High. The Beaverhill Lake Spur/Thickwood Hills High is comparable in paleotopographic significance to the Grosmont High, and separates the GPV from the Ells paleovalley to the north (Hauck et al., 2017).

The margins of the study area approximate the margins of the GPV in the east, south and west, and the point of confluence with other secondary paleovalleys in the north. It covers approximately 85 townships (townships 65-80, ranges 9-17, west of the 4th meridian) or approximately 7,900 km^2. Well density in the study area decreases steadily to the south. Previously published research focussed on the study area has been sparse, and is limited to the aforementioned work of Ranger and Pemberton (1997).

1.4 Methods

Thirty-three publicly available cores were logged at the Alberta Energy Regulator's Core Research Centre in Calgary, Alberta, Canada. Cores were described at the centimetre-scale, and details were recorded using the core logging software AppleCORE (donated to SFU by Mike Ranger). Core descriptions include grain size, lithology, physical sedimentary structures, accessory features, ichnofossils, bioturbation index (BI), bitumen staining, and significant contacts. Cores were described in detail from the SCU to the top of the McMurray Fm and described more generally in the Wabiskaw Member.

Cores were photographed at the box scale, 1/3 box height scale, and close up photos were taken of select features. Photos were adjusted in Adobe Photoshop to increase the clarity of the features displayed in the core.

Cores selected for logging intersected all three formation tops (SCU, McMurray, and Wabiskaw) and had accompanying gamma ray, neutron/density, and resistivity geophysical well logs. There were no cores that met these criteria south of Township 74. Cores were depth corrected to ensure that the surfaces seen in the core corresponded to wireline logs, and wireline log signatures of the surfaces were then used to interpret non-cored wells and generate regional maps.

The Sub-Cretaceous Unconformity, the top of the McMurray Fm, and the top of the Wabiskaw Member were picked in 1823 wells. Structure-contour maps were generated for each of these three surfaces, and isopach maps of the McMurray to SCU, Wabiskaw to SCU, and Wabiskaw to McMurray were also generated. All maps were produced, using Petrel (donated to SFU by Schlumberger), and the convergent

interpolation method was used to initially contour maps. Minor re-contouring was performed by hand to improve clarity and remove artificial oddities produced by the contouring algorithm. A polygon was drawn around the margins of the GPV and used as the mapping boundary limit for the software.

Of the 1823 wells, 1424 wells had publically available LAS data according to the GeoScout (donated to SFU by GeoLOGIC Systems) software's database. LAS data is not standardized, therefore the dataset was first meticulously sorted and refined in order to filter out any incorrect information. One thousand three hundred and fifty-three wells had usable suites of logs, and these were imported into Petrel. Facies associations, parasequence sets, and allogenic surfaces were identified in each well. This was done by using wells with logged cores as control points, and correlating geophysical log signatures to non-cored wells.

Isopach maps of each facies association were made for each parasequence and were generated using Petrel. The isochore interpolation method was used to initially contour maps, and minor re-contouring was performed by hand. Probable outcrop edges of the SCU exposure at the onset of parasequence set deposition (i.e., at the base) and at the top of each parasequences set were mapped.

In general, the progression of generating subsurface maps starts with core descriptions, progressing to facies and facies association designations, then to depositional interpretations. Depositional interpretations are then used as a guide to assist with correlating between wells in order to create both maps and cross-sections. This is a cyclic and iterative process that shifts back and forth from vertical observations of core data to lateral observations from maps and cross-section data. As a result of the cyclic and iterative nature of data analysis and interpretation, each chapter in this thesis is interconnected, as the data and interpretations from each chapter carry over into one another.

1.5 Research Objectives and Thesis Outline

The primary objective of this thesis is the mapping the regional parasequence sets, associated channel belts, and allogenic surfaces of the Grouse Paleovalley (GPV)

within the McMurray Formation, in order to develop a depositional model and refine the stratigraphic framework for the area. This data will be integrated at a later stage into a regional model of the entire McMurray Sub-Basin. To achieve the goals of this project, the following objectives are defined and the thesis is organized as follows:

Chapter 2:

- Map the structure of formation tops within the GPV. These maps are used to determine if any structural features affect the strata within the study area.
- Map the thicknesses of the McMurray Fm and Wabiskaw Member in the GPV. These maps display the distribution of sediment and provide insight into how the SCU controlled accommodation space.

Chapter 3:

- Broadly define facies and facies associations of the regional parasequence sets within the GPV. Facies associations are used to map strata between allogenic surfaces.
- Define parasequence sets and associated channel belts in the GPV. These parasequence sets are used to map allogenic flooding surfaces across the GPV.

Chapter 4:

- Map facies associations within each parasequence set in the GPV. This contributes to defining depositional settings for each parasequence set.
- Propose a stratigraphic model for the parasequence sets within the GPV.

Chapter 5:

- Summary of conclusions.

2 General Architecture and Structure of the Grouse Paleovalley

The Grouse Paleovalley is a secondary paleovalley demarcated by north-south trending carbonate ridges. Core and wireline log data were used to map the SCU, McMurray Fm top, and Wabiskaw Member top. Structure maps were created using each surface to show the present-day orientation of these surfaces within the GPV. Isopach maps of the McMurray Fm and Wabiskaw Mbr display variations in thickness, and how they relate to the filling of accommodation space/Devonian paleotopography.

2.1 Structure Maps

The SCU structure map shows the pronounced topography of the surface and the topographic highs that define the boundaries of the GPV (Fig. 2.1). The structure on the top of the McMurray Fm shows a relatively consistent shallowing from southwest to northeast, with a basinward dip of 0.077° towards approximately 229° (Fig. 2.2). Structural dip of the top of the McMurray Fm shows a gradual reorientation and shallowing north of Township 76, with a dip of 0.075° towards 214°.

The structure on the top of the Wabiskaw Member is more uniform than that on top of the McMurray Fm, but shows the same general trends in dip direction and magnitude. The structure on the top of the Wabiskaw Member is consistent with the structure of the Mannville Group in the region (Fig. 2.3; Hayes et al., 1994). No major post-depositional faults or karst features are observed.

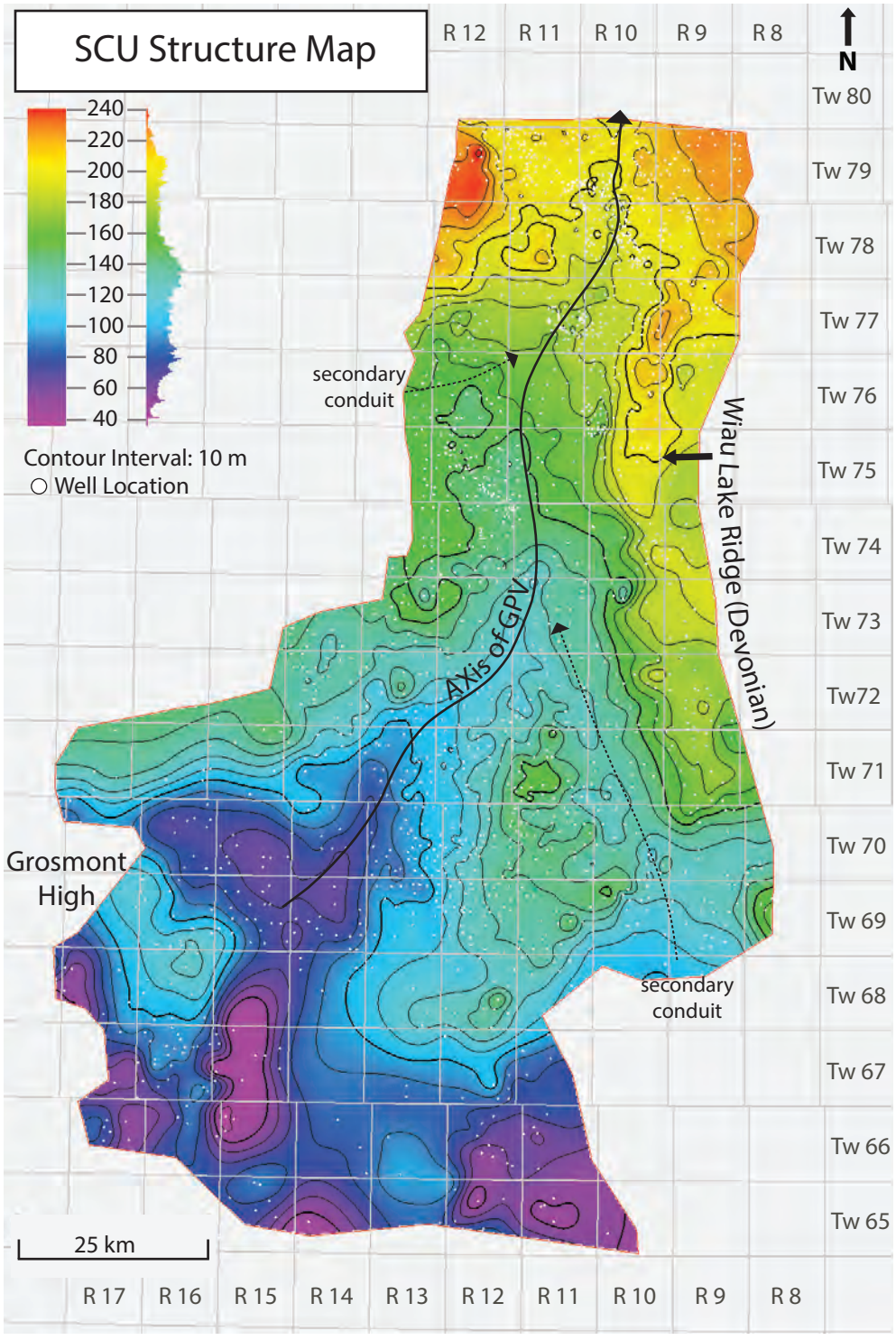

Figure 2.1 - Structure contour map of the Sub-Cretaceous Unconformity (SCU) in the study area. The long black arrow denotes the main axis of the Grouse Paleovalley (GPV). The dotted arrows denote secondary conduits. Hot colors represent highs, cool colors represent lows. Note the histogram on the right side of the elevation scale which displays the frequency distribution of the elevation in the mapped surface.

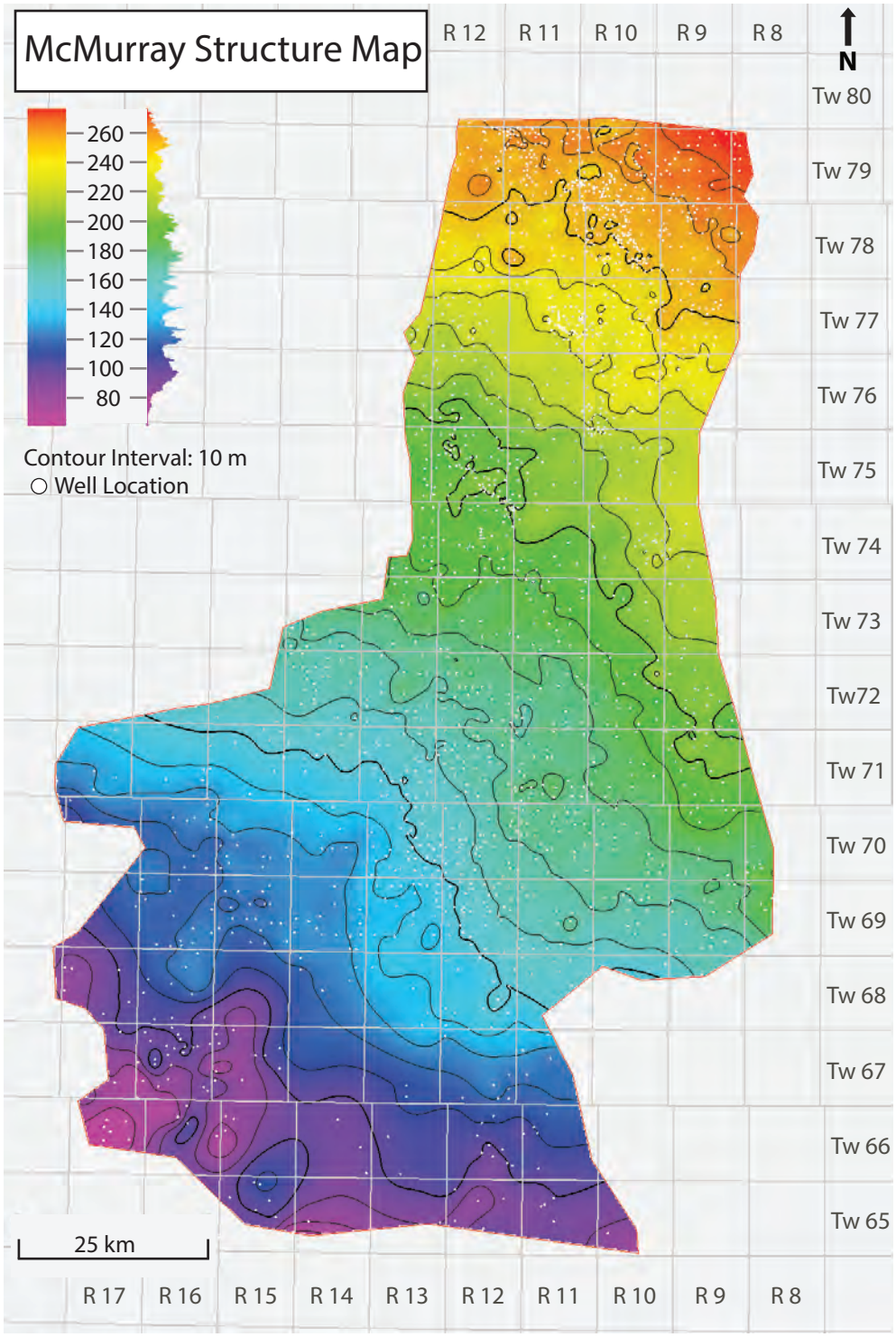

Figure 2.2 - Structure contour map of the top of the McMurray Formation in the study area. Hot colors represent highs, cool colors represent lows. Note the histogram on the right side of the elevation scale which displays the frequency distribution of the elevation in the mapped surface.

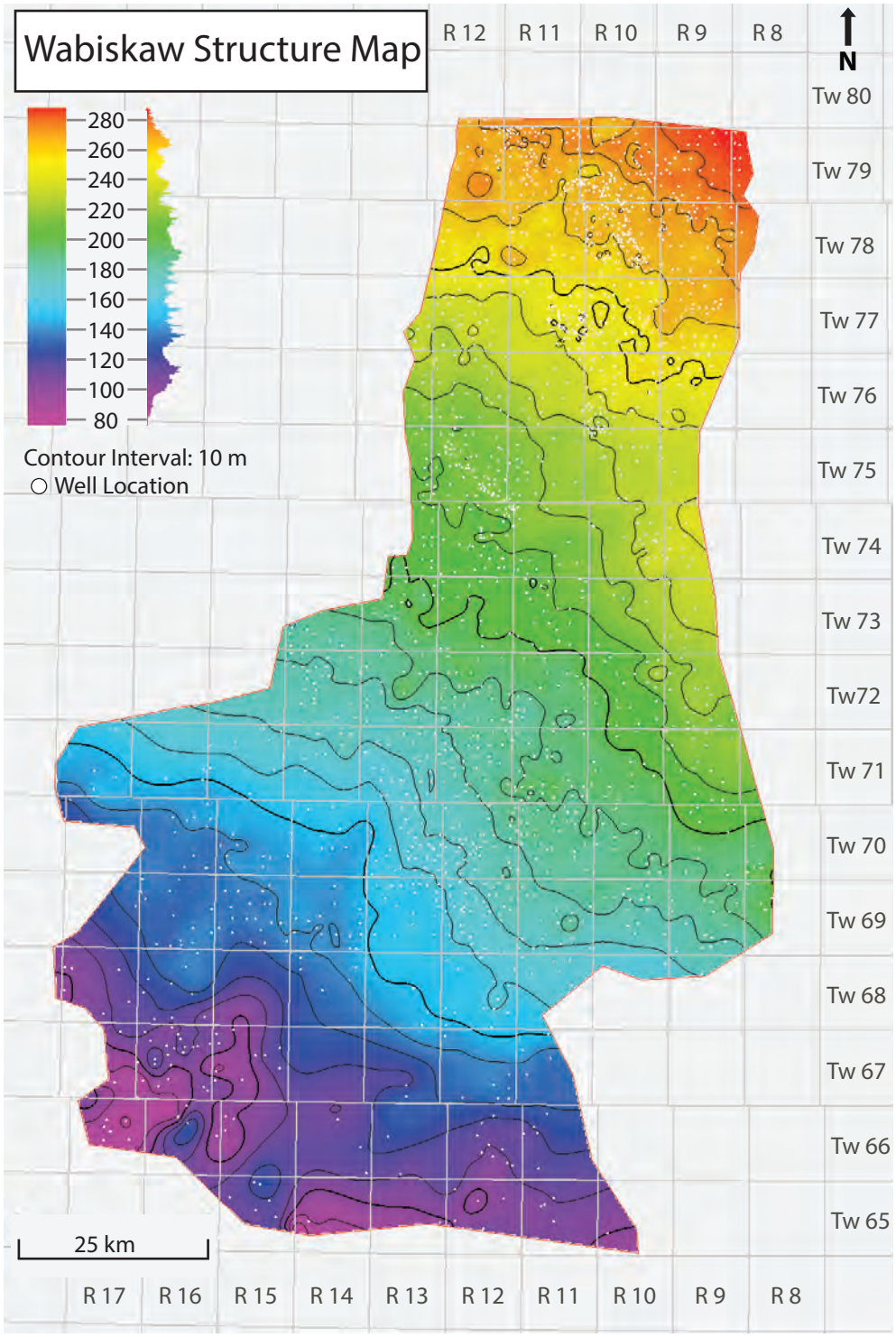

Figure 2.3 - Structure contour map of the top of the Wabiskaw Member in the study area. Hot colors represent highs, cool colors represent lows. Note the histogram on the right side of the elevation scale which displays the frequency distribution of the elevation in the mapped surface.

2.2 Formation Isopach Maps

The thickness of the McMurray Formation varies markedly and ranges from 0 to 65 m (Fig. 2.4). Within the study area, the thickness of the McMurray is greatest along the axis of the GPV and displays an approximate, linear north-south trend. Along the eastern, southern, and western edges of the study area, the McMurray Formation thins. It eventually thins to zero in the southwest as it approaches the Grosmont High.

The Wabiskaw – SCU isopach map shows a north-south-oriented thick (warm colors, Fig. 2.5), which defines the axis of the paleovalley. Thins (cool colors, Fig. 2.5) occur over the top and along the margins of paleotopographic highs that flank the study area. The topographic high on the east side of the study area is called the Wiau Lake Ridge and constitutes part of the Cooking Lake Formation subcrop (Fig. 2.5, Hauck et al., 2017). A NNE-trending paleotopographic low connects the GPV to the main fairway, centered in township 71, Range 10W4 (Fig. 2.5). A second paleotopographic low exists in a west-east trend and connects the GPV to an unnamed relatively short and shallow north-south-oriented paleovalley centered in Township 76, Range 12W4 (Fig. 2.5). The isopach thickness of Wabiskaw to SCU thins to the southwest as it approaches the Grosmont High.

Although the structure maps of the top of the McMurray and top of the Wabiskaw Mbr look similar, the isopach map of the Wabiskaw Mbr reveals that the two surfaces do not track one another (Fig. 2.6). Regionally, the Wabiskaw Member increases in thickness to the south, although in the southernmost portion of the study area, it thins as it onlaps the Grosmont High. Two significant thicks exist through the middle of the study area. The narrower thick, which occurs in Township 75 and has a west-east trend, is probably the product of erosion and infilling at the top of the McMurray Formation during deposition of the Wabiskaw Member. The wider thick occurs between Township 70 and 74, and has a southwest-northeast trend. The change in thickness of Wabiskaw deposits results in a slight distortion of the allogenic surfaces that demarcate the regional parasequence sets.

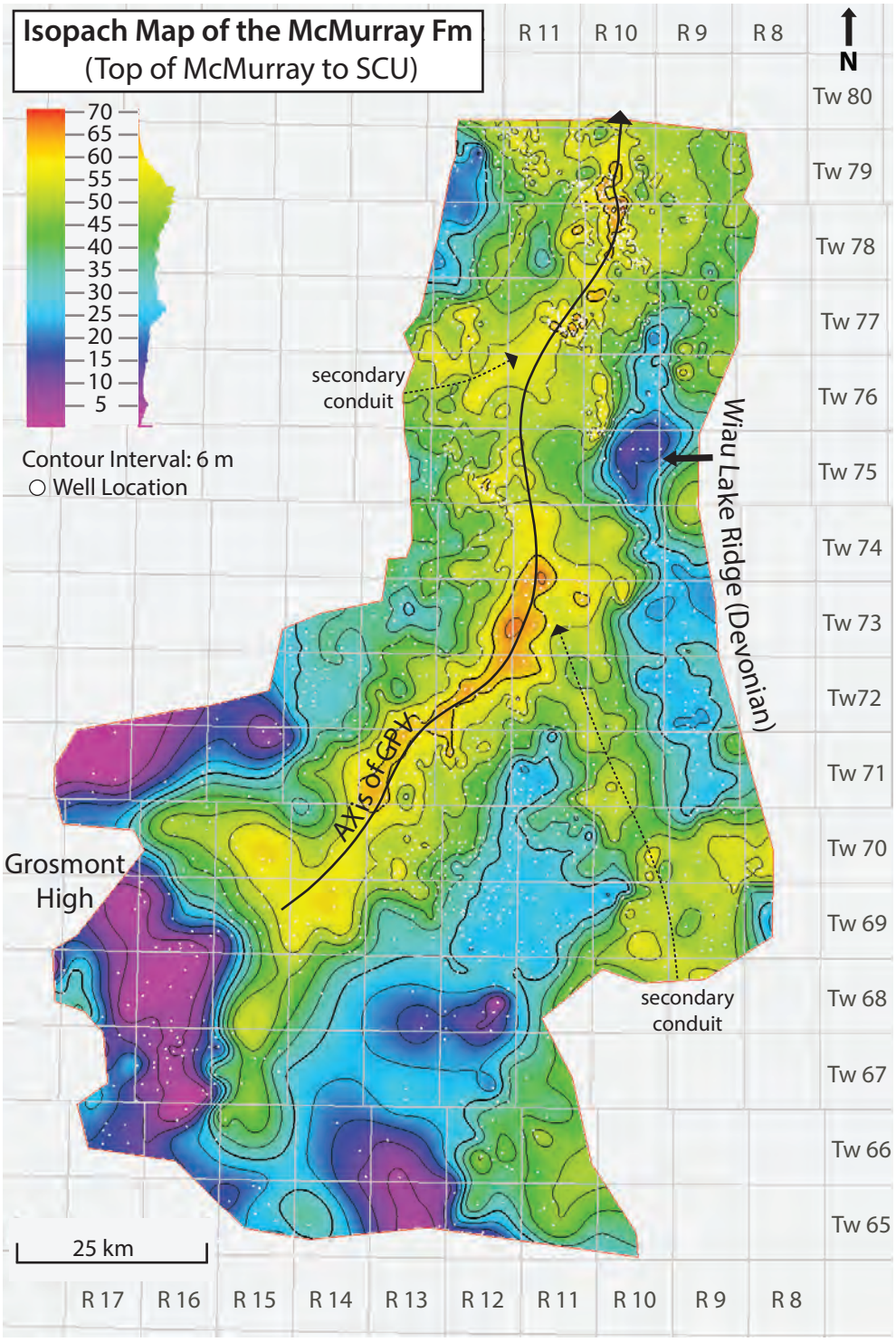

Figure 2.4 - Isopach map from the top of theMcMurray Formation to the Sub-Cretaceous Unconformity in the study area. The long black arrow denotes the main axis of the GPV. The dotted arrows denote secondary conduits. Hot colors represent thicks, cool colors represent thins. Note the histogram on the right side of the thickness scale which displays the frequency distribution of thickness in the mapped surface.

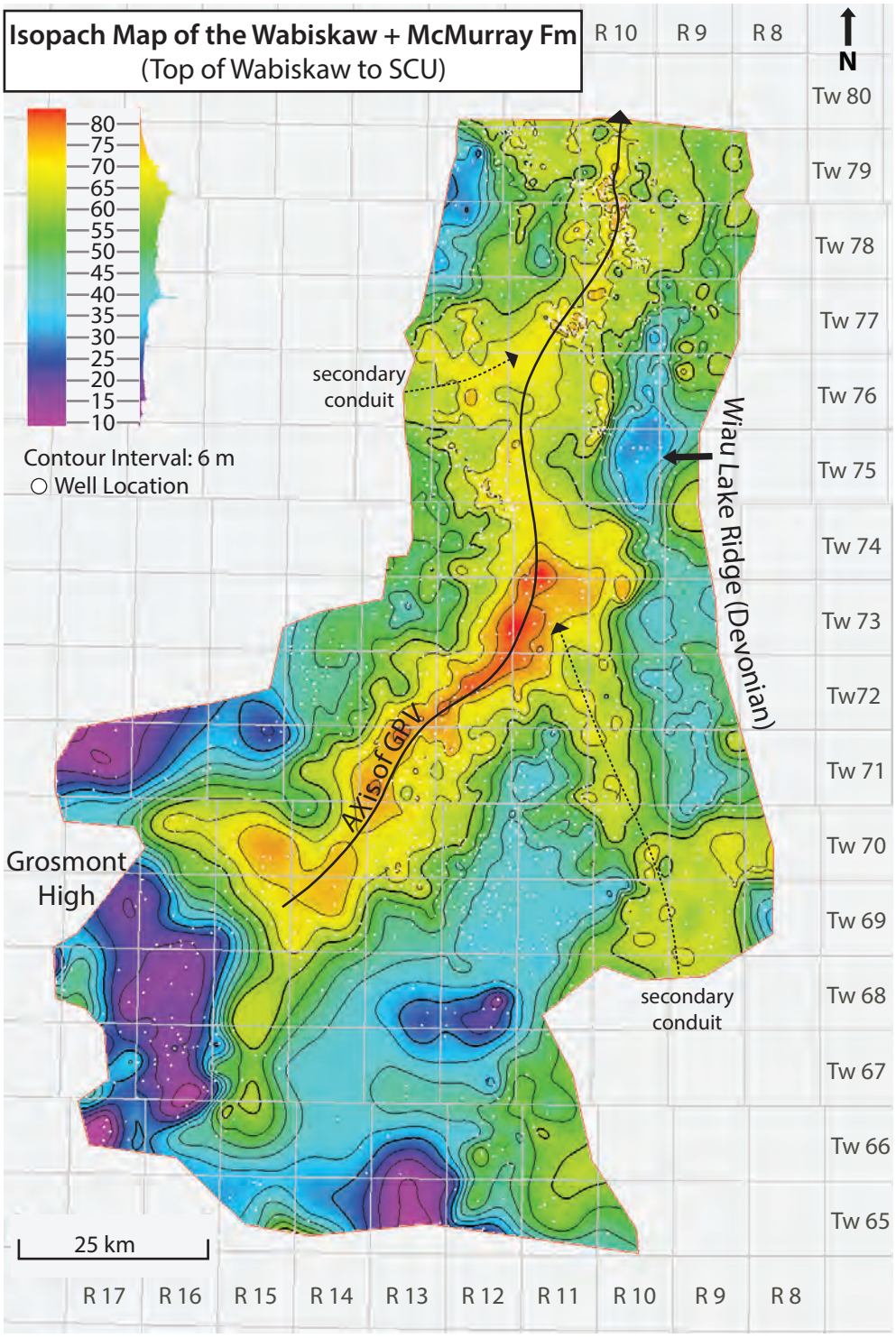

Figure 2.5 - Isopach map from the top of the Wabiskaw Member to the Sub-Cretaceous Unconformity in the study area. The long black arrow denotes the main axis of the GPV. The dotted arrows denote secondary conduits. Hot colors represent thicks, cool colors represent thins. Note the histogram on the right side of the thickness scale which displays the frequency distribution of thickness in the mapped surface.

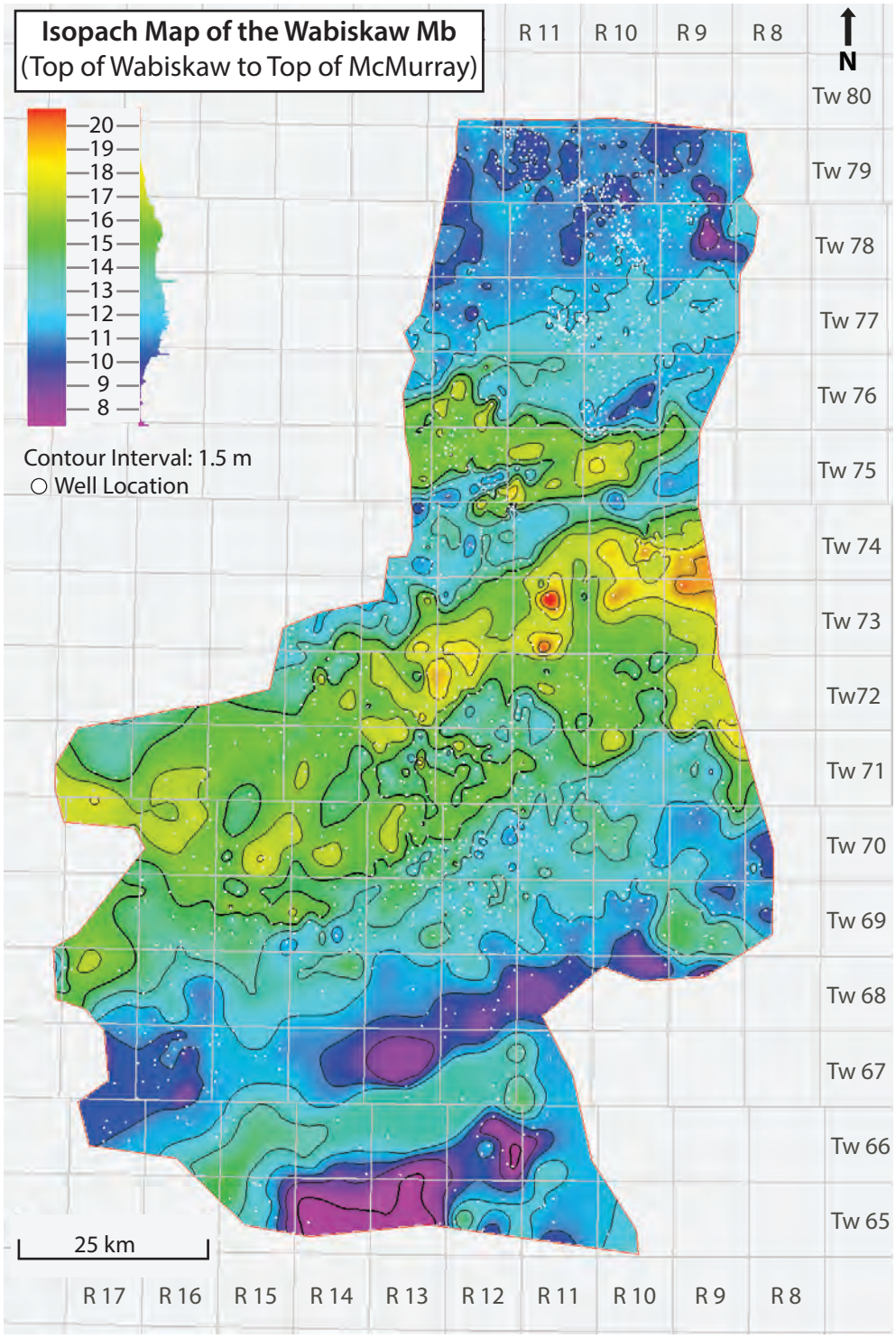

Figure 2.6 - Isopach map from the top of the Wabiskaw Member to the top of the McMurray Formation in the study area. Hot colors represent thicks, cool colors represent thins. Note the histogram on the right side of the thickness scale which displays the frequency distribution of thickness in the mapped surface.

3 Facies, Facies Associations, and Parasequences of the Grouse Paleovalley

Ten facies were described from the regional parasequence sets of the McMurray Fm and Wabiskaw Mbr in the GPV, which are grouped into four facies associations (Table 3.1). Facies associations represent general depositional environments, such that that they can be mapped using wireline logs. Regional parasequences sets are described, and the thickness of each facies association found within each parasequence set is graphed.

Facies Association 1 (FA1) is interpreted to represent deposition within a wave/storm-dominated deltaic environment. Facies Association 2 (FA2) is interpreted to represent deposition within a sheltered shoreface to bay-margin setting. Facies Association 3 (FA3) is interpreted to represent brackish channels resulting from either tidal or tidal-fluvial processes. Finally, Facies Association 4 (FA4) is interpreted to represent a marine lower shoreface to upper offshore environment.

Grain sizes of the deposits in the regional parasequence sets within the study area range from upper fine- (fU) to lower very fine-grained sand (vfL), with only rare occurances of lower medium-grained sand (mL). No significant coal beds/deposits were observed in the study area, but carbonaceous mudstone was observed rarely, associated with FA2 and FA3. FA3 is interpreted and discussed in more detail, as its occurrence can be explained by multiple working hypotheses. The focus of the study is on the upper McMurray and not the Wabiskaw Member, therefore the Wabiskaw Member is only described and discussed in general terms.

Facies Association	Facies Number	Facies	Grain Size	Bedding scale	Sedimentology	Bioturbation Intensity	Dominant trace fossils	Dominate Process Interpretation	Depositional Environment	Para-sequence	Contacts / notes
1 –Wave/ storm dominated delta	1	Shale with parallel and lenticular sand and silt laminae	vfU to vfL	mm scale silt laminae	Irregular to parallel laminated shale. Parallel and lenticular silt laminae, rare, rare syneresis, wavy oscillatory rippled sand may occur at base.	1-4	**Pl**, Te, Cy (Traces are diminutive)	Low energy, minor energy fluctuations	Distal prodelta	Z	Sharp basal contact. Ravinement surface at base and max flooding in lower portion
	2	Lenticular to wavy heterolithic bedding with oscillation ripples	f to vfL	Sand beds cm to dm scale, shale beds cm to dm scale	Abundant syneresis cracks locally present in mud, lenticular to wavy bedding, oscillation ripples, carbonaceous debris, rare micro-HCS, rare soft sediment deformation	0-3	**Pl**, Te, Cy,Sk (Traces are diminutive)	Fluctuations in energy, low to high energy, oscillatory-bidirectional combine energy, storm	Wave storm dominated proximal prodelta to distal delta front	Z	Sand content increasing upwards
	2	Oscillation rippled to hummocky cross stratified sand	f to vfL	Sand beds cm to dm scale, shale beds cm scale	Abundant erosion and scour surfaces, abundant oscillation ripples, micro-HCS, hummocky cross stratified sand, thin shale beds, rare syneresis cracks	0-2	**Pl**, **fu**, Cy, Sk (Traces are diminutive)	High energy, oscillatory-bidirectional combine energy, storm	Wave/storm dominated delta front	Z	Sand content increasing upwards
2 – Protected shoreface to tidal flat	4 4A	Bioturbated mudstone and sandstone	vfU to vfL	cm to dm scale	Bioturbation overprints sandy mudstone and muddy sandstone interbeds, carbonaceous debris, rare preservation of oscillatory structures	2-5	**Pl, Cy, Sk, Gy, Te,** Th, Pa (Traces are diminutive)	Bidirectional energy	Distal protected/ sheltered shoreface to tidal flat	X & Y	Sand content increasing upwards
	4B	Bioturbated sandstone interbeddded with mudstone to oscillatory rippled sand	vfU to vfL	cm to dm scale	Abundant bioturbated muddy sandstone, low angle undulatory parallel laminations, oscillation ripples, Carbonaceous debris, rare mud clasts	1-4	**Pl, Cy, Sk, Gy, Te,** Th, Pa (Traces are diminutive)	Bidirectional energy, oscillatory-bidirectional combine energy in sand dominated beds towards top of unit	Proximal protected/ sheltered shoreface to tidal flat	X & Y	Sand content increasing upwards
3 – Brackish channel (tidal channel or tidal-fluvial channel)	5	Rippled and cross bedded sandstone	mL to vfU	cm to dm with mm scale mud beds	cross bedding, prograding current ripples with reactivation surfaces, oscillatory ripples, Carbonaceous debris, mud rip up clasts, sand dominated with thin flaser mud beds	0-2	**Cy**, Sk, Pl (Traces are diminutive)	High energy, unequal bidirectional energy dominate with some oscillatory energy	Subtidal (sand dominated) channel	X & Y	Sharp erosional base, often coarser grain size than below, often bitumen saturated
	6	Bioturbated wavy interbedded sandstone and mudstone	fU to vfL	mm to dm scale	Wavy bedding often overprinted with bioturbation, IHS, oscillatory ripples, current ripples, reactivation surfaces, double mud drapes, flaser to lenticular bedding, carbonaceous debris, rare syneresis cracks	2-4	**Pl, Cy, Sk, Gy,** Pa, Te (Traces are diminutive)	Bidirectional energy with periods of quiescence (slack)	shallow subtidal to lower intertidal (Heterolithic) channel	X & Y	Sand content decreasing upwards

	7	Bioturbated mudstone with thin sand beds and laminae	fU to vfL	mm to cm, some dm	Bioturbation overprinting remnant thin/lenticular sand beds and sand and silt laminae. carbonaceous debris, uncommon syneresis cracks,	2-5	**Pl, Cy, Sk, Gy,** Pa, Te, roots (Traces are diminutive)	Low energy, bidirectional energy with significant periods of quiescence	Lower intertidal to upper intertidal (mud dominated) channel	X & Y	Sand content decreasing upwards
2,3	8	Carbonaceous mudstone			Abundant carbonaceous debris, rootlets, some soft sediment deformation and convolute bedding	0-1	**Roots**, Pl	Subaerial exposure and pedogenic alteration	Pedogenically altered terrestrial setting	X & Y	Uncommon, found at top of FA2, FA3
4 – Marine lower shoreface to upper offshore	9	Bioturbated glauconitic lithic silty sandstone	fU to vfL	Not discernible due to bioturbation	Bioturbation overprinting sedimentary structures, abundant glauconite and lithic fragments.	4-6	**Di, Te, Th, As, Pl, Pa, Sk**, **Ph, Co**, He Cy, Ar, Zo (robust and relatively diverse traces)	Moderate energy, Likely oscillatory	Marine lower shoreface	Wabiskaw	Large trace subtend from F10 into underlying McMurray deposits, Sharp erosive contact with underlying McMurray Formation, increasing silt content upwards
	10	Bioturbated muddy siltstone with sand laminae	vfL	mm	Bioturbation overprinting physical structures, thin unbioturbated sand laminae	4-6	**Te, Th, As, Pl, Pa, Sk**, **Ph, Co, Ch, He**, Ar, Zo, Cy (robust and relatively diverse traces)	low energy, with storm events	Marine upper offshore	Wabiskaw	Gradational contact with F10.

Table 3.1 - Facies that occur in the upper McMurray within the study area. Dominant trace fossils of each facies are in bold. *Planolites* (Pl), *Teichichnus* (Te), *Cylindrichnus* (Cy), *Skolithos* (Sk), *Gyrolithes (*Gy*)*, *Thalassinoides (*Th*)*, *Palaeophycus* (Pa), *Diplocraterion* (Di), *Asterosoma* (As), *Arenicolites* (Ar), *Chondrites* (Ch), *Phycosiphon* (Ph), *Helminthopsis* (He), *Cosmorhaphe* (Co), *Zoophycos* (Zo), fugichnia (fu), medium lower sand (mL), fine upper sand (fU), fine sand (f), very fine upper sand (vfU), very fine lower sand (vfL), hummocky cross-stratification (HCS).

3.1 Facies Descriptions and Interpretations

3.1.1 Facies 1: Shale with parallel and lenticular silt laminae

3.1.1.1 Description:

Facies 1 consists of light grey shale with intercalated laminae (typically 2-4 mm thick) of silt (Figs. 3.1 and 3.2). This facies commonly has a sharp basal. Facies 1 may grade into or be sharply overlain by Facies 2.

Facies 1 is dominated by irregular to parallel laminae. Silt laminae are less common (10-20%), are mm-scale, and are parallel stratified or show lenticular (starved) ripples. Very fine-grained sand layers are uncommon and are only present in the lowermost 10 cm of the facies, where they are sharp based and display oscillation ripples. Dark grey, organic-rich mud layers are rare and only occur in the lowermost 10 cm of Facies 1, and are intercalated with the very fine-grained sand laminae. Syneresis cracks are locally present, but uncommon.

Facies 1 displays sporadically distributed burrows at the bed scale, with bioturbation intensities ranging from BI 1-4. The ichnological suite is of low diversity and traces fossils are diminutive. The most common biogenic structure is *Planolites*, with subordinate occurrences of *Teichichnus* and *Cylindrichnus*.

3.1.1.2 Interpretation:

The predominance of irregular to parallel laminae suggests that mud was deposited from suspension or via flocculation from hypopycnal plumes in a low energy subaqueous setting (Bhattacharya and MacEachern, 2009). Occurrences of parallel and lenticular silt laminae suggests that energy levels and sediment input were locally elevated to allow emplacement of these laminae (Bhattacharya and MacEachern, 2009). Localized occurrences of syneresis cracks indicate short-lived events of salinity reduction occurred in the system (e.g., MacEachern et al., 2005). Ichnologically, the sporadically distributed, low-diversity, diminutive traces also suggest that there was a notable combination of physico-chemical stresses acting on the environment, leading to conditions unfavorable for infaunal colonization, but with sedimentation rates sufficiently

low, certain depositional intervals allowed sediment re-colonization during ambient conditions (e.g., MacEachern et al., 2005; Bhattacharya and MacEachern, 2009).

The normally graded, sharp based, very fine-grained sand to organic-rich mud layers in the lowermost 10 cm of Facies 1 reflect waning energy conditions in this interval (e.g., Mulder et al., 2003; MacEachern et al., 2005). Additionally, the presence of oscillation ripples suggests deposition in an environment where orbital wave motion affected sediment at the bed, either under fair-weather conditions (above fair-weather wave base) or from episodic storm-related conditions (above storm wave base) (e.g., Harms, 1969; Komar, 1974; Miller and Komar, 1980). The organic-rich mud layers of this interval suggests input of terrestrially derived carbonaceous material (MacEachern et al., 2005). The sharp-based, normally graded very fine-grained sand to oscillation-rippled silt interval may be the result of ravinement. Overall, the sedimentological and ichnological characteristics of Facies 1 suggest a prodeltaic setting in a restricted bay.

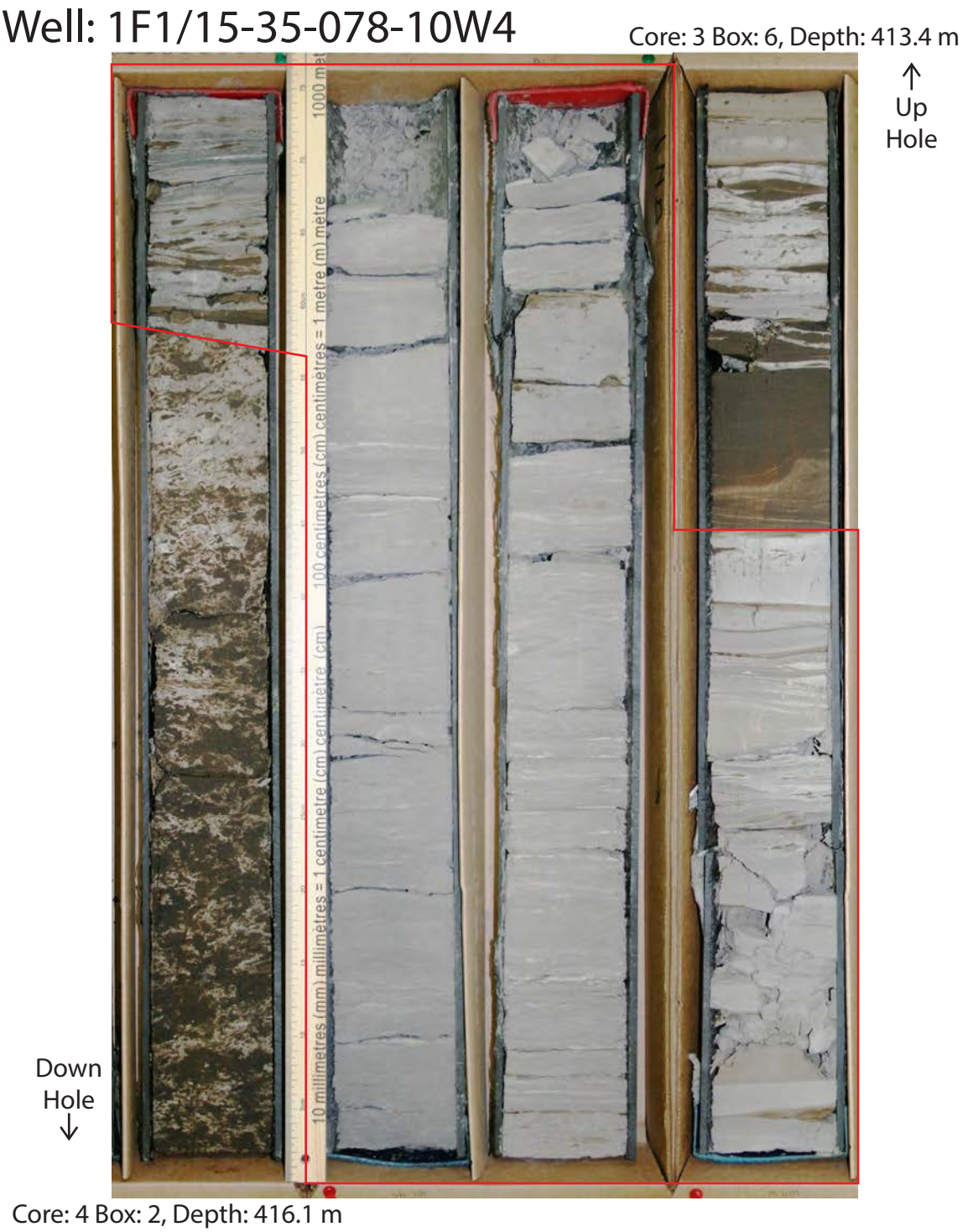

Figure 3.1 - Stitched core photograph of Facies 1- shale with parallel and lenticular sand and silt laminae. The red outlined area indicates the position of Facies 1.

Figure 3.2 - Core photograph of Facies 1 A) Sharp basal contact of F1 with oscillation rippled sand. The red line denotes the base of F1. Well: 1F1/15-35-078-10W4, core: 4 box: 2 depth: 415.5 m B) shale with lenticular bedding. Well: 1F1/15-35-078-10W4, core: 4 box: 1 depth: 414.6 m. Soft-sediment deformation (SSD), *Planolites* (Pl), *Teichichnus* (Te), oscillation ripples (OR).

3.1.2 Facies 2: Lenticular to wavy heterolithic bedding with oscillation ripples

3.1.2.1 Description:

Facies 2 commonly varies between 40% - 60% mud and 60% - 40% sand (Figs. 3.3 and 3.4). Sand bed thickness are cm- to dm-scale, and grain sizes range from lower very fine- to fine-grained sand. Mud beds are also cm- to dm-scale in thickness. Sand content increases upwards within Facies 2.

Abundant syneresis cracks are locally present in the mud beds. Heterolithic beds commonly display lenticular to wavy bedding and oscillation ripples. Oscillation ripples may appear aggradational. Carbonaceous debris is locally common. Micro-HCS and soft-sediment deformation features are present, but rare.

Bioturbation is variable within the heterolithic intervals of Facies 2, where BI ranges from 0-3. There is an overall sporadic heterogeneous distribution of trace fossils within the facies. Traces are commonly found in the muddier intervals and are less common in the sandier intervals. The most common trace fossil is *Planolites*, with subordinate occurrences of *Teichichnus, Cylindrichnus* and *Skolithos*. The ichnogenera are diminutive.

3.1.2.2 Interpretation:

Fluctuations in mud and sand content suggests fluctuating low to high energy conditions, were common during deposition of Facies 2. The presence of oscillation ripples suggests deposition in an environment where orbital wave motion, generated by wind-driven waves, affected sediment at the bed (Harms, 1969; Komar, 1974; Miller and Komar, 1980). Rare, but significant, storm events are manifest in the presence of micro-HCS beds that are generated by orbital wave motion of storm waves (Dott and Bourgeois, 1982). Abundant syneresis cracks with in the mud beds suggests that the system was subject to periods of freshet conditions that caused a salinity contrast at or near the bed (MacEachern et al., 2005). Alternatively, storm associated fluvial discharge may care buoyant mud plumes that may flocculate and capture freshwater and form syneresis cracks (MacEachern and Bann, 2008). Locally common carbonaceous detritus suggests that pulses of terrestrially derived organic debris entered the system as a result of heightened river discharge (MacEachern et al., 2005). Rare soft-sediment deformation

features associated with unbioturbated mud intervals is consistent with increased sedimentation rates and rapid mud deposition (Alexander et al., 1991).

The low bioturbation indices, diminutive burrows, and low-diversity of trace fossils indicates that physico-chemically stressful conditions were likely affecting the environment (Gingras et al., 2011). All traces represent facies-crossing opportunistic forms and are consistent with forms observed in brackish-water environments (MacEachern and Gingras, 2007). Traces are typically not observed in sandy intervals as physical energy and/or deposition rates were likely too high to allow for infaunal colonization. Only the muddier intervals that do not display soft-sediment deformation or syneresis cracks are bioturbated. This suggests that physico-chemically stressed conditions were common and opportunistic organisms were able to colonize the bed only during ambient conditions (Rhoads et al., 1978; Ekdale et al., 1984; Ekdale, 1985; Whitlach and Zajac, 1985; MacEachern et al., 2005; Gingras et al., 2011).

The abundance of wave-generated features, locally common syneresis cracks and organic debris, and rare soft-sediment deformational features, in addition to the sporadic heterogeneous distributions of impoverished trace fossil suites, strongly supports wave-/strom-dominated deltaic deposition in a salinity-stressed environment (e.g., Moslow and Pemberton, 1988; MacEachern and Pemberton, 1992; MacEachern et al., 2005; Maceachern and Bann, 2008; Gingras et al., 2011). Facies 2 is therefore interpreted to represent deposition within a wave- to storm-dominated distal delta front to prodeltaic environment in a restricted brackish embayment setting.

Well: 1F1/15-35-078-10W4

Core: 4 Box: 2, Depth: 411.8 m

Core: 3 Box: 6, Depth: 414.1 m

Figure 3.3 - Stitched core photograph of Facies 2 – lenticular to wavy heterolithic bedding with oscillation rippled sand. The red outlined area indicates the position of Facies 2.

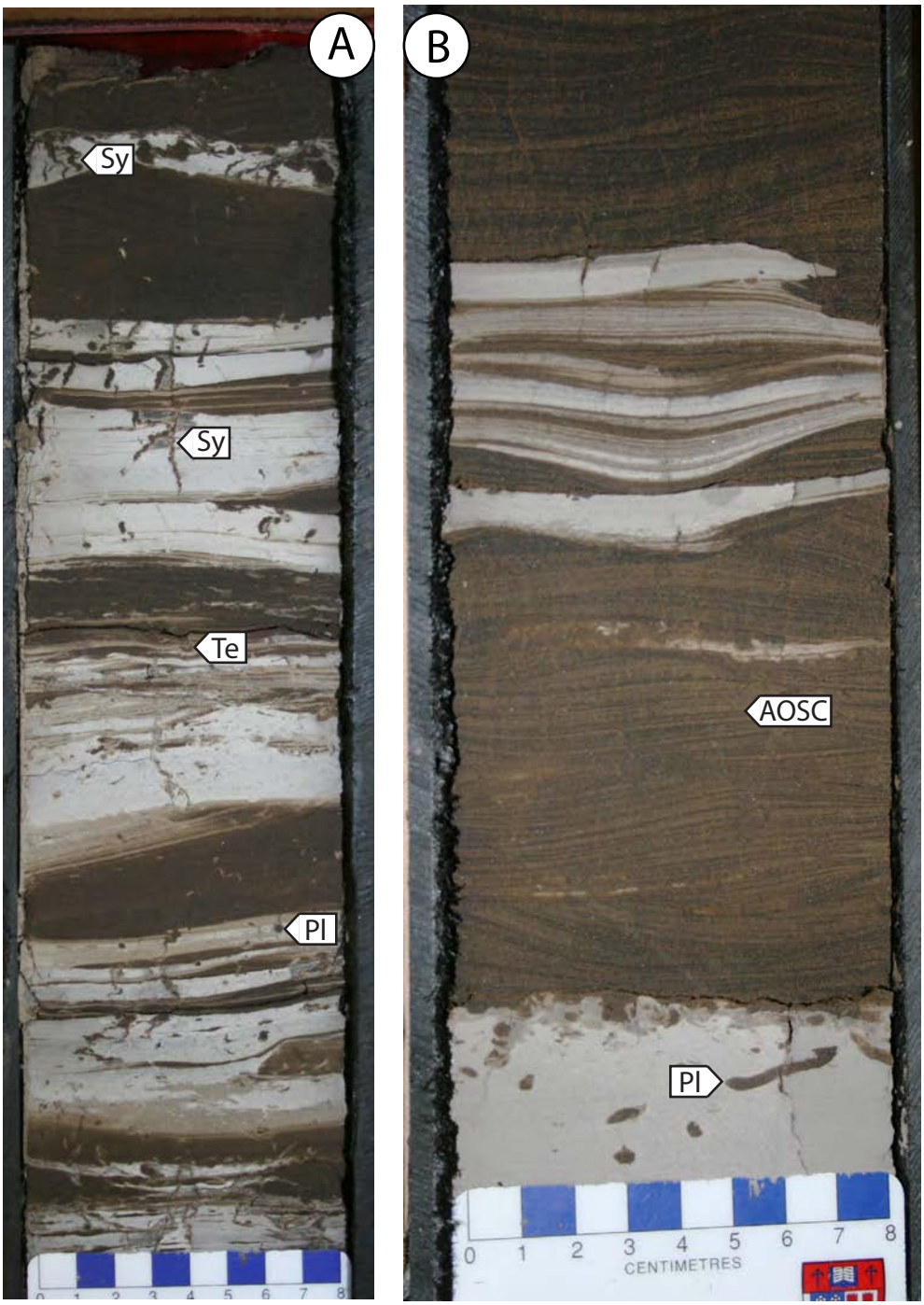

Figure 3.4 - Core photograph of Facies 2. A) Interbedded sand and mud displaying abundant syneresis cracks. Well: 1F1/15-35-078-10W4, core: 3 box: 6 depth: 412.7 m. B) Interbedded sand and mud with oscillation ripples to micro-HCS. Well: 1F1/15-35-078-10W4, core: 3 box: 5 depth:
412.5 m. Aggradational oscillation ripples (AOSC), syneresis cracks (Sy), *Planolites* (Pl), *Teichichnus* (Te).

3.1.3 Facies 3: Oscillation-rippled to hummocky cross-stratified sand facies

3.1.3.1 Description:

Facies 3 consists predominantly of lower very fine- to fine-grained sand (Figs. 3.5 and 3.6). There are abundant cm- to dm-thick sand beds and uncommon cm-thick mud beds. Sand content increases upwards in Facies 3. The sand beds contain abundant erosion and scour surfaces. There are also abundant oscillation ripples, micro-HCS, and hummocky cross-stratified sand intervals. Thin muds layers contain uncommon syneresis cracks.

Facies 3 displays reduced bioturbation intensities, ranging only from BI 0-2. The ichnological suite is of low diversity and traces are diminutive. The most common trace fossil is *Planolites*, and escape traces (fugichnia). There are also subordinate occurrences of *Cylindrichnus* and *Skolithos*.

3.1.3.2 Interpretation:

Facies 3 comprises multiple oscillatory-generated bedforms that have erosional and scoured surfaces between them. The presence of hummocky cross-stratified sands and micro-HCS suggests storm deposition (e.g., Dott and Bourgeois, 1982). Oscillation-rippled sands may represent waning storm deposition or ambient fairweather conditions where the orbital motion of wind-generated waves affected the bed (Dott and Bourgeois, 1982; Mulder et al., 2003; MacEachern et al., 2005). Uncommon, thin mud layers with syneresis cracks suggests periods of suspension sediment settling or clay flocculation under salinity stressed conditions (e.g., flocculation of mud from buoyant plumes; cf. MacEachern et al., 2005; MacEachern and Bann, 2008).

The traces present are facies-crossing opportunistic forms and escape structures, indicating periods of rapid and/or episodic deposition (MacEachern et al. 2005). The overall low diversity of traces and lack of abundant traces suggests that stressful physico-chemical conditions prevailed, where only opportunistic generalists were able to colonize the sediment (Gingras et al. 2011).

The sedimentology and ichnology observed in Facies 3 suggests that this facies was deposited within an environment subject to overall high depositional energies and

rates. The presence of thin mud beds with syneresis cracks in F3 indicates a deltaic setting. Facies 3 is interpreted to represent deposition within a wave- to storm-dominated delta-front environment in a restricted, brackish-water embayment.

Well: 1F1/15-35-078-10W4

Core: 3 Box: 2, Depth: 407.4 m

Core: 3 Box: 5, Depth: 412.6 m

Figure 3.5 - Stitched core photograph of Facies 3 – oscillation rippled to hummocky cross-stratified sand. The red outlined area indicates the position of Facies 3. ARS (allogenic ravinement surface), FS (flooding surface (autogenic)), WAB (Wabiskaw Member). Mud drapes support the interpretation that F3 was deposits in a deltaic setting.

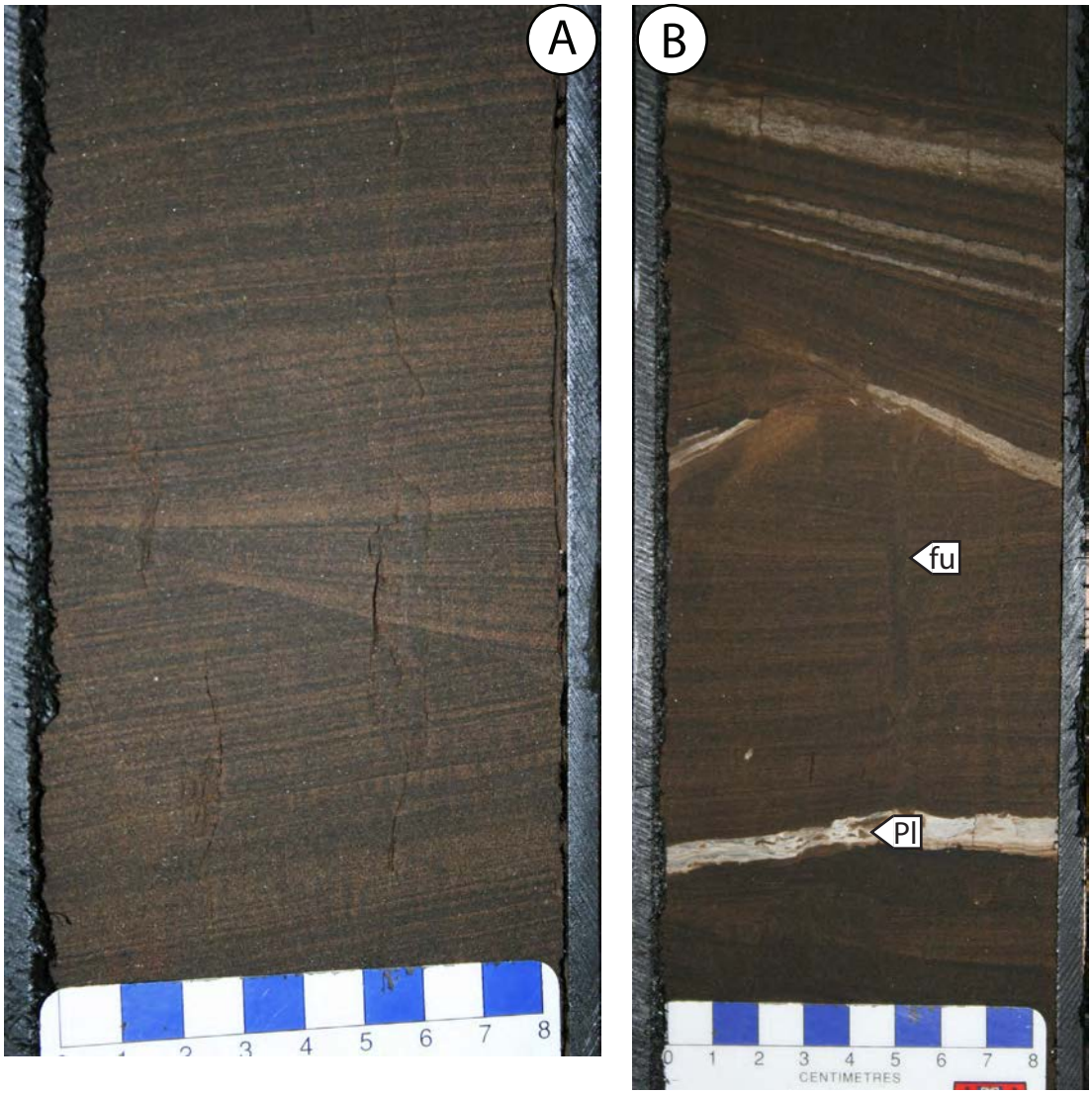

Figure 3.6 - Core photograph of Facies 3. A) Micro-hummocky cross-stratified to hummocky cross-stratified sand. Well: 1F1/15-35-078-10W4, core: 3 box: 5 depth: 412.0 m. B) Hummocky cross-stratified (HCS) in sand. Well: 1F1/15-35-078-10W4, core: 3 box: 4 depth: 411.1 m. Planolites (Pl), Fugichnia (fu).

3.1.4 Facies 4: Sub-Facies 4A: Bioturbated mudstone and sandstone

Facies 4 consists of bioturbated sand and mud. Facies 4 is divided into two sub-facies based on differences in lithologic ratios of sand and mud and prevalence of oscillation ripples. Sub-Facies 4A is mud dominated will higher BI values and less common oscillation ripples compared to F4B, which is sand dominated with reduced BI values and increased occurrences of oscillation ripples. Sub-Facies 4B has a gradational contact with underlying Sub-Facies 4A, and it is often difficult to pick the exact location where F4A ends and F4B beings.

3.1.4.1 Description:

The basal contact of Sub-Facies 4A (F4A) is sharp. Facies 4A varies between 90% mud and 10% sand to 50% mud and 50% sand, with sand content increasing upwards (Figs. 3.7 and 3.8). Beds range from cm to dm in thickness. The grain size of sand ranges from upper very fine- to lower very fine-grained. Oscillatory structures in the sand beds and localized carbonaceous debris are observed, but are uncommon.

Bioturbation commonly disturbs sedimentary structures and bed contacts. Sub-Facies 4A displays sporadically distributed burrows at the bed scale, and BI ranges from 2-5. Bioturbation indices often decreases upwards associated with the increase in sand content upwards. The ichnological suite is of low diversity and all ichnogenera are diminutive. The most common trace fossils are *Planolites, Cylindrichnus, Skolithos, Gyrolithes, and Teichichnus*, with subordinate occurrences of *Thalassinoides* and *Palaeophycus*.

3.1.4.2 Interpretation:

The suite of trace fossils in Sub-Facies 4A comprises relatively simple traces that are diminutive in size, are of low diversity, and are relatively abundant; characteristics typical of a brackish-water suite (Pemberton et al., 1982; Pemberton and Wightman, 1992; Gingras et al., 1999; Gingras and MacEachern, 2012).

Oscillation ripples suggest wave activity (possible wind waves or low energy swells). Episodic storm events could result in rapid emplacement of sediment and oscillation-rippled sand, as well as terrestrially derived carbonaceous detritus that preclude any bioturbation (MacEachern and Gingras, 2007). Facies 4A is interpreted to

represent the distal deposit of Facies 4. The sedimentology and ichnology observed in Sub-Facies 4A suggests that this facies was deposited within a restricted embayed sheltered (bay-margin) shoreface.

Well: 1AA/05-08-076-11W4

Core: 23 Box: 1, Depth: 472.5 m

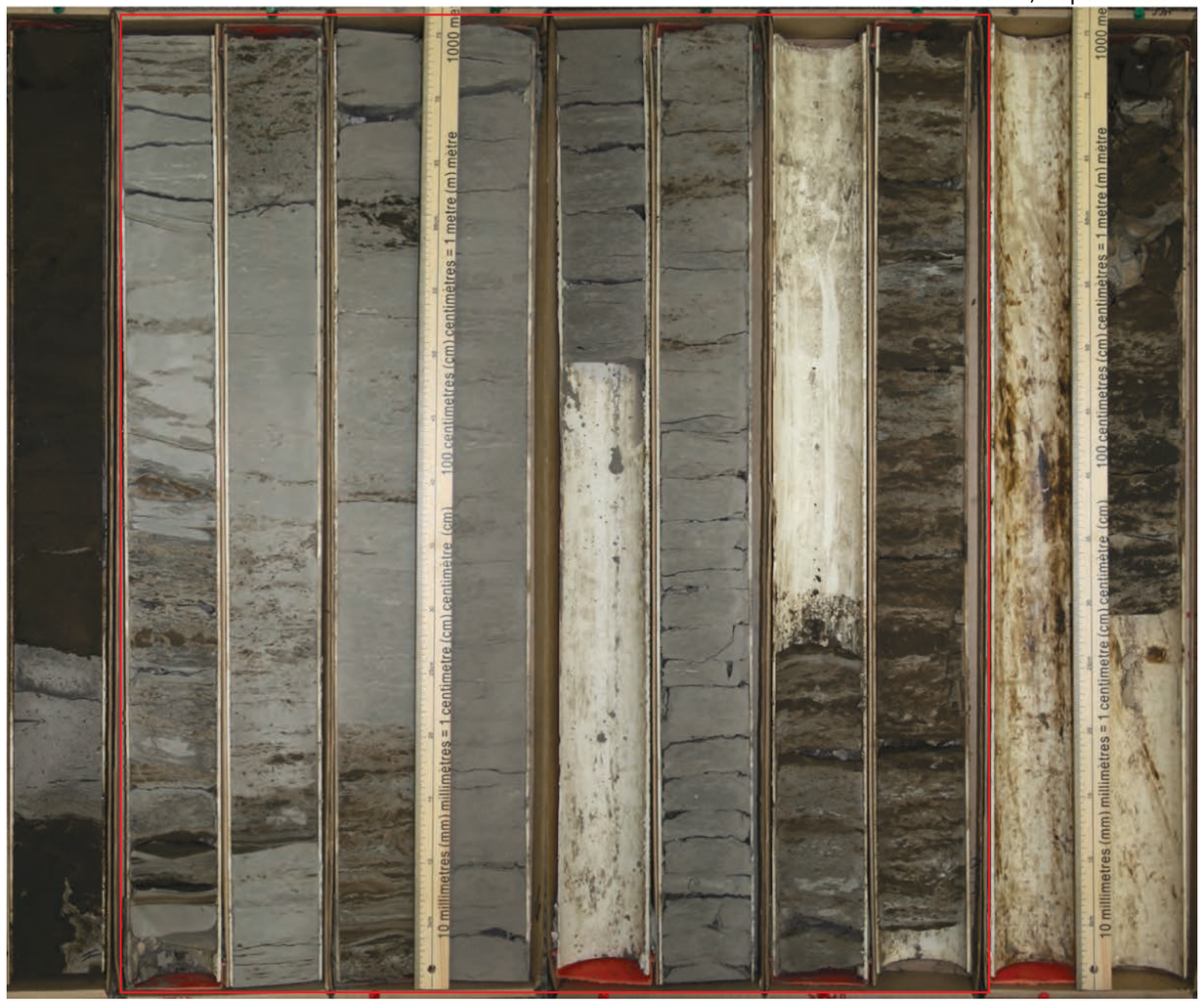

↑ Up Hole

Down Hole ↓

Core: 25 Box: 2, Depth: 478.1 m

Figure 3.7 - Stitched core photograph of Sub-facies 4A - Bioturbated mudstone interbedded with sand passing upwards into bioturbated sandstone interbedded with mudstone. The red outlined area indicates the position of Sub-facies 4A.

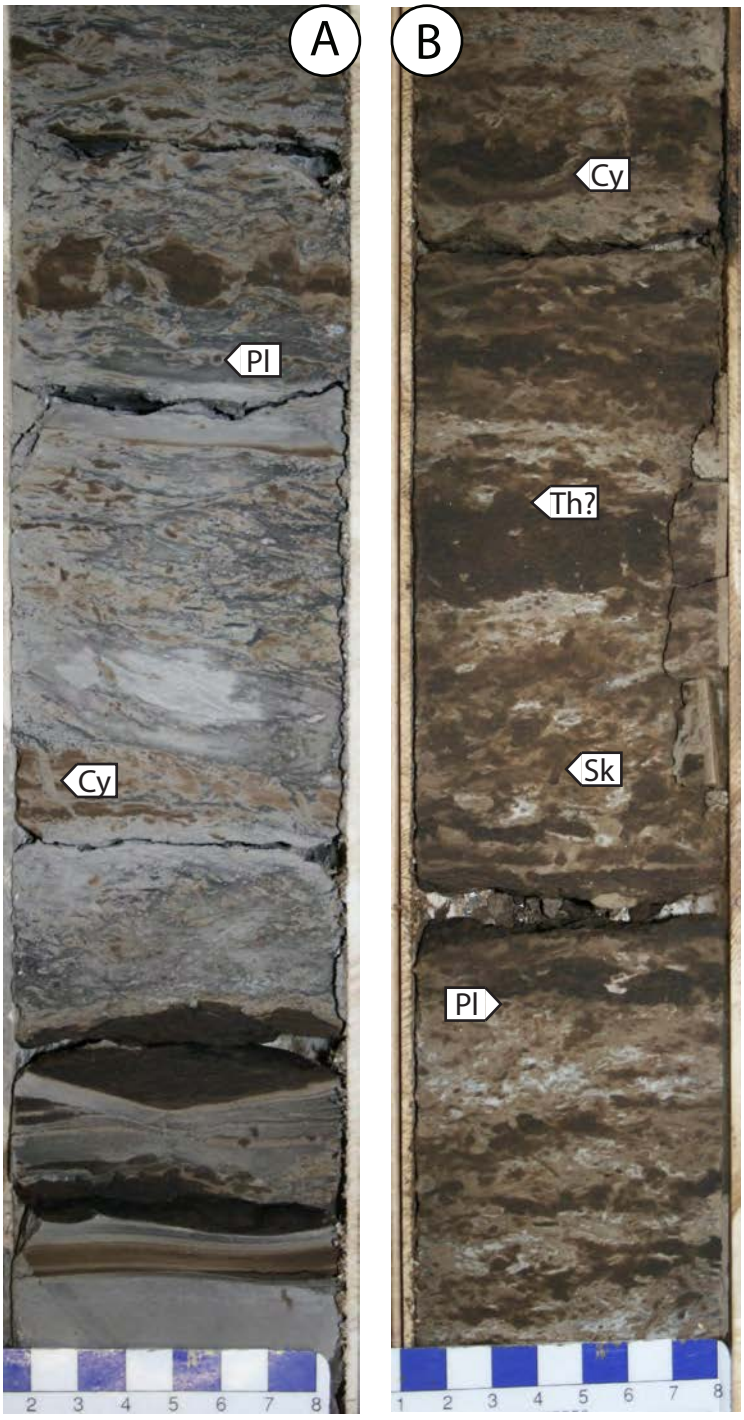

Figure 3.8 - Core photograph of Sub-facies 4A. A) Mud-dominated base of F4A. Well: 100/05-08-076-11W4, core: 25 box: 2 depth: 478.0.m. B) Bioturbated interbedded sand and mud. Well: 100/05-08-076-11W4, core: 24 box: 1 depth: 473.7 m. *Cylindrichnus* (Cy), *Planolites* (Pl), *Skolithos* (Sk), and *Thalassinoides* (Th).

3.1.5 Facies 4: Sub-Facies 4B: Bioturbated sandstone interbedded with mudstone to oscillation-rippled sand

3.1.5.1 Description:

Sub-Facies 4B (F4B) has a gradational lower contact with F4A. The sand content of F4B increases upwards, and varies between 50% - 20% mud and 50% - 80% sand (Figs. 3.9 and 3.10). Beds thicknesses range from cms to dms. The grain size of sand ranges from upper to lower very fine. Low-angle undulatory parallel lamination commonly overlie scour surfaces on underlying beds. Oscillation ripples are common in the upper portion of F4B. Carbonaceous debris is uncommon and mud clasts are rare, but where present are rounded to sub rounded and <1 cm in diameter.

Sub-Facies 4B has sporadically distributed burrows at the bed scale, and BI ranges from 2-4. Mud beds tend to have higher BI values than do the sand beds. The ichnological suites observed in F4B are of low diversity and consists of diminutive forms. The most common trace fossils are *Planolites, Cylindrichnus, Skolithos, Gyrolithes,* and *Teichichnus*, with subordinate occurrences of *Thalassinoides,* and *Palaeophycus*. Comparable to Sub-Facies 4A, suites observed in Sub-Facies 4B consist of relatively simple, diminutive traces.

3.1.5.2 Interpretation:

The low diversity and high abundance of these traces suggests a salinity stressed, or brackish-water environment (Pemberton et al., 1982; Pemberton and Wightman, 1992; Gingras et al., 1999; Gingras and MacEachern, 2012).

Sand intervals with oscillation ripples and lower BI values could represent seasonal deposition whereby episodic storm events result in rapid emplacement of sediment and oscillation-rippled sand, as well as terrestrially derived carbonaceous detritus that precluded bioturbation (Dalrymple et al., 1991; Gingras et al. 1999; Yang et al., 2005; MacEachern and Gingras, 2007). Sub-Facies 4B is interpreted to represent the proximal form of Facies 4. The sedimentology and ichnology observed in Facies 4B suggests that this facies was deposited within a restricted or sheltered, embayed (bay-margin) shoreface setting.

Well: 1AA/05-08-076-11W4

Core: 20Box: 2, Depth: 467.4 m

↑ Up Hole

Down Hole ↓

Core: 24 Box: 1, Depth: 473.8 m

Figure 3.9 - Stitched core photograph of Sub-facies 4B - Bioturbated sandstone interbeddded with mudstone to oscillation rippled sand. The red outlined area indicates the position of Sub-facies 4B.

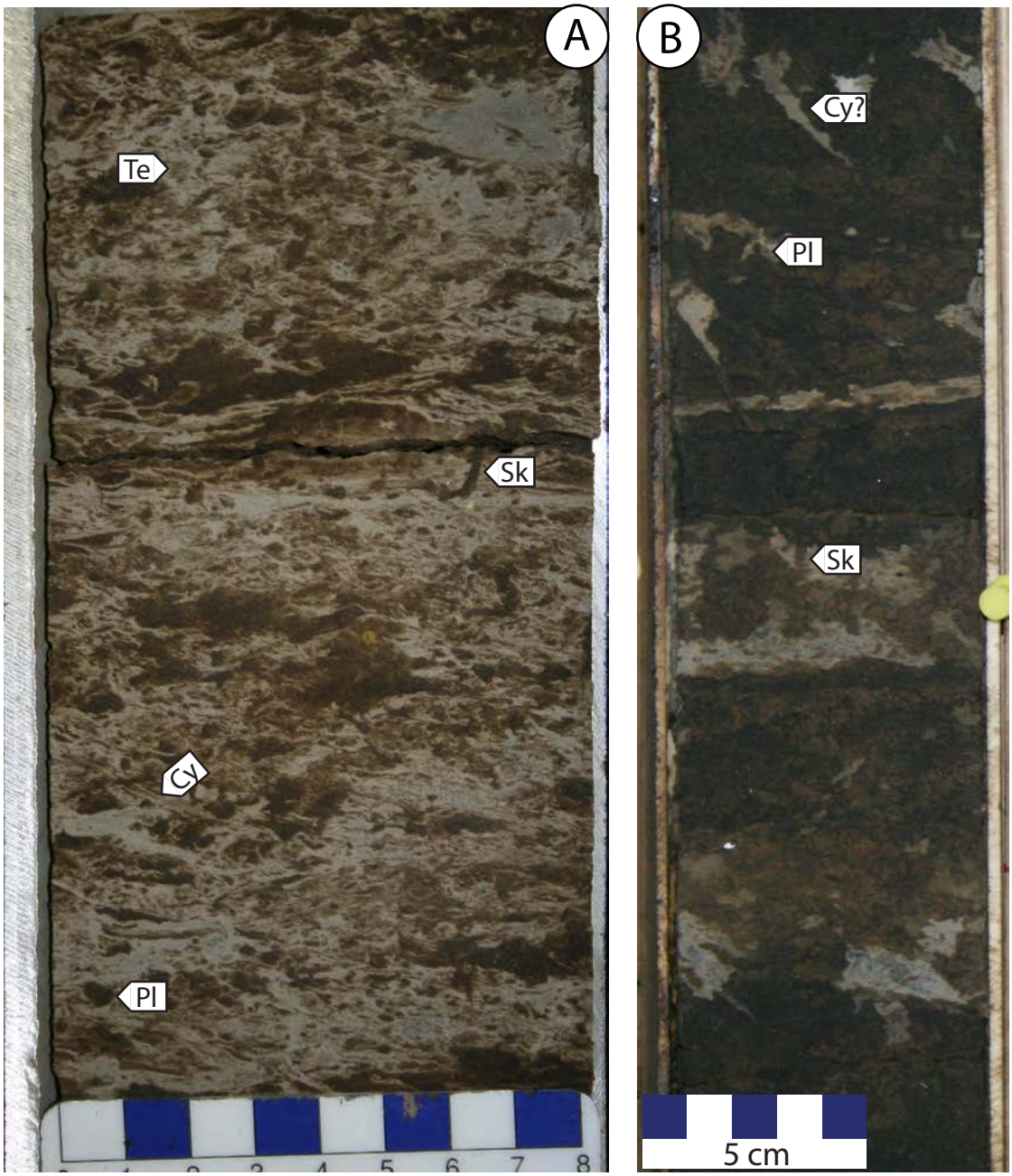

Figure 3.10 - Core photograph of Sub-facies 4B. A) Bioturbated sand and mud. Well: 1AA/06-19-77-09W4, core: 7 box: 3 depth: 373.6. B) Bioturbated sandy portion of F4B. Well: 100/05-08-076-11W4, core: 21 box: 1 depth: 468.9 m. *Planolites* (Pl), *Skolithos* (Sk), *Teichichnus* (Te), and *Cylindrichnus* (Cy).

3.1.6 Facies 5: Current rippled and cross-bedded sandstone

3.1.6.1 Description:

Facies 5 has a sharp basal contact with underlying strata (Figs. 3.11 and 3.12) and consists of lower medium- to upper very fine-grained sand. Sand beds thicknesses range from cm- to dm-scale. The base of Facies 5 typically contains cross-bedded to massive appearing sands. Cross-bed foresets commonly are oriented in the same direction. These sands may or may not have subrounded to angular intraformational mud rip-up clasts. Distribution of mud clasts varies from a few dispersed clasts in sand to intervals of clast-supported breccia. Mud clasts range in size from 1 mm to larger than the width of the core (>10cm). Overlying this interval, sand with thin, uncommon mud laminae occurs. Muds may be flat lying, undulatory, or occur as flaser bedding. This interval is commonly dominated by migrating current ripples intercalated with scour surfaces bounding low-angle oscillation ripples and reactivation surfaces (Fig. 3.13). Carbonaceous debris may be locally present.

Facies 5 displays sporadically distributed burrows, with BI ranging from 0-2. The ichnological suites are of low diversity and contain diminutive forms. The most common trace fossil is Cylindrichnus, with subordinate occurrences of *Skolithos* and *Planolites.* Although uncommon owing to the low BI values, *Cylindrichnus* can be found throughout Facies 5, whereas *Skolithos* and *Planolites* generally occur within intercalated the mud layers.

3.1.6.2 Interpretation:

Sharp basal contacts indicate erosional events. Cross-beds can form in water with sufficient water depth, velocity and sand, and can be found in a wide range of environments, including fluvial settings (Jackson, 1976, Harms et al., 1982), tidal settings (Barwis, 1978; Fenies and Faugeres, 1998, Hughes, 2012), mixed tidal-fluvial settings (Shchepetkina et al., 2016; Sisulak and Dashtgard, 2012), eolian settings, and turbidites. The angularity of intraformational mud rip-up clasts are interpreted to be the result of short transportation distances and rapid burial, likely as a result of bank erosion (e.g., Smith, 1972). Low-angle, undulatory bedding is interpreted to be the result of sheet flow and the migration of current ripples record lower flow regime currents.

Low bioturbation indices, diminutive burrows, and low diversity of trace fossils indicates that physico-chemically stressful conditions affected the environment (Gingras et al., 2011). Sand-dominated zones lacking bioturbation are not interpreted to be the result of freshwater conditions, but instead are interpreted as the product of a dynamic environment with high sedimentation rates and variable but persistent (quasi-steady) current flow. Such environments typically display reduced bioturbation intensities due to rapid accumulation of sediment, poor larval recruitment, and difficulty of infauna to establish permanent dwelling structures in mobile substrates (MacEachern and Gingras, 2007; Gingras and MacEachern, 2012). All trace fossils observed represent facies-crossing opportunistic forms, and are consistent with those observed in brackish-water settings (Beynon et al., 1988; Gingras et al., 1999; MacEachern and Gingras, 2007).

The abundance of sand, mud rip-up clasts, and current-generated sedimentary structures, in addition to impoverished ichnofossil suites suggest a stressed, relatively high-energy, channelized environment. Therefore, Facies 5 is interpreted to occur in a subtidal brackish-water channelized setting.

Well: 1AA/09-36-074-12W4

Core: 9 Box: 1, Depth: 490.1m

↑ Up Hole

Down Hole ↓

Core: 19 Box: 1, Depth: 411.9m

Figure 3.11 - Stitched core photograph of Facies 5 – Current rippled and cross bedded sandstone. The red outlined area indicates the position of Facies 5.

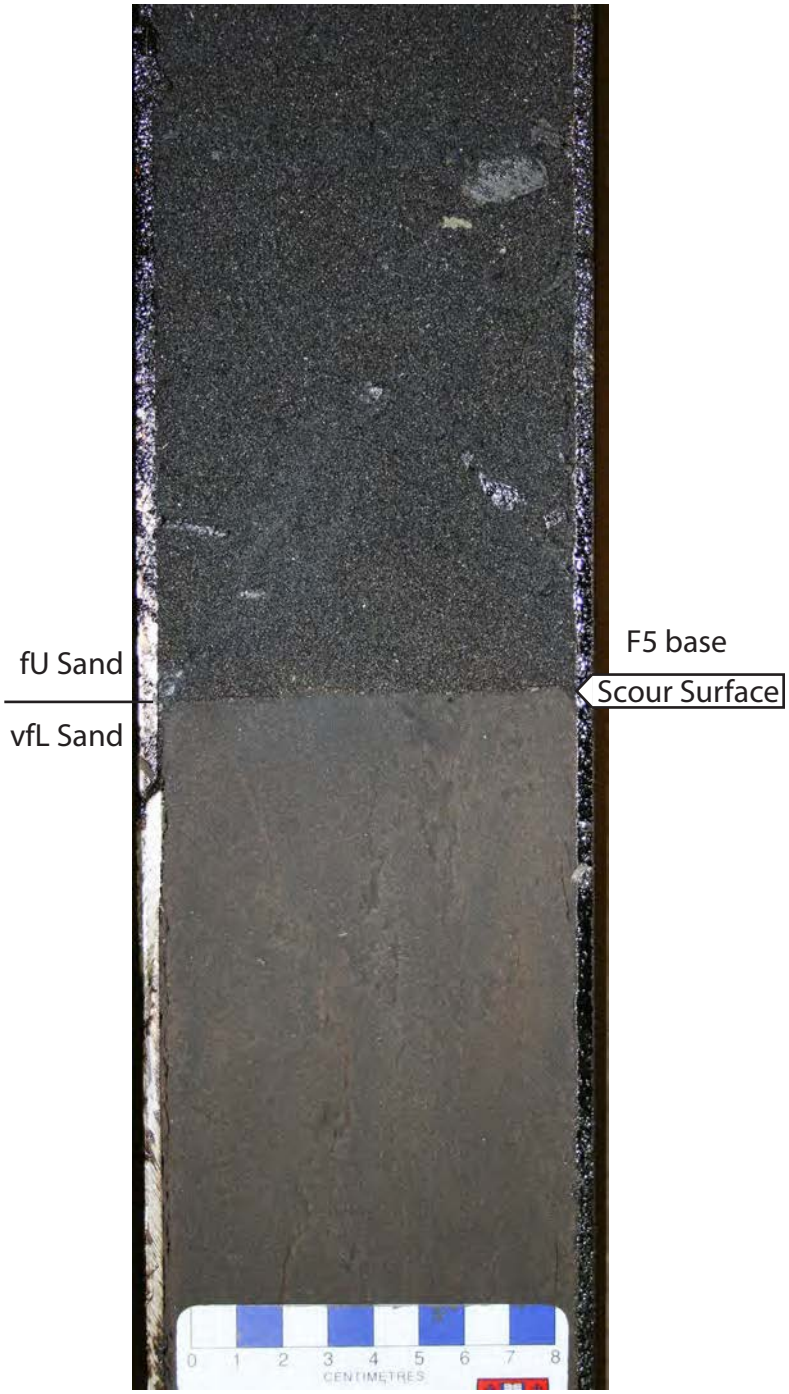

Figure 3.12 - Core photograph of erosional sharp base of Facies 5 overlying middle McMurray. Well: 1AA/09-36-074-12W4, Core: 10, Box: 4, Depth: 502.4m. Upper fine-grained sand (fU), lower very fine-grained sand (vfL).

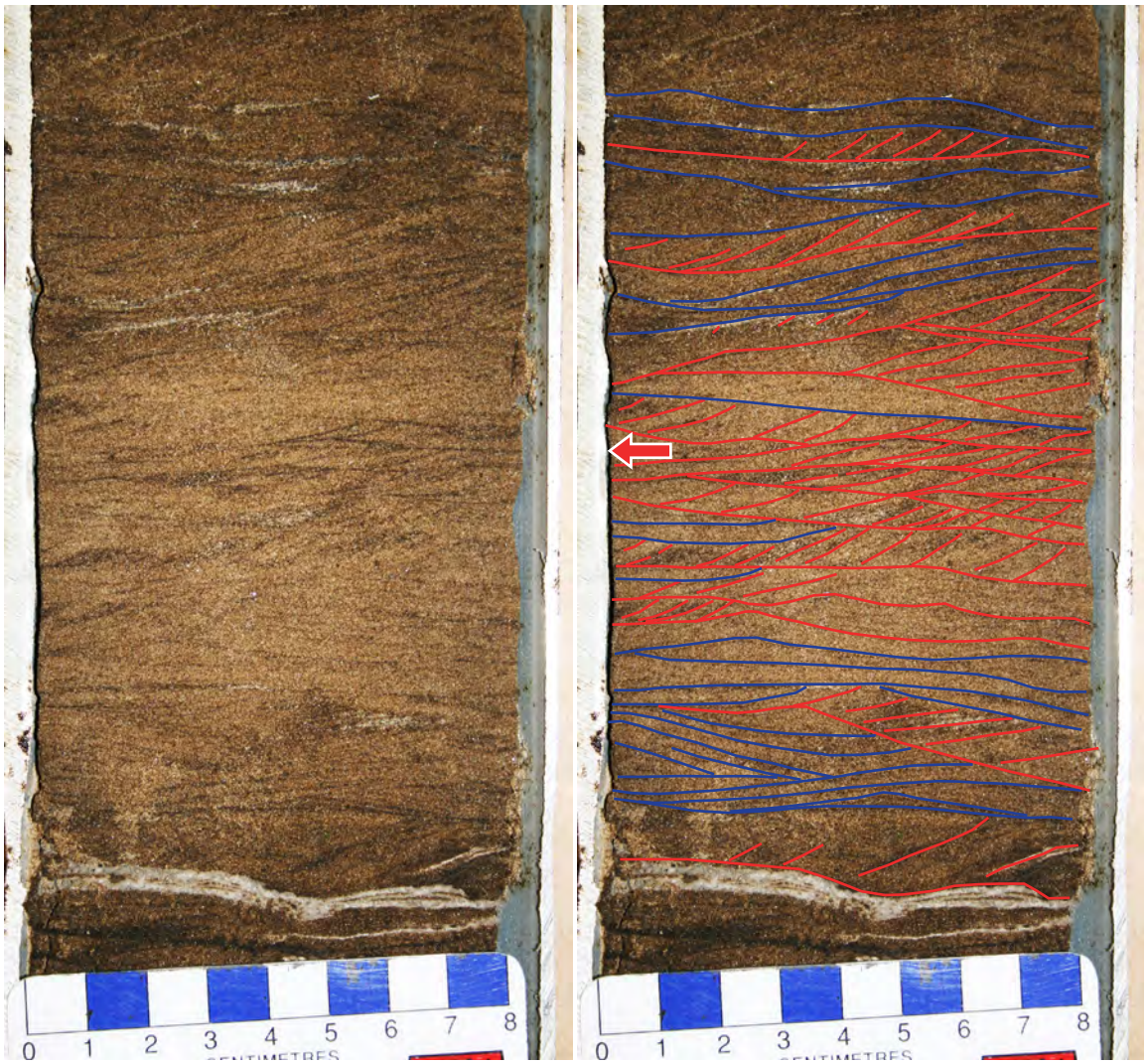

Figure 3.13 - Core photograph of Facies 5 (Left) and line sketch of sedimentary structures. Current ripples and cross-bedded sandstone interpreted to display differing flow energies. Blue surfaces denote low-angle undulatory bedding and red structures denote migrating current ripples. The red arrow is the interpreted flow direction during the deposition of the migrating ripples. Well: 1AA/06-19-077-9W4, Core: 11, Box: 2, Depth: 398.9m.

3.1.7 Facies 6: Sporadically bioturbated wavy interbedded sandstone and mudstone

3.1.7.1 Description:

Facies 6 is gradational with underlying Facies 5, and consist of upper fine- to lower very fine-grained sand intercalated with mud (Figs. 3.14 and 3.15). Beds are typically mm- to dm-scale in thickness. Mud contents increase upwards from sand dominated (80% sand, 20% mud) at the base to mud dominated (30% sand, 70% mud) at the top. Thinner mud beds and laminae (mm to cm scale) commonly show lenticular to wavy bedding, double mud drapes, rare syneresis cracks, and local carbonaceous debris. Thicker mud beds (cm to dm scale) interbedded with sand beds may show a consistent low-angle inclination and preferred orientation. These beds appear as inclined heterolithic stratification (IHS).

Bioturbation intensity varies, with some Facies 6 deposits having BI values of 2 while others have BI values up to 4. Trace fossils in Facies 6 are diminutive. Bioturbation is sporadically distributed and may disrupt sedimentological features. There is an overall sporadic heterogeneous distribution of trace fossils within the facies. Trace fossils are commonly found in muddier intervals and are less common in sandier intervals. The ichnological suite observed in Facies 6 is of low diversity. The most common trace fossils are *Planolites, Cylindrichnus, Skolithos, Gyrolithes,* with subordinate occurrences of *Palaeophycus* and *Teichichnus*.

3.1.7.2 Interpretation:

Heterolithic bedding is interpreted to be the result of variable flow conditions possibly related to neap-spring cycles and/or seasonal cycles. Inclined heterolithic stratification is common to channel margins and bar margins, including lateral migration. IHS can be found in fluvial environments (Thomas et al., 1987; Smith, 1987; Wood et al., 1988), tidal-fluvial environments (Thomas et al., 1987; Smith, 1987; Sisulak and Dashtgard, 2012; Johnson and Dashtgard, 2014) through to tidal environments (Pearson and Gingras, 2006; Santos and Rossetti, 2006; Hughes, 2012; Brivio et al., 2016). Double mud drapes are interpreted to result from semidiurnal tidal periodicities in a subtidal setting (Visser, 1980; Mackay and Dalrymple, 2011). Current-generated lenticular and wavy bedding is interpreted to form from tidal processes (Reineck and

Wunderlich, 1968). Syneresis cracks are regarded to indicate subaqueous conditions subject to salinity variations (Burst, 1965).

Diminutive and low diversity trace fossil assemblages indicate that physico-chemical stressors were affecting the environment (Gingras et al., 2011). All traces in the suite represent facies-crossing opportunistic forms and are consistent with brackish-water environments (Pemberton et al., 1982; Beynon et al., 1988; Pemberton and Wightman, 1992; MacEachern and Gingras, 2007). Traces are less common in sand beds, interpreted to indicate that deposition rates were higher than during deposition of mud beds (cf. Gingras et al. 2011). Colonization of the mud beds is interpreted to occur through larval recruitment, which is dependent on basin circulation patterns and tidal exchange (Moser and McIntosh, 2001; Gingras et al., 2002). This suggests that physico-chemically stressed conditions were common and unpredictable such that only opportunistic organisms could colonize the strata.

The overall increase in mud content, heterolithic bedding, and IHS, in addition to the sporadically heterogeneous distribution of impoverished trace fossils suites, suggests stressed channelized deposits that experienced waning and waxing of current flow. Therefore, Facies 6 is interpreted to represent a shallow, subtidal to lower intertidal portion of a brackish-water channel.

Well: 1AA/09-36-074-12W4

Core: 7 Box: 1, Depth: 475.5 m

Up Hole ↑

Down Hole ↓

Core: 9 Box: 1, Depth: 490.1 m

Figure 3.14 - Stitched core photograph of Facies 6 - Sporadically bioturbated wavy interbedded sandstone and mudstone. The red outlined area indicates the position of Facies 6.

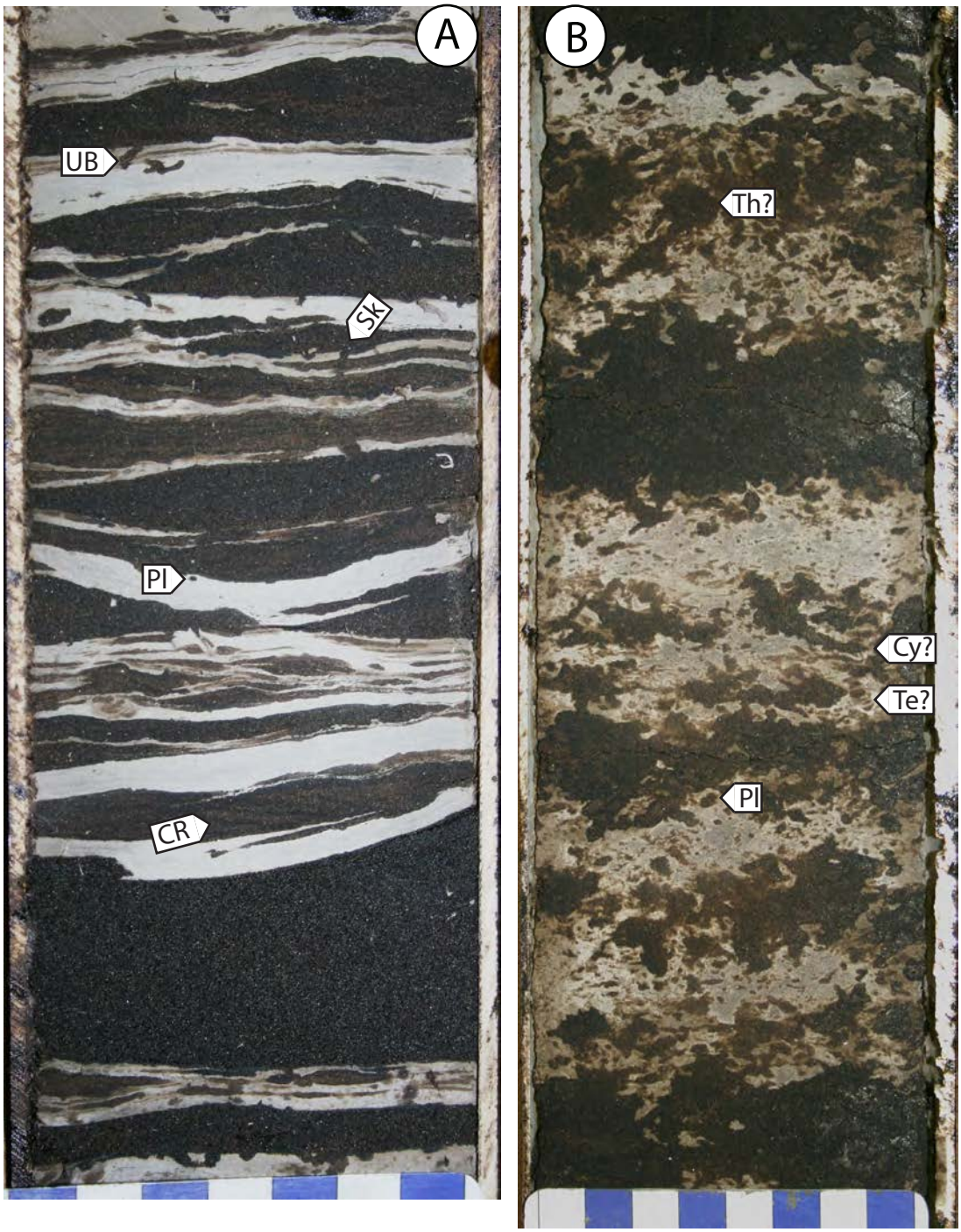

Figure 3.15 - Core photograph of Facies 6. A) Sporadically and weakly bioturbated wavy interbedded sandstone and mudstone with bioturbation intensities between BI 1 and 2. Well: 1AA/07-24-079-12W4, Core: 9, Box: 2, Depth: 444.1m. The dark beds are bitumen stained sandstone and the light grey beds are mudstone. B) More pervasively bioturbated wavy interbedded sandstone and mudstone with bioturbation intensities between BI 3 and 5. Bioturbation within the bitumen stained sands are difficult to discern. Well: 1AA/06-19-077-9W4 Core: 10, Box: 3, Depth: 392m. Current ripple (CR), *Planolites* (Pl), unidentified burrows (UB), *Teichichnus* (Te), *Thalassinoides* (Th), and *Cylindrichnus* (Cy).

3.1.8 Facies 7: Sporadically bioturbated mudstone with thin sand beds and laminae facies

3.1.8.1 Description:

Facies 7 has a gradational base with underlying occurrences of Facies 6. Facies 7 contains upper fine- to lower very fine-grained sand, in mm- to dm- thick beds (Figs. 3.16 and 3.17). Facies 7 is dominated by thick mud beds with thin (cm-scale) sand and silt beds and mm-scale laminae. Beds may show a consistent, shallow dip and orientation. Locally distributed carbonaceous debris and rare syneresis cracks occur. The upper contact of Facies 7 may be difficult to identify, as the contact is commonly associated with an overlying, mud-dominated facies (e.g., Facies 4A). The key difference in distinguishing Facies 7 from Facies 4 is that the sand content in F7 decreases upwards, whereas the sand content in F4 increases upwards.

Sedimentological features are typically disrupted by bioturbation. Bioturbation intensities range from BI 3-5. The trace fossil suite of Facies 7 is of low diversity and consists of diminutive forms. The most common trace fossils are *Planolites, Cylindrichnus, Skolithos,* and *Gyrolithes*, with subordinate occurrences of *Palaeophycus, Teichichnus*. The facies also contains rare rootlets.

3.1.8.2 Interpretation:

Increasing mud contents upwards indicates an overall reduction in flow energy. Interbedded mud and sand appear to have consistent, shallow dips, and are interpreted as mud-dominated IHS. Current-generate lenticular bedding is interpreted to form from tidal processes (Reineck and Wunderlich, 1968).The rare occurrence of rootlets indicates deposition near a terrestrial/subaerial environment.

Diminutive and low-diversity trace fossils indicate that physico-chemical stresses affected the environment (Gingras et al., 2011). Tidal exchange is interpreted to facilitate larval recruitment resulting in colonization of the beds (Moser and McIntosh, 2001; Gingras et al., 2002). All traces observed represent facies-crossing, opportunistic forms consistent with those observed in brackish-water settings (Pemberton et al., 1982; Beynon et al., 1988; Pemberton and Wightman, 1992; MacEachern and Gingras, 2007). Relatively high intensities of bioturbation suggest preferential colonization and slower deposition rates relative to the underlying Facies 5 and Facies 6.

The dominance of mud with lenticular sand beds, mud-dominated IHS, and relatively high bioturbation intensities composed of stressed ichnological suites suggests that deposition occurred in the upper portion of a brackish-water channel. Therefore, Facies 7 is interpreted to represent the lower intertidal to upper intertidal portion of a brackish-water tidal or tidal-fluvial channel.

Well: 1AA/09-36-074-12W4

Core: 6 Box: 2, Depth: 471.1 m

↑ Up Hole

Down Hole ↓

Core: 7 Box: 1, Depth: 476.9 m

Figure 3.16 - Stitched core photograph of Facies 7 - Sporadically bioturbated mudstone with thin sand beds and laminae. The red outlined area indicates the position of Facies 7.

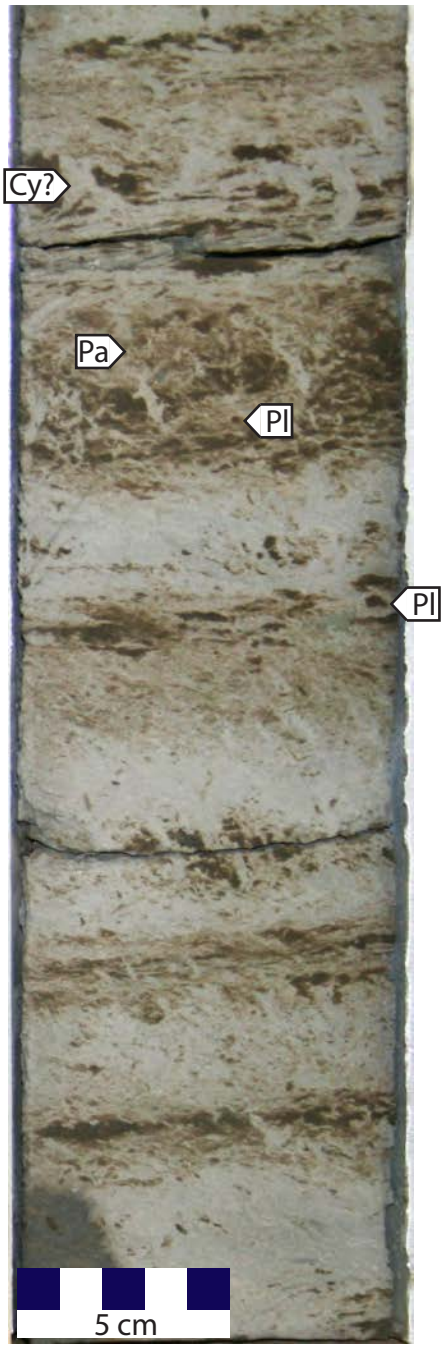

Figure 3.17 - Core photograph of Facies 7. Pervasively bioturbated sandy mudstone with bioturbation intensities between 4 and 5.Well: 1AA-09-36-74-12W4, Core: 6, Box: 2, Depth: 473.2m. *Planolites* (Pl), *Palaeophycus* (Pa), *Cylindrichnus* (Cy), and *Teichichnus* (Te).

3.1.9 Facies 8: Carbonaceous-detritus bearing mudstone

3.1.9.1 Description:

Facies 8 is not commonly encountered and where present has a gradational basal contact with the underlying strata; typically either F4 or F7. It comprises mudstone, dominated by abundant carbonaceous debris, coalified wood fragments and rhizoliths (Figs. 3.18 and 3.19). There are local occurrences of soft-sediment deformation and convolute bedding, but they are typically uncommon overall. The vast majority of the facies appears structureless.

The BI varies from 0-1, though root traces (rhizoliths) are common. *Planolites* is the only trace fossil observed, and is only rarely encountered.

3.1.9.2 Interpretation:

Since Facies 8 is found to overlie facies interpreted to record brackish-water tidal conditions, the abundant rhizoliths in predominantly structureless mud, in addition to the scarcity of bioturbation, suggests that the substrate was supratidal and subaerially exposed (cf. Gingras and MacEachern, 2012). Facies 8 is therefore interpreted to represent periods of subaerial exposure in a supratidal or coastal plain setting, wherein the mudstone had begun to undergo pedogenic alteration.

Well: 1AA/16-02-079-11W4

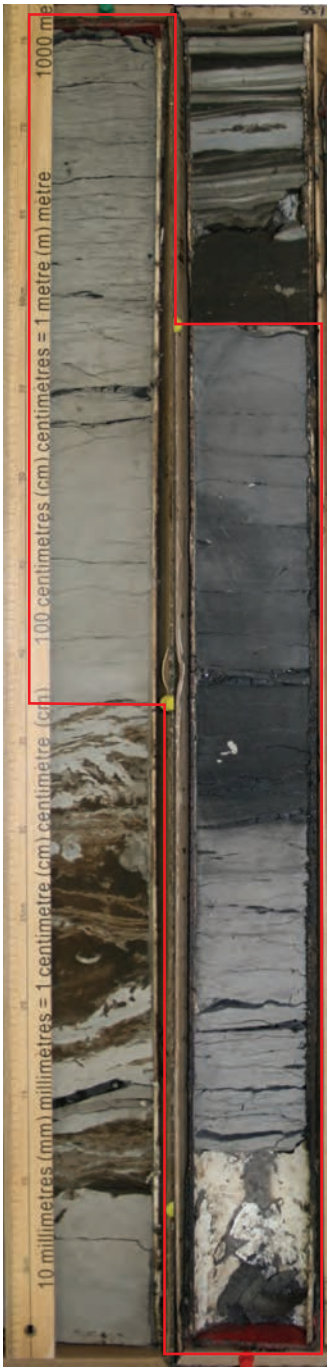

Figure 3.18 -Stitched core photograph of Facies 8 – Carbonaceous-detritus bearing mudstone. The red outlined area indicates the position of Facies 8.

Figure 3.19 - Core photograph of Facies 8 consisting of abundant carbonaceous-detritus in light grey mudstone. Well: 1AA/16-02-079-11W4, core: 9 box: 2 depth: 453.1 m. Coalified wood fragments (CW).

3.1.10 Facies 9: Bioturbated glauconitic silty to muddy sandstone

3.1.10.1 Description:

Facies 9 consists predominantly of lower very fine- to upper fine-grained sand. Bedding is typically not discernible, owing to the high intensity of bioturbation (Figs. 3.20 and 3.21). Silt contents increase upwards within the facies, and Facies 9 contains abundant glauconitic and lithic fragments intermixed with the sand. Facies 9 is in gradational contact with overlying Facies 10. Facies 9 erosionally overlies the McMurray Formation facies.

Facies 9 has markedly elevated bioturbation intensities with relatively robust, and diverse traces. Bioturbation indices range from 4-6. The most common trace fossils include *Diplocraterion, Teichichnus, Thalassinoides, Asterosoma, Planolites*, *Phycosiphon*, *Palaeophycus, Chondrites,* and *Skolithos.* There are subordinate occurrences of *Cylindrichnus, Arenicolites, Cosmorhaphe,* and *Zoophycos*. Large traces, such as *Diplocraterion* and *Thalassinoides*, subtend from Facies 9 into the underlying McMurray Formation facies.

3.1.10.2 Interpretation:

The presence of robust and diverse ichnogenera overprinting all primary sedimentary features indicates that no significant physico-chemical stresses were acting on the system at the time of deposition (cf. MacEachern and Bann, 2008). The presence of traces typical of marine conditions (e.g., Cosmorhaphe, Phycosiphon, Asterosoma, and Zoophycos) suggests that normal marine salinities prevailed during deposition (cf. MacEachern et al. 2007; MacEachern and Bann, 2008). The abundant overprinting of traces and presence of abundant glauconite suggests that slow and continuous rates of deposition predominated (cf. Odin and Matter, 1981; Stonecipher, 1999; MacEachern and Bann, 2008)

The erosive contact between Facies 9 (within the Wabiskaw) and all underlying McMurray Formation facies, is interpreted to be an allogenic TSE (transgressive surface of erosion). The large subtending traces from Facies 9 are interpreted to record an omission suite, varying from palimpsest softground to firmground conditions. Overall, Facies 9 is interpreted to represent a marine, lower shoreface environment.

Well: 1AA/02-23-079-W4

Core: 17 Box: 1, Depth: 408.4 m

↑ Up Hole

Down Hole ↓

Core: 19 Box: 1, Depth: 411.9 m

Figure 3.20 - Stitched core photograph of Facies 9 - Bioturbated glauconitic silty to muddy sandstone. The red outlined area indicates the position of Facies 9.

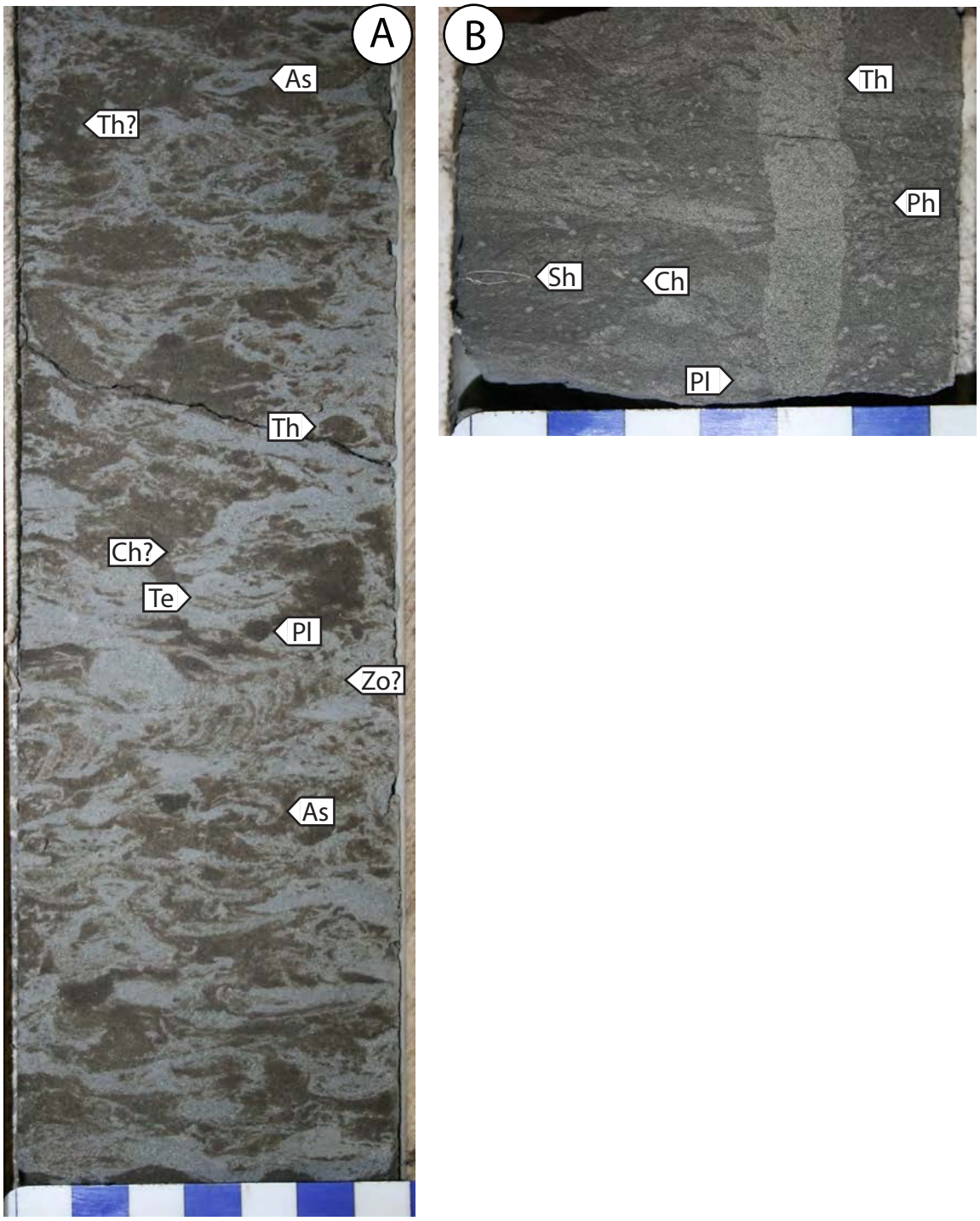

Figure 3.21 - Core photograph of Facies 9. A) Glauconitic silty to muddy sand with robust traces, showing BI 4-5. Well: 1AA/08-11-78-10W4, core: 7 box: 2 depth: 367.7 m. B) Glauconitic muddy sand with robust traces and BI 4. Well: 1AA/08-1-078-10W4, core: 3 box: 2 depth: 357.7 m. *Thalassinoides* (Th), *Teichichnus* (Te), *Planolites* (Pl), *Asterosoma* (As), *Chondrites* (Ch), Shell (Sh), *Zoophycos* (Zo) and *Phycosiphon* (Ph).

3.1.11 Facies 10: Bioturbated muddy siltstone with sand laminae

3.1.11.1 Description:

Facies 10 comprises silt with subordinate amounts of clay and lower very fine-grained sand (Figs. 3.22 and 3.23). The sand is only observed as laminae. Facies 10 is gradational with underlying Facies 9. Bioturbation typically overprints primary physical structures. Thin, unbioturbated, parallel laminated glauconitic sand is uncommon. Rare oscillation ripples are also observed associated with the thin sand laminae.

Similar to Facies 9, Facies 10 exhibits elevated bioturbation intensities with relatively robust traces and a diverse trace fossil suite. Bioturbation indices range from 4-6. The most common trace fossils are *Teichichnus*, *Thalassinoides*, *Asterosoma*, *Planolites*, *Palaeophycus*, *Helminthopsis, Chondrites, Phycosiphon, Cosmorhaphe,* and *Skolithos*. There are subordinate occurrences of *Cylindrichnus*, *Arenicolites*, and *Zoophycos*.

3.1.11.2 Interpretation:

Robust and diverse suites of ichnogenera indicate that conditions were likely stable at the time of deposition and that there were no significant physico-chemical stresses in the setting (MacEachern and Bann, 2008). The presence of traces typical of marine conditions (e.g., *Phycosiphon, Cosmorhaphe, Astersoma Zoophycos*, and *Helminthopsis*) suggests that normal marine salinities prevailed at the time of deposition (cf. MacEachern et al., 2007; MacEachern and Bann, 2008). The predominance of deposit-feeding and grazing structures observed in Facies 10 is typical of the suites attributable to the archetypal *Cruziana* Ichnofacies (MacEachern et al., 2007; MacEachern and Bann, 2008).

The uncommon intercalation of thin, lower fine-grained sand laminae with rare oscillation ripples suggests periodic very weak tempestite deposition (Dott and Bourgeois, 1982). Overall, Facies 10 is interpreted to represent a marine, upper offshore environment with a very weak storm climate.

Well: 1AA/02-23-079-W4

Core: 7 Box: 1, Depth: 398.2 m

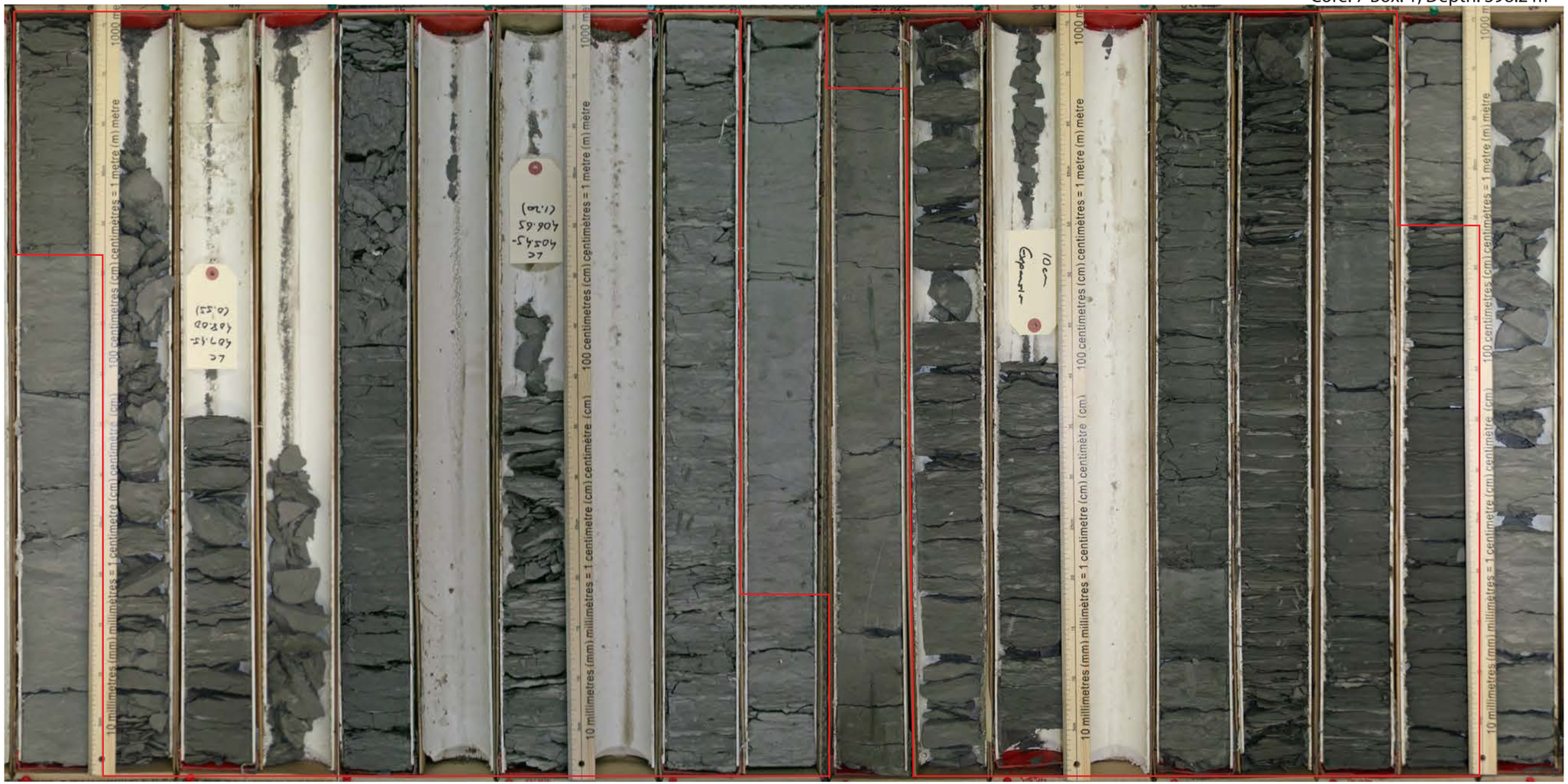

Core: 17 Box: 1, Depth: 409.0 m

Figure 3.22 - Stitched core photograph of Facies 10 - Bioturbated muddy siltstone with sand laminae. The red outlined area indicates the position of Facies 10.

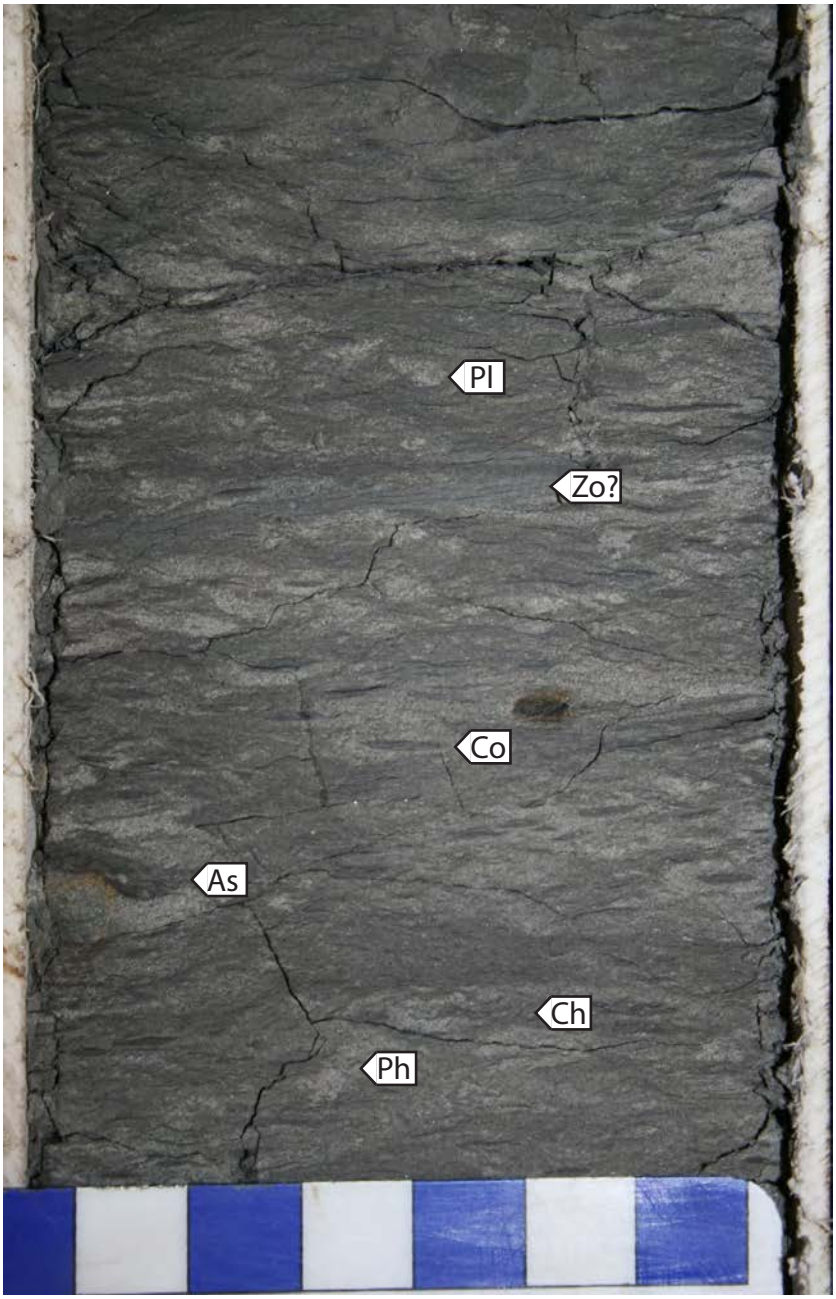

Figure 3.23 - Core photograph of Facies 10 - bioturbated muddy silt. Well: 1AA/08-11-78-10W4, core: 5 box: 1 depth: 361.9 m. *Cosmorhaphe* (Co), *Chondrites* (Ch), *Asterosoma* (As), *Zoophycos* (Zo), Planolites (Pl), and *Phycosiphon* (Ph).

3.2 Facies Association 1 - Wave/Storm Dominated Delta

3.2.1 Description

Facies Association 1 comprises shales with parallel and lenticular sand and silt laminae (F1) above the sharp basal contact, which is overlain by lenticular to wavy heterolithic bedding with oscillation ripples (F2), which is overlain with oscillation rippled to hummocky cross stratified sand (F3). These facies stack vertically to form a coarsening-upwards succession. A second coarsening-upwards succession may occur.

A complete succession begins with a sharp basal contact overlain by wavy bedded to oscillatory rippled very fine sand and shale (F1). These are overlain by shales with parallel and lenticular, mm-scale silt laminae, a unit which dominates the lower portion and is characterized by BI values of 1 to 4, with diminutive suites of trace fossils. The most common trace fossil is *Planolites*, with subordinate occurrences of *Teichichnus* and *Cylindrichnus.* Stratigraphically upwards, fine- to lower very fine-grained sands occur as lenticular to wavy heterolithic bedding and becomes abundant (F2). Sand and shale beds thicknesses range from cm- to dm-scale. The mud beds contain abundant syneresis cracks, whereas the sand beds contain oscillation ripples and carbonaceous debris. Rare micro-HCS and soft-sediment deformation is also present. The heterolithic bedsets have a sporadic heterogeneous distribution of bioturbation (cf. Gingras et al., 2011). The sand beds have BI values of 0-1, with a diminutive monospecific assemblage of *Planolites*. Intercalated mud beds have a BI ranging from 1-3, with diminutive *Planolites*, *Teichichnus*, *Cylindrichnus*, and *Skolithos*. Stratigraphically upwards, oscillation ripples, micro-HCS, and hummocky cross-stratified sands dominate with only a few thin shale beds (F3). There is abundant erosion and scour surfaces associated with the sand bedforms. BI values range from 0-2, with diminutive traces. The most common trace fossils are *Planolites* and fugichnia, with subordinate occurrences of *Cylindrichnus*, and *Skolithos*. The upper contact of FA1 is sharp.

3.2.2 Interpretation

Facies Association 1 has the most consistent appearance in core compared to the other facies associations. Facies 1 is genetically related to and gradationally transitions to Facies 2, which is genetically related to and gradationally transitions to

Facies 3. A flooding surface may be amalgamated with or occur slightly above the ravinement surface. Mud beds are interpreted to be deposited due to the suspension settling of flocculated muds or fluid (dynamic) muds (MacKay and Dalrymple, 2011). Syneresis cracks occur in the mud beds and are attributed to salinity differences due to mixing of fresh and marine waters. Ichnological suites comprise impoverished marine traces and indicate physico-chemical stresses attributed to a deltaic setting (e.g., MacEachern et al., 2005, La Croix et al., 2015). Overall, wave energy increases upwards and bioturbation intensities decreases upwards, consistent with shallowing during progradation and concomitant increasing depositional energies. Micro-hummocky cross-stratification and oscillation ripples are interpreted to be the result of orbital flow from waves (including storms). FA1 is interpreted to transition from below fair-weather wave base to above fair-weather wave base in a wave dominated, strongly storm influenced environment. The second coarsening upwards succession is interpreted to be the result of autogenic flooding. Overall, the succession records progradation from distal prodelta (F1), to proximal prodelta - distal delta front (F2), through to to delta front (F3) in a wave-/storm-dominated delta in a brackish-water setting (Fig. 3.24).

Well: 1F1/15-35-078-10W4

Core: 3 Box: 2, Depth: 407.4 m

Core: 4 Box: 2, Depth: 416.1 m

Figure 3.24 - Stitched core photograph displaying FA1 (wave-/storm-dominated delta), Well: 1F1/15-35-078-10W4.ARS (allogenic ravinement surface), FS (flooding surface (autogenic)), WAB (Wabiskaw Member).

3.3 Facies Association 2 - Protected Shoreface to bay-margin

3.3.1 Description

Facies Association 2 overlies a sharp basal surface and forms a coarsening-upwards succession (Fig. 3.24). FA2 starts with bioturbated mudstone and sandstone (F4A) that gradational transitions to bioturbated sandstone interbedded with mudstone to oscillatory rippled sand (F4B), and capped with carbonaceous mudstone (F8) locally.

A complete succession begins with a sharp basal contact dominated by bioturbated sandy mudstone (F4A). Grain sizes range from upper very fine to lower very fine. Interbeds of sand and mud range from cm- to dm- in thickness. Bioturbation commonly obscures bedding. Oscillation structures in sand beds are present but most commonly reworked by bioturbation. Carbonaceous debris are also present locally. BI values range from 2-5 with low-diversity suites of diminutive trace fossils. The most common elements are *Planolites, Cylindrichnus, Skolithos, Gyrolithes,* and *Teichichnus,* with subordinate occurrences of *Thalassinoides,* and *Palaeophycus*. Stratigraphically upwards, the muddy sandstone becomes increasingly dominated by sand beds. Sand beds may contain oscillation ripples, low-angle undulatory parallel lamination, carbonaceous debris, and rare mud clasts (F4B). BI values in this portion of FA2 ranges from 1-4, and contains trace fossil suites similar to F4A. Although rare, FA2 may have carbonaceous-rich mudstone with rootlets and soft sediment deformation capping the succession (F8).

3.3.2 Interpretation

The basal contact is interpreted as an erosional surface. Heterolithic interbedded sand and mud is interpreted to be the result of fluctuating energy conditions (Hughes, 2012). Oscillatory structures in the lower portion of FA2 are interpreted to be related to storm waves, whereas oscillatory structures in the upper portion of FA2 are interpreted to be deposited by ambient (fairweather) waves (Harms, 1969; Komar, 1974; Miller and Komar, 1980).

The minimal number of preserved sedimentary structures is interpreted to be the result of sheltered conditions. The ichnological suites consist of facies-crossing forms

and are typical of a tide-dominated brackish-water setting (Gingras et al., 2012). The carbonaceous-rich mudstones at the top of some expressions of FA2 are interpreted to represent supratidal conditions. The gradual transition from bioturbated sandy mudstone to muddy sandstone (F4A) to bioturbated muddy sandstone to oscillation rippled sand (F4B) is interpreted to reflect shallowing from distal to proximal subaqueous conditions, passing into intertidal and (more rarely) supratidal conditions. FA2 is interpreted to reflect progradation of a sheltered (protected) bay-margin shoreface environment.

Well: 1AA/05-08-076-11W4

Core: 21 Box: 1 Depth: 468.1m

Up Hole ↑

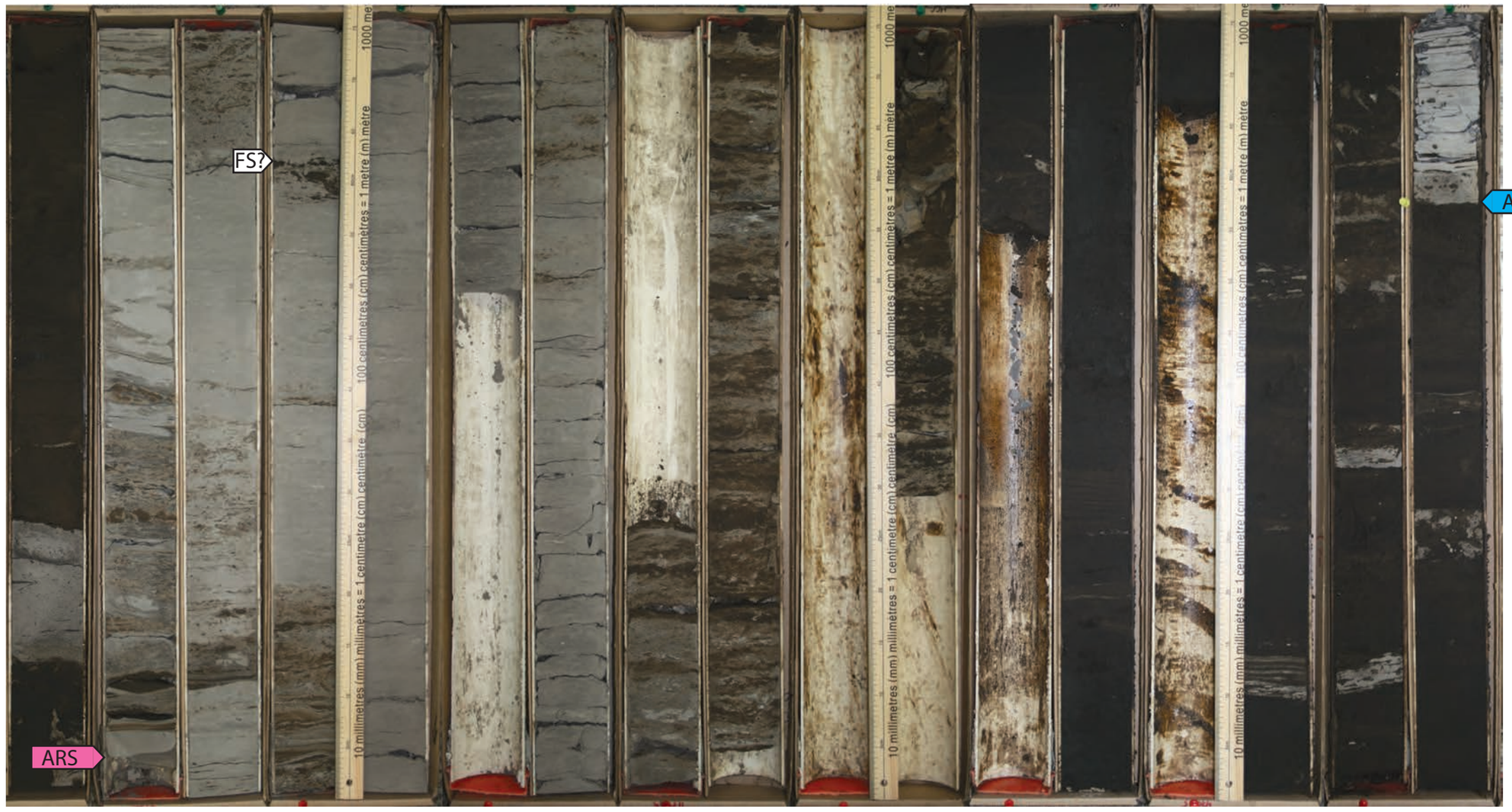

Down Hole ↓

Core: 25 Box: 2 Depth: 478.1m

Figure 3.25 - Stitched core photograph displaying FA2, showing the distal to proximal transition of a sheltered shoreface/bay-margin. Well: 1AA/05-08-076-11W4. ARS (allogenic ravinement surface), FS (flooding surface (autogenic)).

3.4 Facies Association 3 – Brackish-Water Channels

3.4.1 Description

Facies Association 3 overlies a sharp basal contact and consists of rippled and cross bedded sandstone (F5) that transitions to bioturbated interbedded sandstone and mudstone (F6), and passes into bioturbated mudstone with thin sand beds and laminae (F7). This vertical stack of facies forms a fining upwards succession.

A complete succession begins with a sharp basal contact overlain by lower medium- to upper fine-grained cross-bedded sand (F6), locally with sub-rounded to angular mud intra-clasts. This interval has a much lower gamma-ray API than any of the other facies in the study; typically less than 45 API, unless mud clasts are present. Overlying the basal interval of cross-bedded sand is upper fine- to lower fine-grained sand with migrating current ripples cut by low angle oscillation. Flaser bedding and carbonaceous debris may be present locally. Sand beds thicknesses range from cm- to dm-scale, with intercalated mm-scale mud laminae. BI values are low and range from 0-2, with suites characterized by diminutive trace fossils. The most common trace fossil is *Cylindrichnus,* with subordinate occurrences of *Skolithos* and *Planolites*. Stratigraphically upwards, mud beds become more common and thicker (from mm- to cm- with some dm-scale layers, F6). Thicker (>10 cm) mud beds may dip in the same direction and have consistent shallow inclinations. The thinner mud beds (<10 cm) and mud laminae can be flat lying or undulatory, but do not show consistent dip angles or directions. This interval commonly consists of bioturbated, potentially inclined, interbedded sandstone and mudstone beds. Sedimentary structures, where not obscured by bioturbation, consist of lenticular to flaser bedding, with oscillation ripples, current ripples, reactivation surfaces, double mud drapes, and rare syneresis cracks. BI values range from 2-4, with diminutive trace fossils. The most common trace fossils are *Planolites, Cylindrichnus, Skolithos,* and *Gyrolithes,* with subordinate occurrences of *Palaeophycus* and *Teichichnus.* Stratigraphically upwards, FA3 is dominated by bioturbated sandy mudstone, where bioturbation overprints virtually all primary sedimentary structures (F7). Remnant lenticular bedding can be distinguished in areas of less intense bioturbation. BI values range from 3-5, with suites of diminutive trace fossils. The most common trace fossils are *Planolites, Cylindrichnus, Skolithos,* and *Gyrolithes,* with subordinate occurrences of *Palaeophycus, Teichichnus*, and rootlets. Although rare, FA3 may have mudstone with

abundant coalified fragments with rootlets and soft-sediment deformation capping the succession. Facies Association 3 is mud-dominated at the top and commonly displays a upper contact with the mud-dominated portion of overlying facies associations, typically FA2.

3.4.2 Interpretations

Two interpretations for FA3 are presented herein. One interpretation considers Facies Association 3 to reflect tidal channel deposits. A tidal channel is a channel formed by bidirectional tidal flow that acts as a conduit for the tidal wave to propagate, commonly within a tidally dominated coastal landscape (Hughes, 2012). An alternative interpretation, suggests that FA3 is the deposit of tidal-fluvial channels. Tidal-fluvial channels are channels that show a transition from a fluvial dominated, sustained freshwater zone, through a mixed tidal-fluvial energy zone of fresh to brackish-water, to a tide-dominated, sustained brackish-water zone (La Croix et al., 2015).

3.4.3 Interpretations: Tidal Channels

Sharp erosive basal contacts are interpreted to represent subaqueous flow conditions capable of removing the underlying sediment. Angular mud clasts are interpreted to represent erosion of cohesive beds by high-flow energy, where clasts have not been transported long distances and are buried rapidly (Smith, 1972). Cross-bedded sands are interpreted to record high-energy flow in one direction. Migrating current ripples scoured by low-angle undulatory structures are interpreted to be the result of unequal flow energies.

The transition from rippled and cross-bedded sandstone (F5) to bioturbated wavy interbedded sandstone and mudstone (F6) is interpreted to represent the transition from subtidal to lower intertidal positions (Terwindt, 1988). The heterolithic interbedding of sand and mud in Facies 6 results from variations in flow energies. These variations are interpreted to be the result of variations in tidal energies. Thin draping mud laminae and beds are interpreted to be deposited due to suspension sediment settling. Therefore,

these beds are interpreted to be deposited during slack water periods. Thin couplets of mud drapes are interpreted as double mud drapes deposited in a semidiurnal tidal environment (e.g., Visser, 1980; Mackay and Dalrymple, 2011). Syneresis cracks are interpreted to occur due to salinity differences (Burst, 1965). Mud beds with consistent dip angles and directions are interpreted as IHS. The trace fossil assemblages in FA3 indicates a stressed marine setting (MacEachern and Gingras, 2007). The stressed trace fossil assemblage along with the sedimentary structures indicates that the environment of deposition is likely a brackish-water intertidal setting (Howard et al., 1975; Barwis, 1978; see MacEachern and Gingras, 2007 for a review).

The transition from bioturbated wavy interbedded sandstone and mudstone (F6) to bioturbated mudstone with thin sand beds and laminae (F7) is interpreted to represent a lower intertidal to upper intertidal setting on the lateral accretion deposits. Due to the dominance of mud and pervasive bioturbation, Facies 7 is interpreted to be a lower energy environment with slower depositional rates, which was more suitable for infaunal colonization. Carbonaceous mudstone (F8), though not commonly encountered in FA3, locally caps the succession. F8 is interpreted to have formed in a supratidal setting. Surpratidal settings generally have a low preservation potential (Terwindt, 1988), which may explain F8's scare occurrence in the succession.

Facies Association 3 is interpreted to record tidal channels accumulation. Sharp erosive basal contacts with coarser sediment at the base and concave upwards morphology are common features of any type channel, including tidal channels (e.g., Fenies and Faugeres, 1998; Ginsberg and Perillo, 2004; Santos and Rossetti, 2006; Brivio et al., 2016). Angular mud clasts are commonly seen in the subtidal portion of tidal channels (e.g., Barwis, 1978; Terwindt 1988; Fenies and Faugeres, 1998; Hughes, 2011; Brivio et al., 2016). Shell lags also commonly occur in tidal channels (Barwis, 1978; Terwindt 1988; Fenies and Faugeres, 1998; Rieu et al, 2005); however, shell lags are not diagnostic (Santos and Rossetti, 2006). Cross-bed foresets oriented in the same direction are a common occurrence in modern tidal channels, and is attributed to unequal ebb and flood energies (Barwis, 1978; Fenies and Faugeres, 1998; Hughes, 2012). Herringbone cross-stratification was not observed in F6. However, this is also uncommon in tidal channels as it is often not preserved, nor is it necessarily indicative of a tidal environment (Alam et al., 1985; Terwindt, 1988).

Current ripples scoured by low-angle undulatory structures are interpreted as tidal bedsets with uneven energies. The occurrence of unidirectional cross beds overlain by current ripples scoured by low-angle undulatory surfaces, has been found in the lower portions of tidal channel attached bars characterized by uneven ebb and flood energies (Barwis, 1978). Since core and related wireline logs used in this study were not oriented, ebb or flood dominance cannot be determined.

Further, slack water mud is commonly not found in the subtidal portions of tidal channels (Barwis, 1978; Fenies and Faugeres, 1998, Brivio et al., 2016). This is due to the relatively high energies that occur in the subtidal portion of tidal channels, which prevent mud from being deposited and/or erodes those slack water muds that were deposited (Brivio et al., 2016).

Inclined heterolithic stratification is commonly associated with the lateral accretion of tidal channels (Dalrymple et al., 1992; Rieu et al. 2005; Santos and Rossetti, 2006; Pearson and Gingras, 2006; Dalrymple and Choi, 2007, Brivio et al, 2016). Tidal channels are typically preserved as lateral accretion deposits if there is channel migration (Dalrymple et al., 1992). For lateral deposition, there must be sufficiently high energies to erode the banks of the channel and sufficient supply of sediment for deposition. Syneresis cracks are also found in tidal channels (Reineck and Singh, 1980). Freshwater water input is interpreted to be minimal and thought to come from small streams or episodic rainfall events.

Tidal channels can occur at a range of scales from single, large deep channels to small marsh creeks (Horton, 1945; Cleveringa and Oost, 1999; Hughes, 2012). Both wide-deep and thin-narrow tidal channels are observed in the GPV. Tidal channels act as conduits for the tidal bulge to propagate, with larger deep tidal channels experiencing higher velocities (~1m/s) compared to smaller salt marsh creeks (~0.1 – 0.6m/s; Ashley and Zeff 1988; Hughes et al. 2009; Hughes, 2012). Tidal channel initiation and evolution have both a vertical and horizontal component. Channels deepen through erosion, compaction, or due to relative sea level rise (Hughes, 2012). Channels shift horizontally through channel migration. Tidal channels widen through headward erosion and bank erosion (Hughes, 2012).

Preservation of tidal channels occurs vertically through infilling or laterally through accretion (Hughes, 2012). Upward fining in tidal channels results from reduced flow energies owing to depositional infill and lateral accretion (Hughes, 2012). Tidal channel widths change as the tidal prism changes; when the tidal prism increases, the width of the tidal channel increases, and as the tidal prism decreases the channel partially fills to reduce its width (Rieu et al., 2005).

Bioturbation is common in the intertidal portions of tidal channels (Pearson and Gingras, 2006). The trace fossils observed in the GPV generally comprise a low-diversity suite of traces, consisting of an impoverished marine assemblage (Beynon et al., 1988; Barnes, 1989; cf. MacEachern and Gingras, 2007 for a review). Trace fossil suites contain elements of both the *Cruziana* and *Skolithos* ichnofacies, with more simple morphologies reflecting generalized feeding strategies (Beynon et al., 1988; Ranger and Pemberton, 1992). Trace fossils in FA3 are facies-crossing forms, meaning that the traces are commonly found in deposits of varying environmental conditions. Trace fossils in FA3 are diminutive compared to their fully marine counterparts due to various physico-chemical stresses acting within the environment (dominantly subaerial exposure, salinity, flow velocity, and sedimentation rates). Bioturbation intensities seen in FA3 increase upwards from BI 0 to 5. This is interpreted as representing a decrease in hydraulic energy and sediment reworking upwards (Gingras et al., 2012). Trace-fossil diversity also increases upwards, but remains low compared to fully marine environments. In the upper portion of FA3, bioturbation intensities are high (up to BI 5), but trace fossil diversities remain low compared to fully marine assemblages. This is interpreted to represent conditions that were tolerable only for opportunistic trace makers (Pemberton et al., 1982, Beynon et al., 1988). Traces are observed subtending from mud beds in FA3. This is interpreted to be the result of trace-makers preferring the lower energy conditions associated with the organic-rich muds (Gingras et al., 2012). The sands within the upper portion of FA3 are also bioturbated.

No features related to tidal inlet systems were observed (i.e., barrier islands, spits, or tidal deltas). Overall, tidal channels typically contain thick subtidal sand with unidirectional cross-bedding that transitions upwards to IHS, which increases in mud content (Figs. 3.26, 3.27; Barwis 1978; Fenies and Faugeres, 1998; Hughes, 2011; Brivio et al., 2016). Bioturbation intensities increase upwards in tidal channels, but

maintain a low-diversity stressed assemblage (Figs. 3.26, 3.27; Barwis 1978; Terwindt, 1988, Fenies and Faugeres, 1998; Hughes, 2011; Brivio et al., 2016).

3.4.4 Alternate Interpretation: Tidal-Fluvial Channels

Sharp erosive basal contacts are interpreted to represent subaqueous flow conditions capable of removing underlying sediment. Angular mud rip-up clasts are interpreted to represent erosion of cohesive beds by high flow energy, where in clasts have not been transported far and were buried rapidly (Smith, 1972; Thomas et al., 1987). Cross-bedded sands are interpreted to be the result of high energy quasi-steady flow. Current ripples bounded by low-angle undulatory scour surfaces are interpreted to be the result of unequal flow resulting from unequal tidal/fluvial energies.

The transition from Facies 5 to Facies 6 is interpreted to represent the transition from subtidal to lower intertidal positions (Terwindt, 1988). The heterolithic interbedding of sand and mud in Facies 6 results from variations in flow energies. These variations are interpreted to be the result of variations in tidal/or and seasonal flow (e.g., Sisulak and Dashtgard, 2012; Johnson and Dashtgard, 2014). Thin mud laminae and beds are interpreted to be deposited due to suspended sediment settling during slack water periods. Thin couplets of mud drapes are interpreted as double mud drapes deposited in a semidiurnal subtidal environment (e.g., Visser, 1980; Mackay and Dalrymple, 2011). Syneresis cracks are interpreted to occur due to salinity variations (Burst, 1965). Mud beds with consistent dip degree and direction are interpreted as IHS. The trace fossil assemblages in FA3 indicates a stressed marine setting (cf. MacEachern and Gingras, 2007 for a review). The stressed trace fossil suite along with the sedimentary structures indicates that the environment of deposition is likely a brackish-water tidal settings (e.g., Barwis, 1978; Beynon et al., 1988; Gingras et al., 1999; MacEachern and Gingras, 2007; La Croix and Dashtgard, 2015; La Croix et al., 2015).

FA3 can be interpreted to represent deposition associated with tidal-fluvial channels. Tidal-fluvial channels commonly have erosional bases absent of shells and may contain mud rip-up clasts (Smith, 1988). Heterolithic bedding is interpreted to be due to energy fluctuations from both tidal and fluvial sources, related to neap-spring

cyclicity and variations in seasonal variations, respectively (Smith, 1988; Sisulak and Dashtgard 2012).

Trace fossils in FA3 are facies-crossing forms, meaning that the traces can be found in deposits associated with a wide range of environmental conditions. Trace fossils in FA3 are diminutive compared to their fully marine counterparts, owing to various physico-chemical stresses acting within the environment (e.g., salinity, periods of subaerial exposure, elevated flow velocities, sediment grain size, and sedimentation rates). Bioturbation intensities seen in FA3 increase upwards from BI 0 to 5. This is interpreted to result from a decrease in hydraulic energy and sediment reworking upwards (Gingras et al., 2012). Trace-fossil diversity also increases upwards, but remains low compared to fully marine deposits. In the upper portion of FA3, bioturbation intensities are high (up to BI 5), through trace fossil diversities remain low. This is interpreted to represent conditions that are tolerable only for opportunistic trace makers (e.g., Pemberton et al., 1982, Beynon et al., 1988). Traces are observed to subtend from mud beds in FA3. This is interpreted to be the result of trace makers preferring lower energy conditions and organic-rich muds (Gingras et al., 2012). The sands within the upper portion of FA3 are also bioturbated. As salinity decreases in a tidal-fluvial channel, so does trace diversity and density, with the freshwater zone containing the lowest BI values and highest degree of trace diminution (La Croix et al., 2015).

There is an overall fining-upward trend from sand-dominated facies, through heterolithic, and into mud dominated successions, a characteristic common to many tidal-fluvial channels (Smith, 1988). Bioturbation intensity increases upwards in tidal-fluvial channels (Smith, 1988). The degree of fluvial input is not well understood. Large continental drainage channels, as described in Benyon et al. (2014) and Blum and Pecha (2014), do not occur in the GPV, but occur further west within the main fairway.

The vertical succession and features of tidal-fluvial channels and tidal channels are similar (i.e., fining upwards, BI increasing upward, IHS, sharp erosional base, mud rip up clasts). The main difference of this alternate interpretation is the evidence of significant fluvial-sediment input into the system. Tidal-fluvial channels often show more sporadic distribution in bioturbation as sand beds related to annual freshet are often less bioturbated than base flow mud beds (Sisulak and Dashtgard, 2012). Tidal-fluvial channels express a landward to seaward transition, from fresh unidirectional flow,

through mixed energy, to brackish-water bidirectional (tidal) flow (Dashtgard et al., 2012). This would be best investigated by comparing and contrasting the features seen in core along the extent of the mapped channel deposits. Described cores were picked over the entire northern portion of the GPV and not selectively chosen to occur in channel deposits, therefore any upstream-downstream trends fall beyond the resolution of this study.

Well: 1AA/09-36-074-12W4

Core: 6 Box: 2 Depth: 471.1m

Core:10 Box:4, Depth: 502.6m

Figure 3.26 - Stitched core photograph displaying FA3 (brackish-water channel). Well: 1AA/09-36-074-12W4. 31.5 m of core displayed. ESS (erosional scour surface), ARS (allogenic ravinement surface).

Well: 1AA/09-36-074-12W4

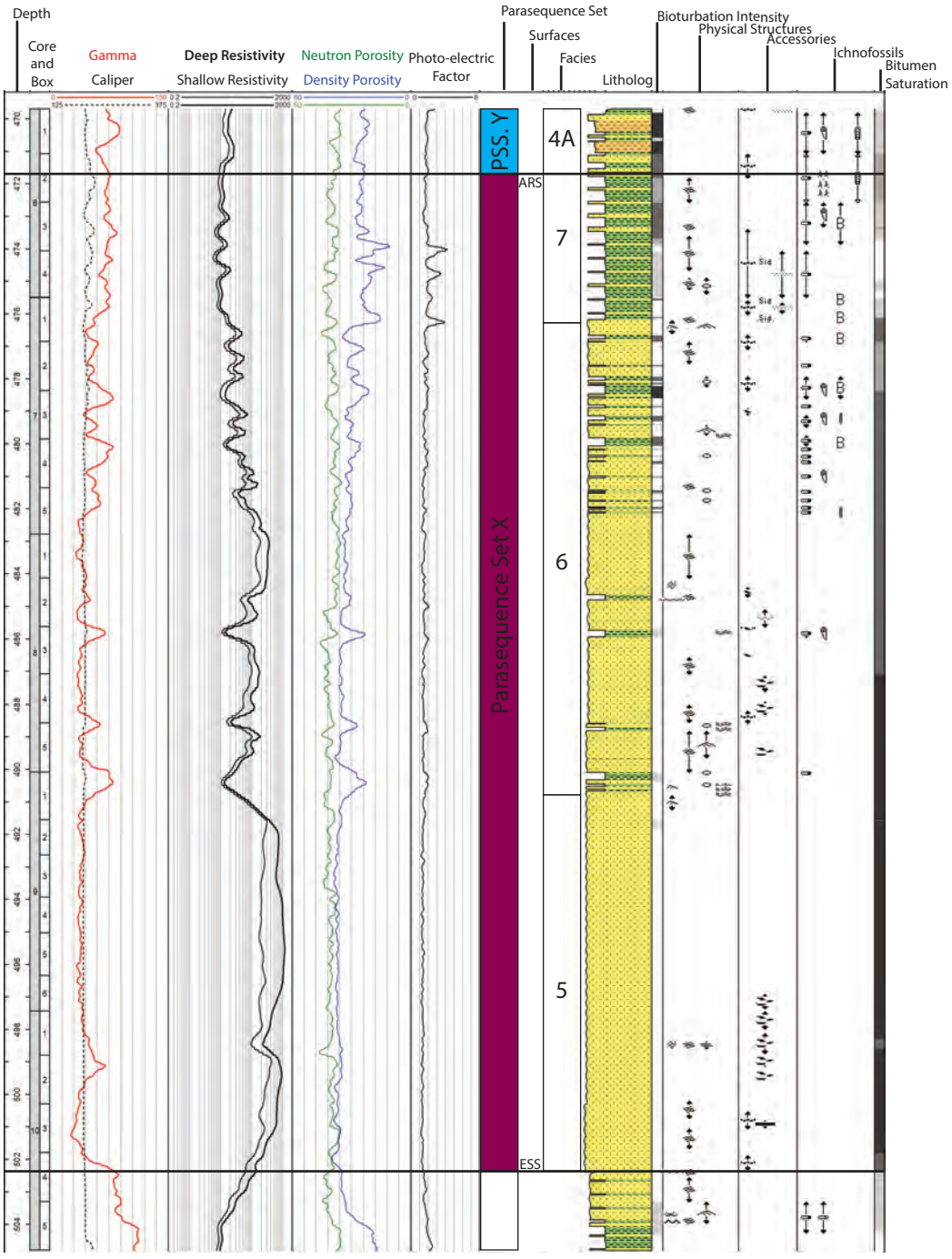

Figure 3.27 - Core description and wireline logs of the core in Figure 3.26 displaying FA3 – brackish-water channel. Well: 1AA/09-36-074-12W4. Note the gradually fining/ mudding/ high API deflection of the gamma-ray log. ESS (erosional scour surface), ARS (allogenic ravinement surface), MFS (maximum flooding surface).

3.5 Facies Association 4 - Marine Lower Shoreface to Upper Offshore

3.5.1 Description

Facies Association 4 (FA4) consists of bioturbated glauconitic silty to mudy sandstone (F9) overlain by bioturbated muddy siltstone with sand laminae (F10). Facies Association 4 displays an overall fining-upwards succession with rare, small coarsening upwards intervals. A complete succession begins with a sharp basal contact dominated by bioturbated, glauconitic silty to muddy sandstone of Facies 9. Grain sizes range from upper fine to lower very fine. Bioturbation overprints almost all primary sedimentary structures and bedding. BI values range from 4-6, and ichnological suites consists of robust and diverse traces. The most common trace fossils are *Diplocraterion, Teichichnus, Thalassinoides, Asterosoma, Planolites, Palaeophycus, Skolithos, Chondrites* and *Phycosiphon,* with subordinate occurrences of *Cylindrichnus, Arenicolites, Cosmorhaphe,* and *Zoophycos.* Stratigraphically upwards, there is a gradational shift to bioturbated muddy siltstone with sand laminae of Facies 10. Sand laminae consists of lower very fine-grained sand, and is commonly not bioturbated. The muddy siltstone, however, is pervasily bioturbated (BI 4-6) with a robust suite of trace fossils. The most common trace fossils are *Teichichnus, Thalassinoides, Asterosoma, Planolites, Palaeophycus, Skolithos, Chondrites, Phycosiphon,* and *Cosmorhaphe,* with subordinate occurrences of *Cylindrichnus, Arenicolites, Helminthopsis,* and *Zoophycos.* There may be layers of glauconitic sand (up to 50cm thick) within this silt dominated interval. Stratigraphically upwards, there is a sharp or gradational contact with an organic rich mudstone.

3.5.2 Interpretation

Facies Association 4 deposits are only found in the Wabiskaw Member. The glauconitic silty to muddy sandstone is commonly seen at the base of FA4; however, it is not present in all cores and across all of the study area. The Wabiskaw Mbr was not the focus of this study, so only very general descriptions and interpretations are made here. Trace fossils within FA4 are more robust and suites are more diverse than in any of the facies associations found within the McMurray Formation. The trace fossil suite is interpreted to represent marine conditions (normal marine salinities) (cf. MacEachern et

al, 2007). FA4 has a sharp contact with the underlying deposits of FA1, and large traces may subtend from FA4 into underlying McMurray deposits and are interpreted to represent an omission suite.

Intense bioturbation indicates slow sedimentation rates under ambient conditions, wherein organisms had ample time to occupy and disrupt the sediment. Thin, unbioturbated sands are interpreted to be the result of high sedimentation rates and depositional energy associated with storms. FA4 is interpreted to represent marine lower shoreface to upper offshore conditions (Fig. 3.28).

Well: 1AA/02-23-079-10W4

Core: 7 Box: 1, Depth: 398.2m

Core: 19 Box: 1, Depth: 411.9m

Figure 3.28 - Stitched core photograph displaying FA4. Well: 1AA/02-23-079-10W4. ARS (allogenic ravinement surface), MFS (maximum flooding surfaces), WAB (Wabiskaw), CLRWTR (Clearwater).

3.6 Regional Parasequence Sets of the McMurray Formation

Three regionally extensive and correlatable parasequence sets (PSS) demarcated by bounding allogenic flooding surfaces define the upper McMurray in the study area (Fig. 3.29, 3.30). In the context of this thesis 'parasequence' is defined as a prograding, coarsening-upward succession bound by autogenic flooding surfaces, often represented by an abrupt change in the gamma-ray signature. The flooding surfaces are interpreted to be transgressive ravinement surfaces or autogenic flooding surfaces, thus the parasequences possibly represent incomplete cycles. The definition of a 'parasequence' as being bound by autogenic flooding surfaces allows for widespread correlation of units across the study area, and adheres to Van Wagoner's (1995) definition that a parasequence is 'a relatively conformable succession of genetically related beds or bedsets bounded by flooding surfaces'. A parasequence can be either a regional correlatable succession bound by allogenic (regional) flooding surfaces or individual delta lobes of limited extent associated with autocyclic shifting of depocenters (Catuneanu, 2006). Consequently, breaks in the stratigraphic record are not always associated with allogenic changes, but can result also from autogenic processes (Muto et al., 2007), and hence, an autostratigraphic approach should be employed when working within the parasequence sets.

A parasequence set is defined by Van Wagoner (1995) as 'a succession of genetically related parasequences forming a distinctive stacking pattern bounded by major flooding surfaces'. Parasequence sets X, Y, and Z were differentiated by apparent changes in stacking patterns. The stratigraphically oldest parasequence set, Parasequence set X, displays a progradational set of typically 2 parasequences. Parasequence set Y displays a retrogradational set of 3-4 parasequences. The stratigraphically youngest parasequence set Z displays a progradational set of typically 2 parasequences. The facies observed in Parasequence set X and Parasequence set Y are essentially identical; however, the stacking patterns are different between each parasequence set and there is an inferred allogenic flooding surface separating each set. Additionally, the parasequences within Parasequence set X are thicker than the parasequences observed in Parasequence set Y. The facies observed in Parasequence set Z are different than those observed in Parasequence set X, even though they both have a similar stacking pattern. Parasequence set Z is separated from the underlying

Parasequence set Y by an inferred allogenic flooding surface. Problems may arise in differentiating between parasequence sets when only 1 parasequence is preserved, likely as a result of erosion or potentially as a result of amalgamation. In these instances the resolution of investigation is not detailed enough to distinguish the parasequence sets. Parasequence sets are likely to correlate to individual allogenic parasequences along strike (cf. Morshedian et al., 2012). Since the parasequences in this study are bound by transgressive ravinement surfaces or autogenic flooding surfaces versus allogenic surfaces the stacking patterns observed are not necessarily the result of base level change and therefore may not reflect shoreline shift.

These parasequence sets extend across the GPV (Fig 3.31, 3.32), but their extents across the entire McMurray Sub-Basin have not been established. The 3 PSS are referred to herein, from oldest to youngest, as X, Y, Z, and this is done to avoid adhering to previously established terminology and enables integration of this data and correlations into future studies. PSS X is equivalent to the Blue or B2 interval, PSS Y is equivalent to the Green or B1 interval, and PSS Z is equivalent to the Red or the combined A2 and A1 intervals (Table 3.2; i.e., Ranger and Pemberton, 1997; Hein et al., 2013). Autogenic surfaces are present within each parasequence set and are correlatable between nearby wells, but do not extend over the entire study area.

<table>
<tr><th colspan="4">Subdivision Nomenclature of the Upper McMurray</th></tr>
<tr><th>Carrigy, (1959)</th><th>Ranger and Pemberton, (1997)</th><th>Hein et al., (2013)</th><th>This Study</th></tr>
<tr><td rowspan="4">Upper</td><td rowspan="2">Red</td><td>A1</td><td rowspan="2">Z</td></tr>
<tr><td>A2</td></tr>
<tr><td>Green</td><td>B1</td><td>Y</td></tr>
<tr><td>Blue</td><td>B2</td><td>X</td></tr>
</table>

Table 3.2 – Subdivisions of nomenclature proposed for the upper McMurray Formation

Well: 1AA/09-16-079-10W4

Core: 1 Box: 2, Depth: 414.9m

Core: 6 Box: 6, Depth: 452.4m

Figure 3.29 - Stitched core photograph displaying the regional parasequences sets of the McMurray Formation and Wabiskaw Member. Well: 1AA/09-16-079-10W4. ARS (allogenic ravinement surface), MFS (maximum flooding surfaces), MRS (maximum regressive surface), FS (flooding surface (autogenic)), WAB (Wabiskaw Member), CLR WTR (Clearwater Formation). The magenta marker denotes PSS X, the cyan marker denotes PSS Y, the yellow marker denotes PSS Z, the grey marker denotes the Wabiskaw Member.

Well: 1AA/09-16-079-10W4

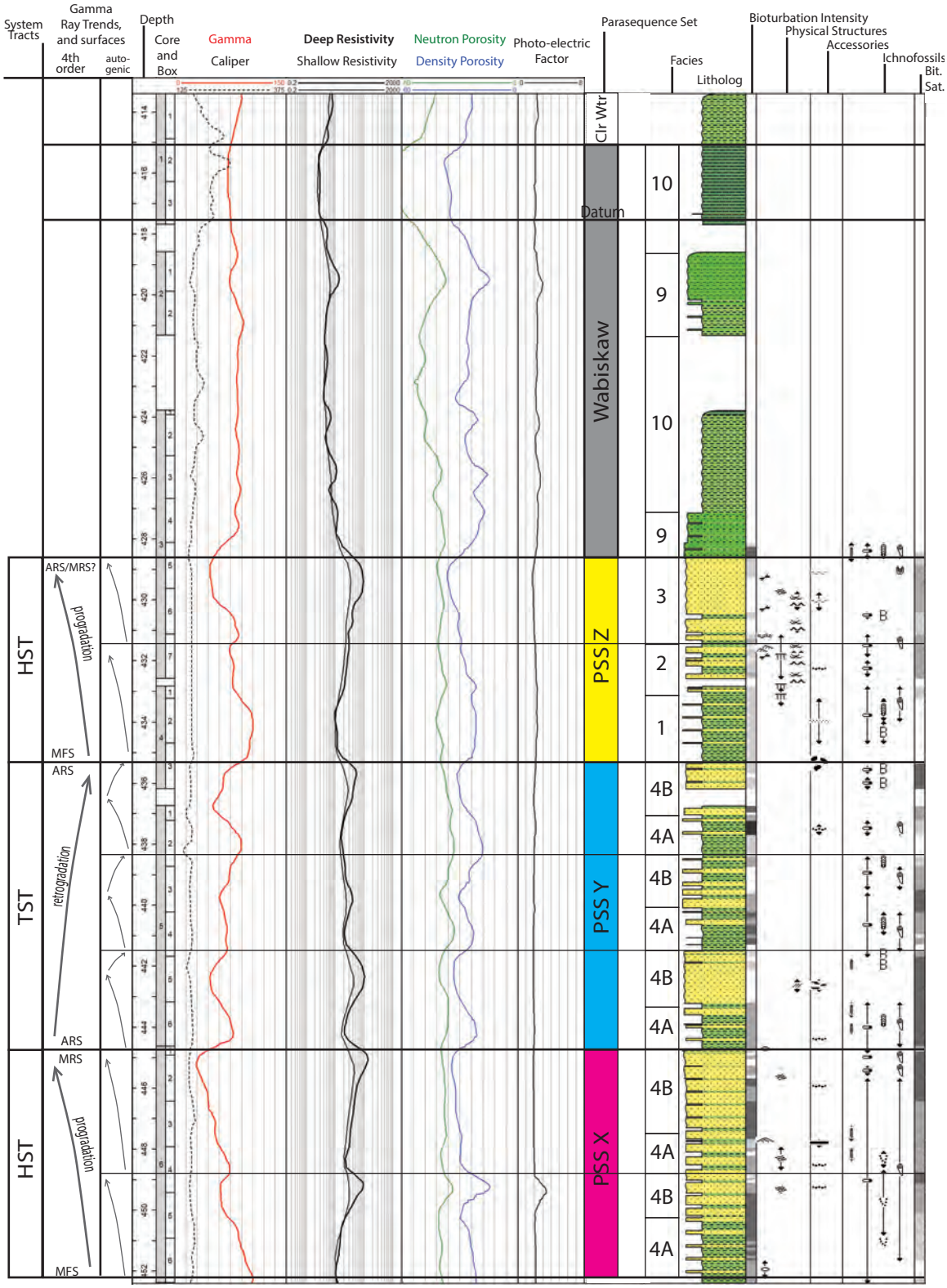

Figure 3.30 - Core description and wireline logs of the core in Figure 3.29 displaying the three parasequences sets of the upper McMurray, well: 1AA/09-16-079-10W4. The core displays the regionally extensive deposits of FA2 and FA1, which have a coarsening-upwards profile demarcated by decreasing API deflections on the gamma-ray log. Deflections are interpreted to be due to progradational regression. Separating such regressive packages are transgressive surfaces. ARS (allogenic ravinement surface), Transgressive surface (T), MFS (maximum flooding surfaces), FS (flooding surface (autogenic)), WAB (Wabiskaw Member), CLR WTR (Clearwater Formation), Bitumen saturation (Bit. Sat.).

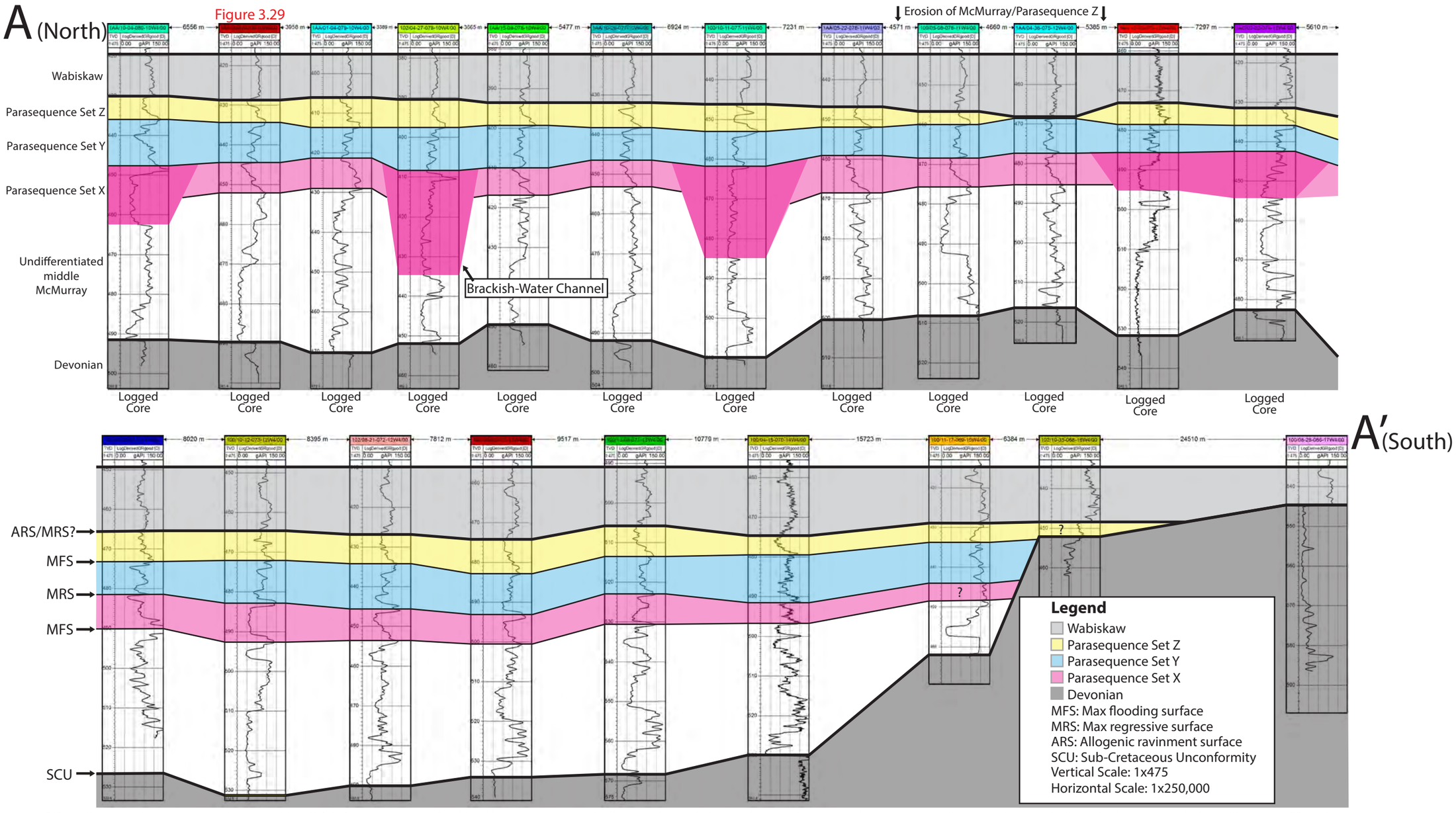

Figure 3.31 - Cross-section A- A' along the axis of the GPV. Parasequence sets of the McMurray onlap onto Grosmont High to the south. The Wabiskaw Mbr increases in thickness from north to south, then begins to thin at township 69 as it approaches the Grosmont High at the southern edge. Surfaces were picked using the full suite of available wireline logs; however, only gamma-ray log signatures are shown in this cross-section due to space limitations and for the purposes of clarity, as they clearly highlight the parasequences. See figure 1.1B for cross-section orientation.

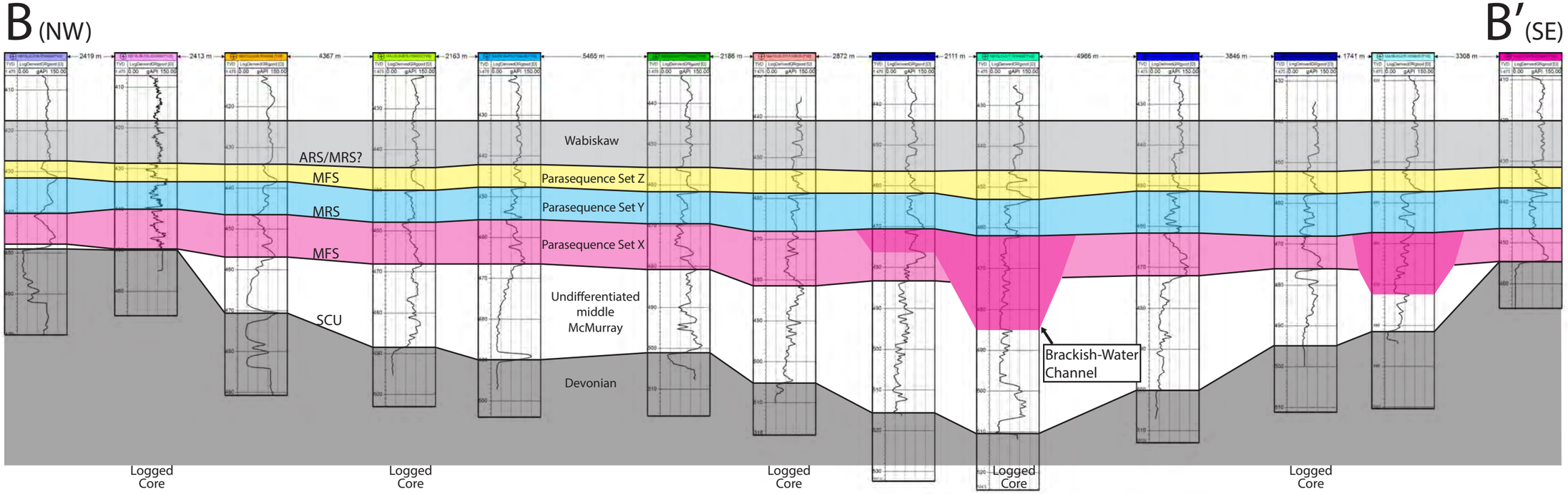

Legend

Wabiskaw | Parasequence Set Z | Parasequence Set Y | Parasequence Set X | Devonian

MRS: Max regressive surface

MFS: Max flooding surface

ARS: Allogenic Ravinement surface

SCU: Sub-Cretaceous Unconformity

Vertical Scale: 1x475

Horizontal Scale: 1x100,000

Figure 3.32 - Cross section B-B', trends perpendicular to the axis of the GPV, and displays the Devonian paleotopographic highs on either side of the valley. See Figure 1.1(B) for cross-section location.

Cross section B (Fig. 3.32) shows the relationship between the regionally extensive parasequence sets and Devonian paleotopography. The allogenic surfaces that bound these parasequence sets most likely exist because the Devonian paleotopography has a less pronounced control on upper McMurray accommodation space and deposition than it had on to older strata. Surfaces stratigraphically lower than PSS X are confined by carbonate highs within and surrounding the study area. As of yet, a functional stratigraphic scheme for the lower part of the McMurray stratigraphy in the GPV has not been proposed.

Parasequence set X is the most affected by Devonian paleotopography in the GPV compared to the other parasequence sets. It is commonly thinner or not present on carbonate highs. Parasequence set X is dominated by facies successions interpreted to record regional protected shoreface to bay-margin (FA2) with local deposits of brackish-water channels (FA3). There may be 1-2 cycles of FA2 deposits separated by autogenic flooding surfaces in a vertical succession. Stacked protected shoreface to bay-margin (FA2) deposits in PSS X have a basal muddy interval that coarsens upwards and is typically 7 to 11 m thick with an average thickness of 8.8 m (Fig. 3.33A). Individual cycles of FA2 deposits were not mapped and fall beyond the resolution of this study. Channel deposits (FA3) incise into the underlying sediment and commonly extend downward past the basal muddy interval of PSS X. Where FA3 deposits do not extend below the basal muddy interval of PSS X, FA3 deposits overly FA2 deposits. FA3 in PSS X ranges from 6 to 40 m in thickness, averaging 22.3 m thick (Fig. 3.33B). The large range in size is interpreted to reflect various scales of brackish-water channels that can exist in tide-dominated settings (Horton, 1945; Cleveringa and Oost, 1999) or be the result of well intersecting the channel axis verses the edge. Parasequence set X is capped by a ravinement/allogenic flooding surface.

Parasequence set X can be identified on gamma-ray wireline logs by two separate signatures, based on which facies association is present (FA2 or FA3). FA2 deposits have low API deflections (deflecting to the left), which are interpreted to represent progradation (Fig. 3.30). Autogenic flooding surfaces occur locally in the vertical succession of PSS X, and are represented on gamma-ray logs as higher API readings. The other wireline signature of PSS X occurs due to the presence of FA3 channels, and are represented as a rightward-deflecting (fining-upwards) gamma-ray signature (Fig. 3.27).

Parasequence set Y is similar to PSS X, in that it is dominated by protected shoreface to bay-margin (FA2) deposits with local deposits of brackish-water channels (FA3). The difference between the stacked FA2 deposits PSS X and PSS Y, is that the sanding-upward profile is less well displayed and contain more mud in PSS Y. Parasequence set Y can have 2-4 cycles of FA2 deposits in a vertical succession, separated by autogenic flooding surfaces. Protected shoreface to bay-margin (FA2) deposits within PSS Y are typically 6 to 11 m thick with an average thickness of 8.6 m (Fig. 3.33C). Brackish-water channel (FA3) deposits vary in thickness, but generally fall between 6 and 38 m and average 18.2 m thick (Fig. 3.33D). The large distribution in the thickness of FA3 deposits is interpreted to be the result of a network of channels with varying sizes or wells intersecting the channel axis verses the edge. Parasequence set Y is capped by an allogenic ravinement and flooding surface.

Observations in core of PSS Y show muddier and more distal deposits, with a greater degree of burrowing, upwards through stacked parasequences (Fig. 3.30). These stacked parasequences show a progression of more distal deposits overlying more proximal deposits and are interpreted to represent a retrogradational stacking pattern of a transgressive systems tract. To confirm this, each parasequence within PSS Y must be mapped; however, this falls beyond the resolution of this study.

The gamma-ray wireline signature of PSS Y has two different expressions due to the occurrence of FA2 and FA3 deposits. The regional correlatable deposits of FA2 have an irregular signature with no simple shape or trend, but can be best described as a small series of stacked low API-deflecting signatures or as displaying a serrated signature (Fig. 3.30). That being said, the gamma-ray signatures are consistent and recognizable in nearby wells. The irregularity in these deposits is due to the occurrence of the aforementioned autogenic flooding surfaces. The other gamma-ray signature in PSS Y is due to deposits of FA3, which display progressive rightward gamma-ray deflections.

Parasequence set Z is the most easily recognizable complex, and consists of wave-/storm-dominated deltaic deposits (FA1). There may be 1-2 cycles of FA1 deposits separated by autogenic flooding surfaces in a vertical succession. The second cycle of FA1 is a remnant of a thicker succession and is often partially or entirely eroded. No significant deposits of brackish-water channels (FA3) were observed in PSS Z in the

GPV. Stacked FA1 deposits in PSS Z normally have a thickness of 4 to 9 m with an average thickness of 6.7 m (Fig. 3.33E). The top of parasequence set Z coincides with the top of the McMurray Formation. Parasequence set Z is partially or entirely eroded in some areas (Fig. 3.30).

The gamma-ray signature of FA1 deposits in PSS Z displays a low API-deflection (Fig. 3.30). In the GPV, there is commonly one low API deflected gamma-ray signature, but a second, smaller and less prominent low API deflection may occur above it.

The top of the McMurray Formation/PSS Z is capped by a regionally extensive transgressive ravinement surface. Marine lower shoreface to upper offshore (FA4) deposits make up the entirety of the Wabiskaw Member. The succession is capped by organic-rich shales, interpreted as a condensed section. The thickness of the Wabiskaw Member is typically 9 to 18 m in the GPV, averaging 13.1 m (Fig. 3.33F).

In general, the boundary between PSS Z and the overlying Wabiskaw Member is typically placed where the gamma-ray profile no longer indicates a coarsening-upward trend (Fig 3.30). The gamma-ray signature is subtle, as that succession is dominated by silty sand (Wabiskaw Mbr) overlying sand (top of McMurray Fm) contact. A straightforward way to determine the contact is by photo-electric (PE) log. The PE log will have a slight increase in value as it passes into the Wabiskaw Mbr due to the presence of glauconitic (Fig 3.30). The datum (top of the Wabiskaw Mbr) is marked on wireline logs by a very high neutron kick and correspondingly low resistivity.

A

Thickness of FA2 deposits, Parasequence Set X

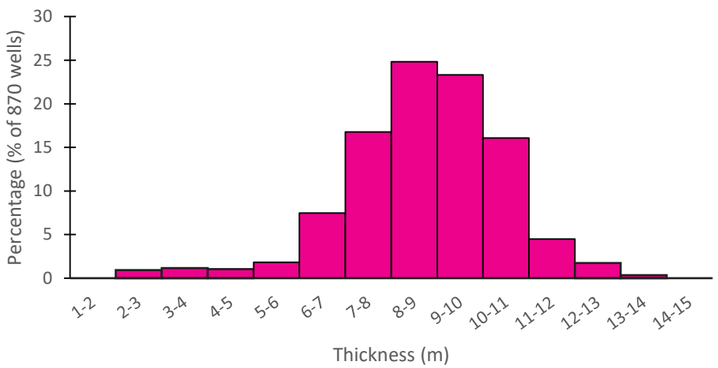

B

Thickness of FA3 deposits, Parasequence Set X

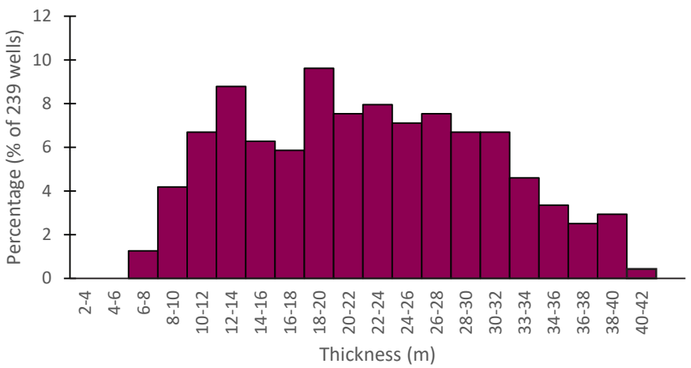

C

Thickness of FA2 deposits, Parasequence Set Y

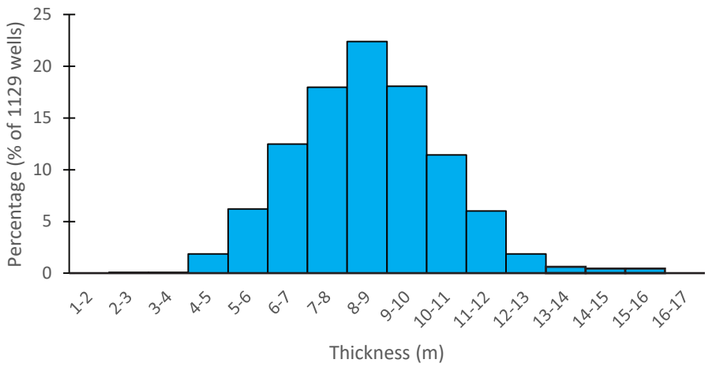

D

Thickness of FA3 deposits, Parasequence Set Y

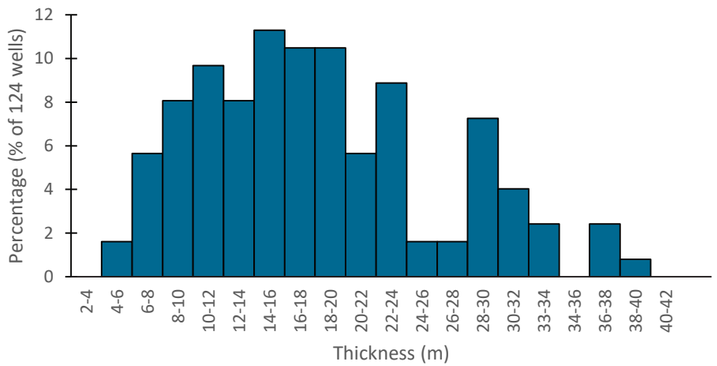

E

Thickness of FA1 deposits, Parasequence Set Z

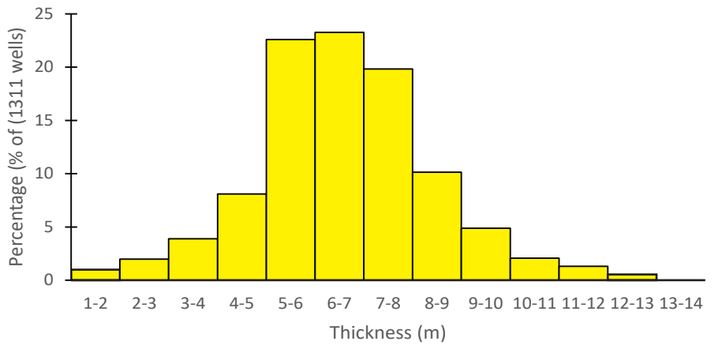

F

Thickness of FA4 deposits, Wabiskaw Member

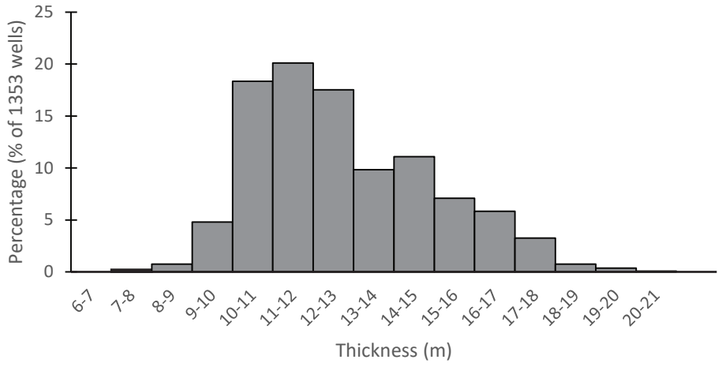

Figure 3.33 - Histogram thickness charts of facies associations for parasequence sets X, Y, Z, and the Wabiskaw Mbr.

3.7 Conclusion

Eight facies occur in the McMurray Formation and two facies occur in the Wabiskaw Member. Three facies associations occur within the regional parasequence sets of the McMurray: wave-/storm-dominated delta (FA1), sheltered shoreface to bay-margin (FA2), and brackish-water channel (FA3). Two working hypotheses of FA3 are presented, which differ mainly in their degree of fluvial input. The Wabiskaw Mbr contains marine lower shoreface to upper offshore (FA4) deposits. Three parasequence sets (X, Y, and Z) are defined. Each parasequence set is demarcated by regional flooding surfaces. Parasequence sets X and Y contain deposits of FA2 and FA3, whereas PSS Z contains deposits of FA1. Deposits of FA1 and FA2, have a fairly consistent distribution in thickness, with the majority of the intevals ranging from 5 – 11 m thick, whereas FA3 deposits show large variations. Deposits of FA4 show a greater distribution in thicknesses than FA1 and FA2, with majority of deposits ranging from 10 – 17 m thick.

4 Facies Association Morphologies and Depositional Interpretations

Parasequence sets and the facies association that occur within them have been mapped across the GPV. Depositional environments are defined, based on core and gamma-ray profiles within each parasequence set, and the depositional architecture are determined. The interpretations of each environmental setting are combined, and an overall basinward direction and coastline orientation are interpreted. The stratigraphic frameworks of Ranger and Pemberton (1997) and Hein et al. (2013) are re-evaluated with a focus on their interpretations regarding relative sea level change, valley incision and preservation, and presence of estuarine deposits. An alternative stratigraphic framework is proposed for the regional parasequence sets and the brackish-water channels in the GPV.

4.1 Mapping Geometries and Trends

Facies associations were mapped for each parasequence set. Mapping was based on correlations defined in Chapter 3, using both facies associations and gamma-ray log signatures. Due to the relatively large size of the study area and lack of high density data, internal stratigraphy of the channel deposits and positions of the autogenic surfaces were not mapped. Small-scale variations are interpreted to occur, but are below the resolution of mapping in this study.

4.1.1 Parasequence Set X

Parasequence set X contains two facies associations; regional deposits of sheltered shoreface to bay-margin deposits (FA2), and brackish-water channels (FA3). In the northern half of the study area, most of the Devonian topography was buried by previous McMurray sediments before the deposition of PSS X (Fig. 4.1). The Wiau Lake Ridge is manifested as a series of small islands along the western portion of the study area. At the southern end of the GPV, allogenic flooding surfaces that demarcate PSS X, onlap the Grosmont High (Fig. 4.1). Since FA2 deposits are regionally extensive throughout the GPV, it is suspected that these deposits also onlap the Grosmont High;

however, this is a low confidence interpretation and deposits may lap out onto the Grosmont High.

Isopach mapping of PSS X reveals only a slight thinning of protected shoreface to bay-margin (FA2) deposits towards the south. However, evidence of significant erosion or non-deposition of FA2 deposits is apparent, where brackish-water channel (FA3) deposits from PSS X or Y downcut and appear to have removed PSS X. Along the margins of the GPV, it is possible that FA2 was not deposited, owing to the influence of Devonian topography

FA3 deposition within PSS X was also affected by the Devonian topography, predominantly in the southern portion of the study area. The majority of FA3 deposits in PSS X occur in the northern half of the study area, where wide and deep successions of FA3 are found exclusively north of Township 73 (Fig. 4.2). The deeper and wider deposits of FA3 are preserved as discontinuous, linear bodies. These linear bodies of FA3 typically trend in a northwest–southeast direction. The shallower, thinner deposits of FA3 are difficult to correlate between wells, and appear to be even more disconnected than their thicker counterparts.

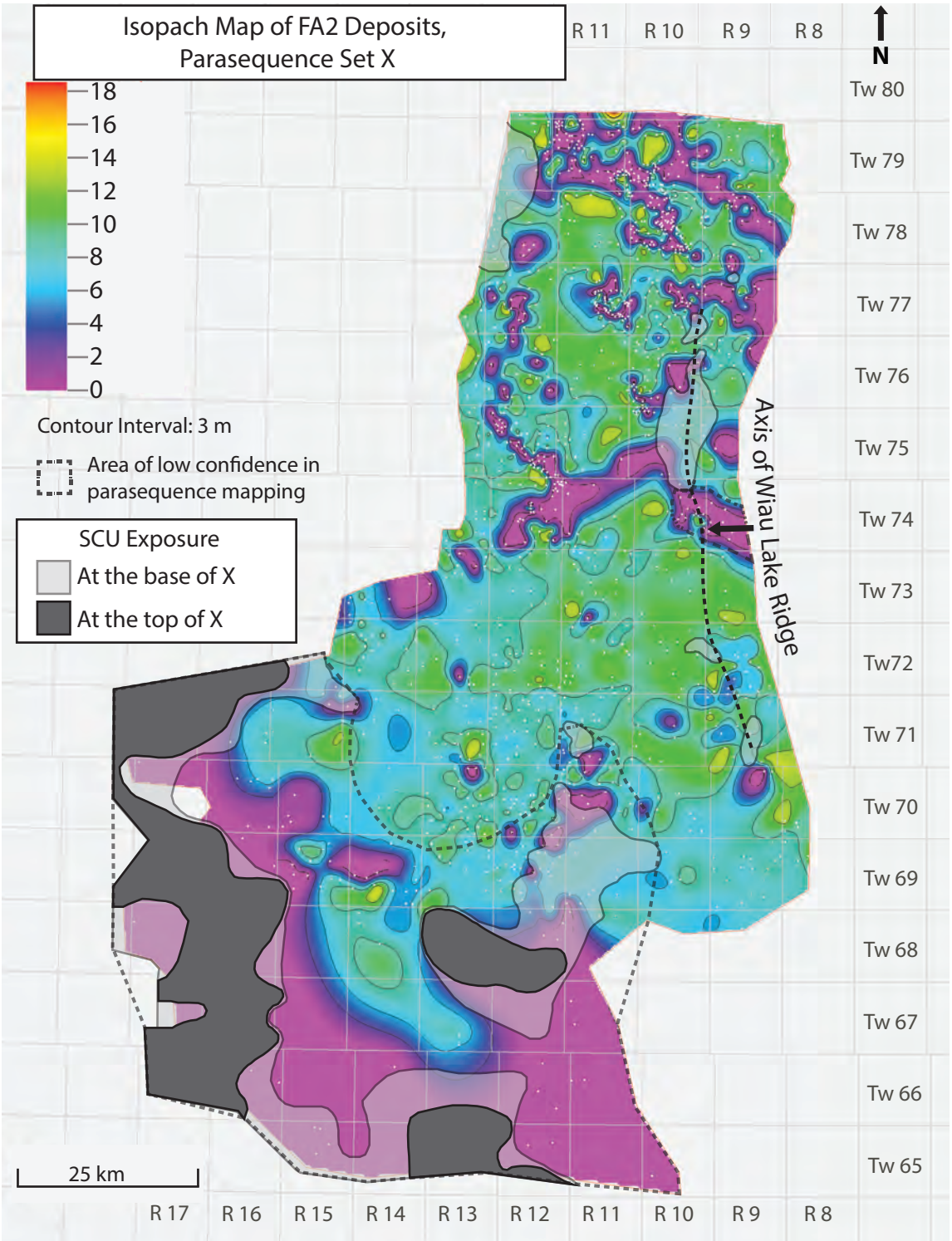

Figure 4.1 - Isopach map of FA2 deposits within PSS X. Translucent grey polygon denotes the carbonate exposure during the onset of PSS X deposition. Opaque grey polygons represent the carbonate exposure at the end of PSS X deposition. Grey dashed polygon line denotes the boundary of low confidence picks. Purple areas have zero thickness due to erosion and/or non-deposition. White dots represent well locations with suitable LAS files that were used in facies association mapping.

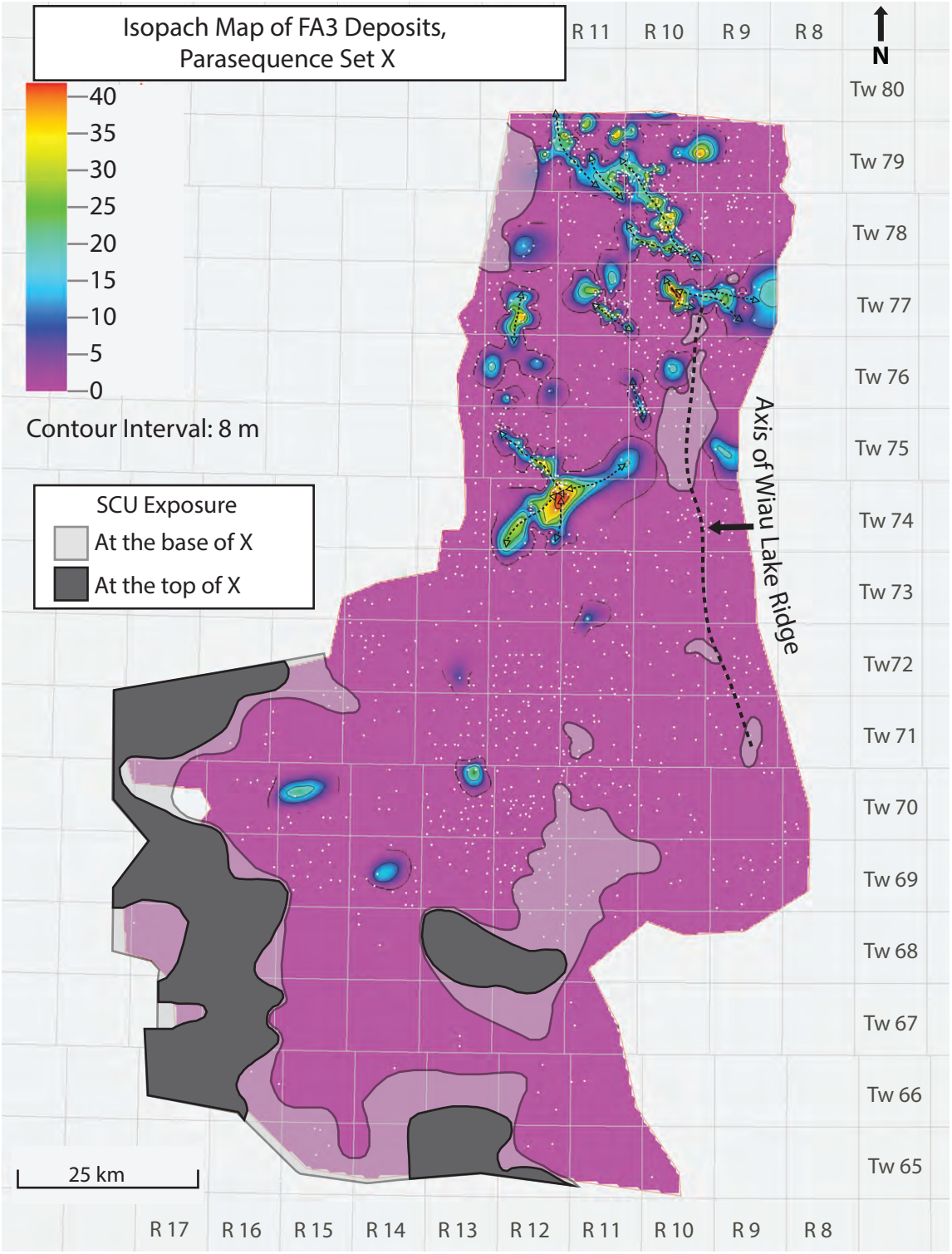

Figure 4.2 - Isopach map of FA3 deposits within PSS X. Black dashed arrows are the interpreted trends of large brackish-water channels. Translucent grey polygons denote the carbonate exposure during the onset of PSS X deposition. Opaque grey polygons represent the carbonate exposure at the end of PSS X deposition.

4.1.2 Parasequence Set Y

Parasequence set Y contains two facies associations; regional deposits of sheltered shoreface to bay-margin deposits (FA2), and brackish-water channels (FA3). The SCU is less pronounced in the south of PSS Y compared to PSS X. Since FA2 deposits are regionally extensive throughout the GPV, it is suspected that these deposits also onlap onto the Grosmont High, however this is a low confidence interpretation (Fig. 4.3). FA2 deposits may lapout onto the Grosmont High. By the onset of PSS Y deposition, the Wiau Lake Ridge was entirely covered by McMurray Fm deposits, and sedimentation was no longer confined by Devonian paleotopography in the GPV, with the exception of the southern edge. Isopach mapping of FA2 deposits in PSS Y, displays no obvious thickness trends. Areas of zero thickness of FA2 deposits are interpreted to be the result of non-depositions, or erosion due to FA3 channel deposits within PSS Y.

A single, thick deposit of FA3 is found in the northeast corner of the study area and trends northwest–southeast (Fig. 4.4). Narrow, thinner FA3 deposits of Parasequence set Y are also found throughout the study area (Fig. 4.4).

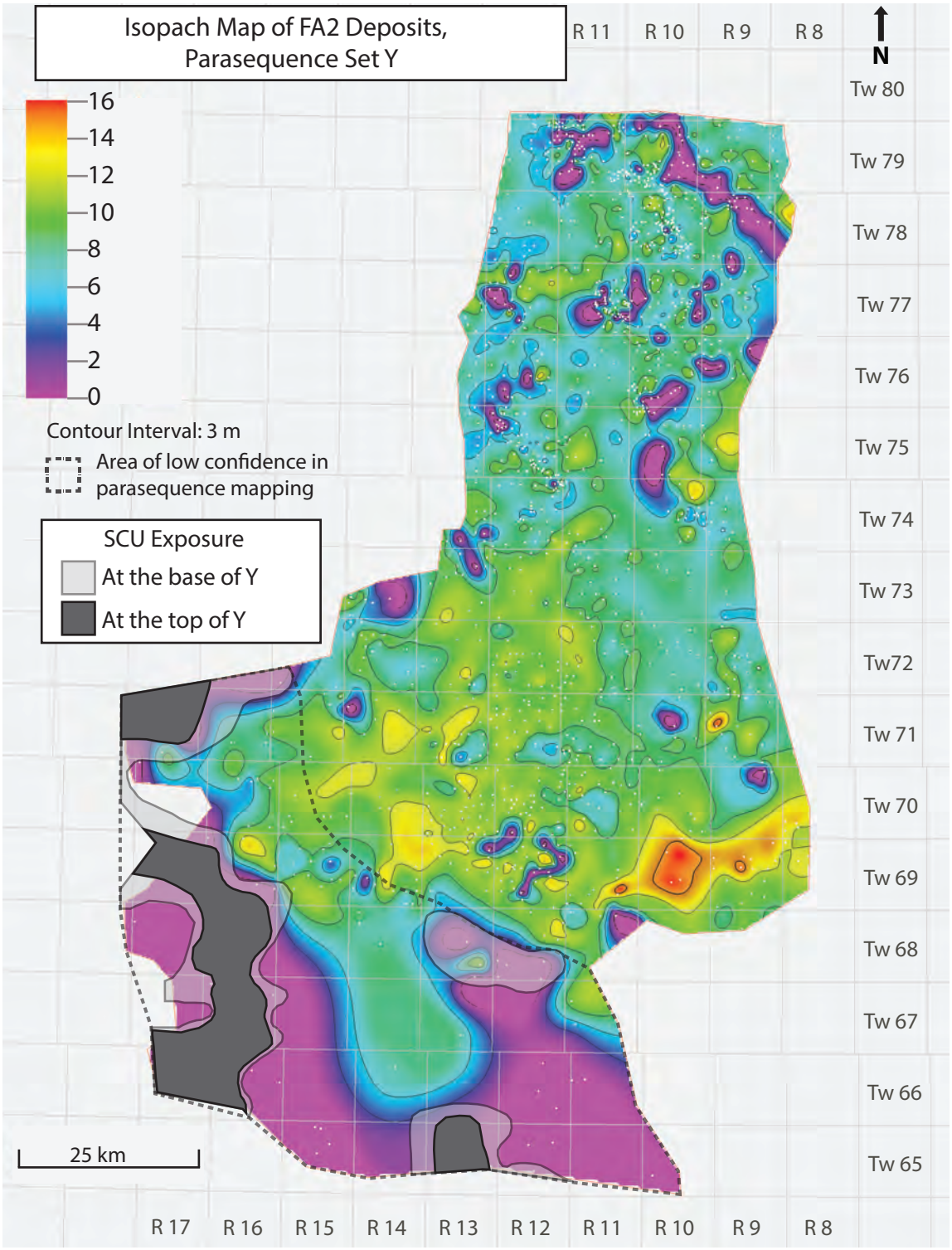

Figure 4.3 - Isopach map of FA2 deposits within PSS Y. Translucent grey polygons denote the carbonate exposure during the onset of PSS Y deposition. Opaque grey polygons represent the carbonate exposure at the end of PSS Y deposition. Grey dashed polygon line denotes the boundary of low confidence picks. Areas of purple are zero thickness due to erosion and/or non-deposition.

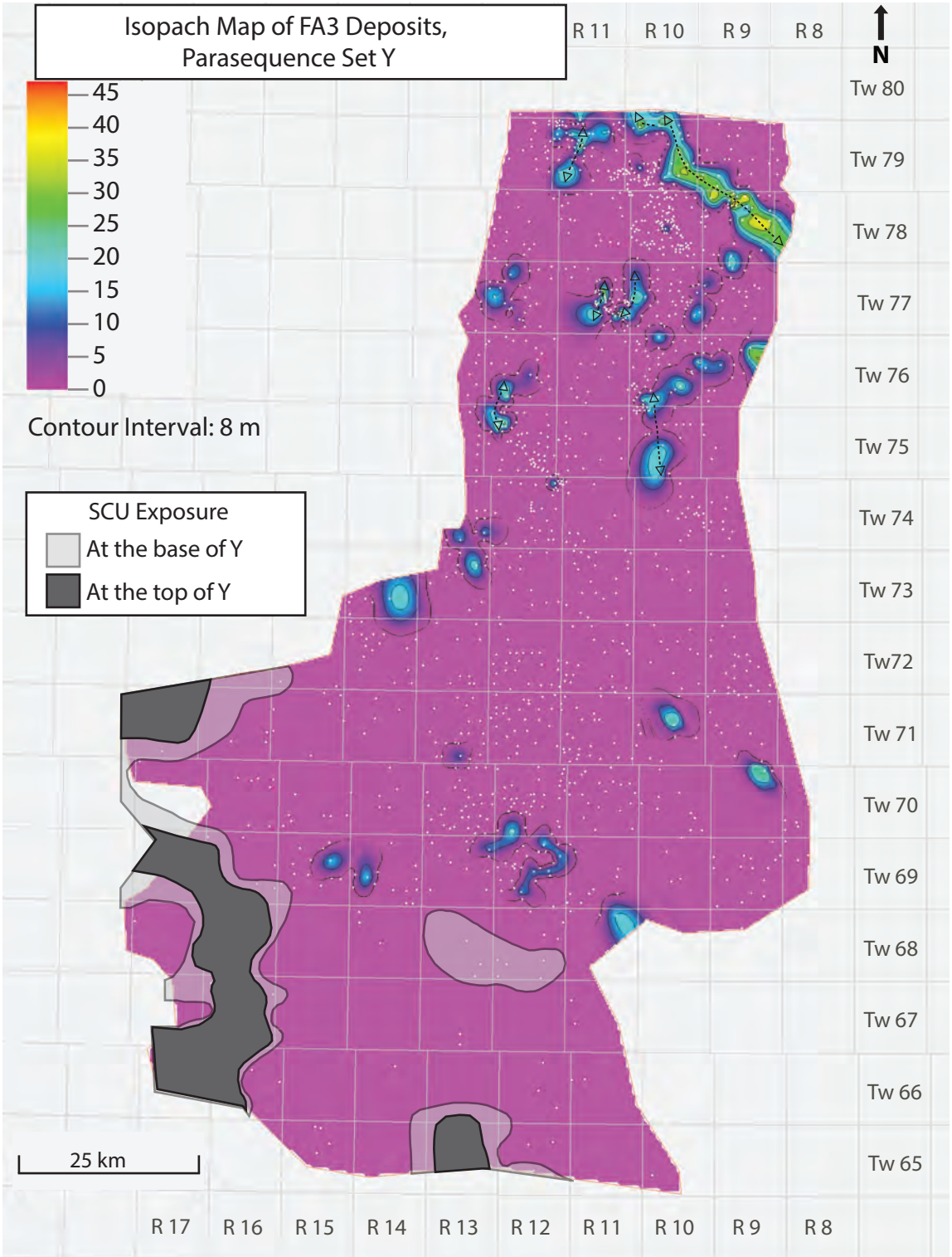

Figure 4.4 - Isopach map of FA3 deposits within PSS Y. Black dashed arrows are the interpreted trends of large brackish-water channels. Translucent grey polygons denote the carbonate exposure during the onset of PSS Y deposition. Opaque grey polygons represent the carbonate exposure at the end of PSS Y deposition.

4.1.3 Parasequence Set Z

Parasequence set Z contains deposits of FA1 (wave-/storm-dominated deltas). The SCU had little effect on deposition of PSS Z within the majority of the study area (Fig. 4.5). The only area where the SCU appears to have affected deposition is in the south, albeit to a lesser degree than its influence on underlying parasequence sets. A large area of PSS Z has a thickness of zero, interpreted to have been due to transgressive erosion associated with the Wabiskaw Member. No wide and deep deposits of FA3 were found associated with PSS Z in the study area. There are at least four long, linear thickness trends of FA1 in PSS Z (Fig. 4.5), all of which are sub-parallel to one another and trend in the southwest–northeast direction.

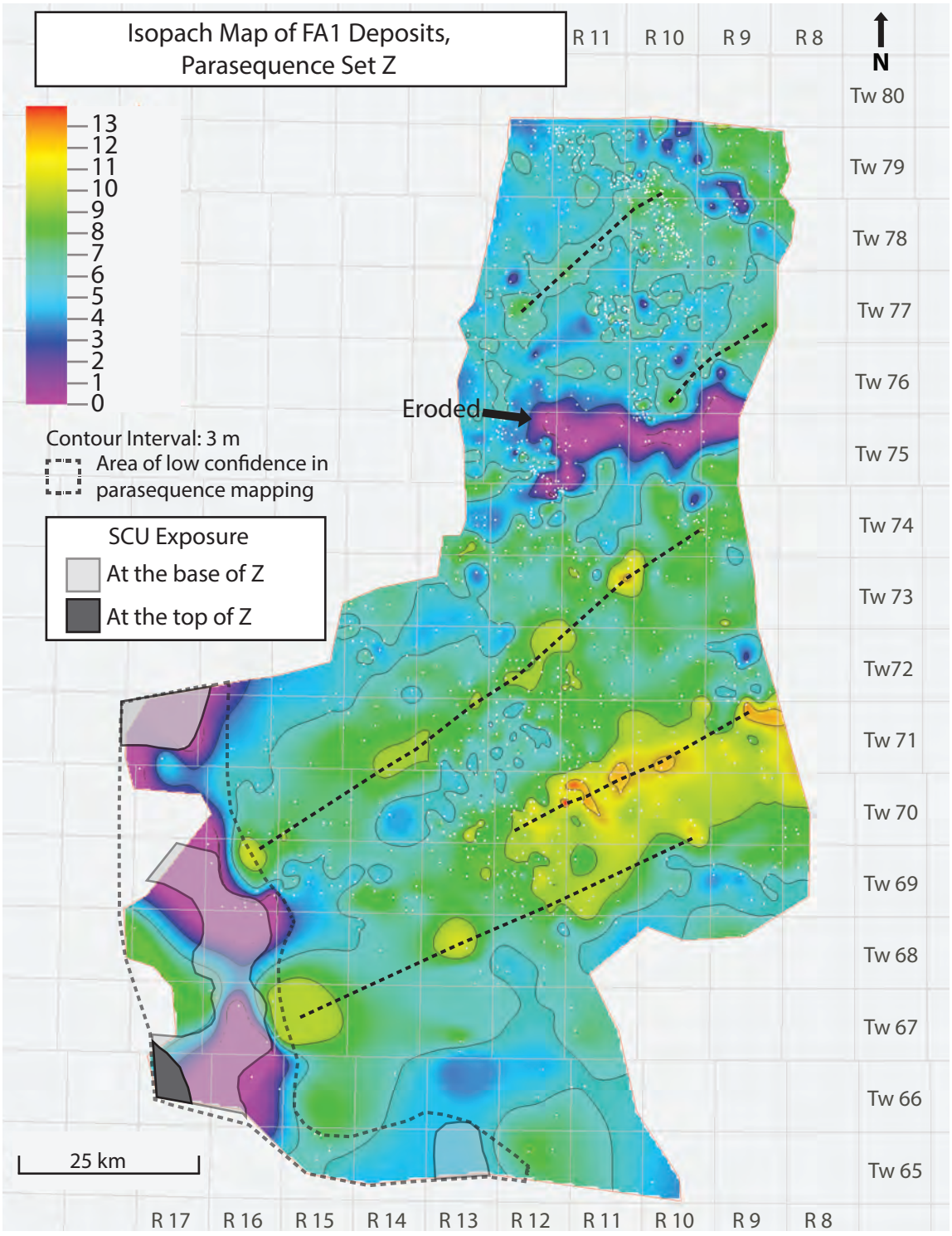

Figure 4.5 - Isopach map of FA1 deposits within PSS Z. Areas of purple are zero thickness due to erosion and/or non-deposition. Black dashed lines are thicks interpreted to represent shore parallel trends of a wave-/storm- dominated delta. Translucent grey polygons denote the carbonate exposure during the onset of PSS Z deposition. Grey dashed polygon line denotes the boundary of low confidence picks. The SCU had only a minor effect on the deposition of PSS Z and there was likely no SCU exposure following the depostion of PSS Z.

4.1.4 Wabiskaw Member

The Wabiskaw Mbr is only affected by the SCU in the south where it onlaps the Grosmont High. There are at least four prominent, sub-parallel linear thickness/thinness trends that run southwest–northeast (Fig. 4.6). The northernmost thick in Figure 4.6 is associated with the area of eroded FA1 deposits in PSS Z (Fig. 4.5).

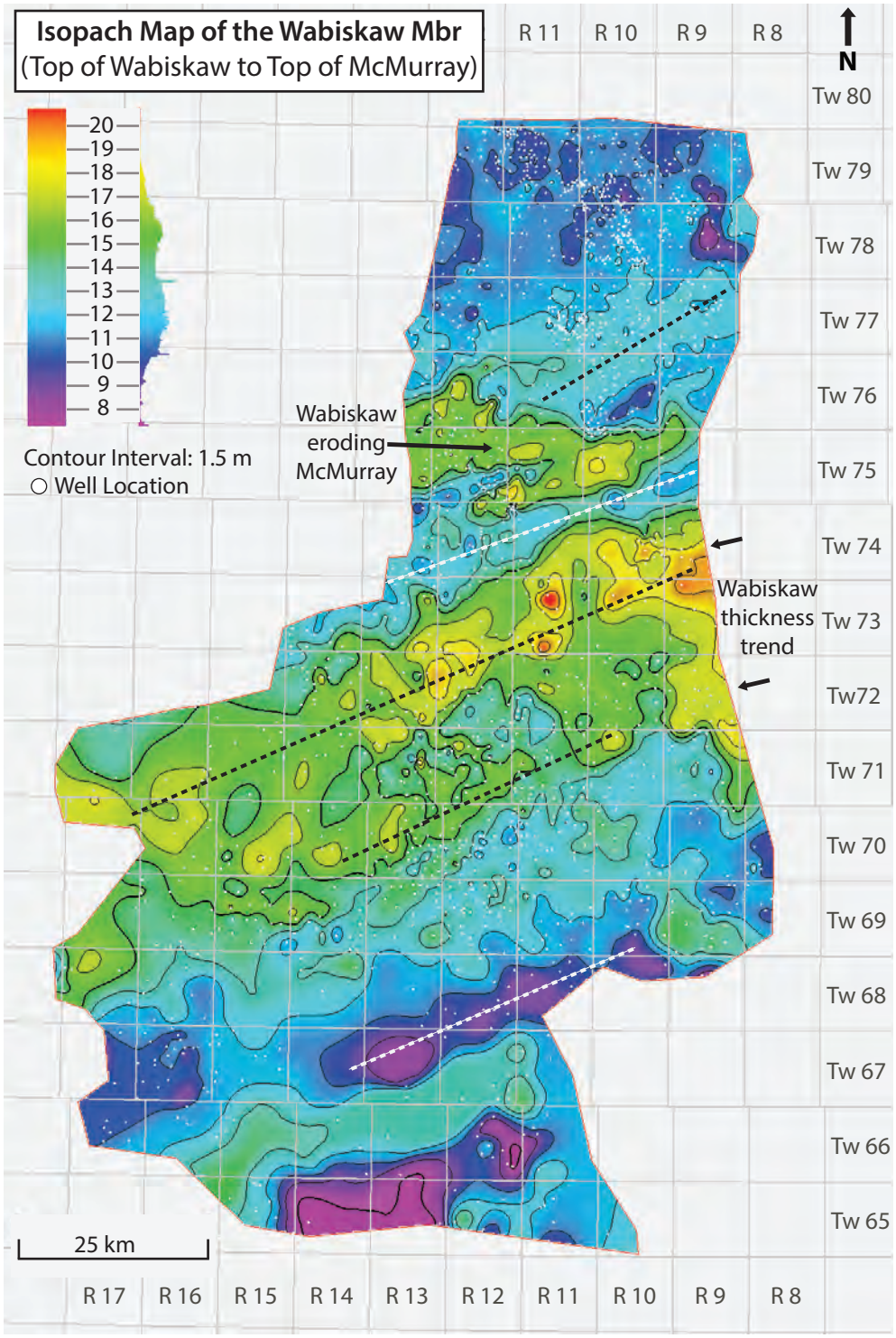

Figure 4.6 - Isopach map from the top of the Wabiskaw Member to the top of the McMurray Formation. Dashed black lines are interpreted to represent shoreline parallel ridges and white dashed lines are interpreted to represent valleys.

4.2 Interpreted Depositional Settings and Discussion

4.2.1 Parasequence Sets X and Y

Parasequence sets X and Y are similar in that they contain the same facies associations. FA2 successions in PSS X represent overall as progradational regression, whereas FA2 successions in PSS Y represent retrogradation. There are virtually no discernable trends in the distribution of FA2 deposits in either parasequence set, and no obvious features associated with tidal inlets (barrier beach ridges and ebb and flood tide deltas). Accommodation space is interpreted to have been low, suggesting that parasequences in these parasequence sets comprise shingled autogenic parasequences separated by minor flooding surfaces. The Beaverhill Lake Spur is interpreted to have sheltered the study area from strong wave energies in the north that may have been experienced elsewhere in the McMurray Sub-Basin (Fig 1.1A, Broughton and Paul, 2013). The exposed Devonian highlands may also have protected the GPV from wave activity during deposition of PSS X (Fig 4.1).

The large FA3 (brackish-water channel) deposits in both PSS X and PSS Y all trend approximately northwest–southeast. It is not uncommon for an entire parasequence set to consist of a brackish-water channels (FA3) with the upper contact terminating at the allogenic bounding surface. However, the upper contact of FA3 deposits may terminate at an autogenic flooding surface within the parasequence set (Fig 4.7, 4.8). Studies of tidal systems indicate that majority of tidal channels trend perpendicular to the coastline (Weimer et al., 1982; Rieu et al., 2005). Consequently, the orientation of the coastline during deposition of PSS X and Y was probably roughly perpendicular to the trend of the brackish-water channels, or southwest–northeast.

The large variations in brackish-water channel thicknesses in PSS X (Fig. 3.33B) and PSS Y (Fig. 3.33D) are likely due to the various scales of tidal channels that occur within a tidal drainage network (Horton, 1945; Cleveringa and Oost, 1999). Deeper channels have a higher preservation potential than do shallower channels in a transgressive setting, due to their position relative to base level (Belknap and Kraft, 1985, Oertel et al., 1991, Rieu et al., 2005). Hence, the preservation of deep FA3 deposits are more continuous than are those associated with shallower FA3 channels in the GPV (Fig. 4.2, 4.4). As well, channels that are of larger scale have a higher

likelihood of being straight (Ginsberg and Perillo, 2004; Hughes, 2012). Larger, straight tidal channels tend to occur seaward, whereas narrower and more sinuous tidal channels occur landward (Marani et al., 2002). Deep FA3 deposits are interpreted to occur near the coastline in the GPV.

Once a channel system has formed, flow and erosive forces are focused at the seaward end of the tidal channel (Hughes et al., 2009; Hughes, 2012). A small narrow channel can funnel the tidal wave, which results in hypersynchronous conditions. This leads to further erosion and further funneling, resulting in expansion of the tidal channel and higher flow velocities. The majority of tidal exchange is confined within larger channels where flow velocities can be very high, and this results in scouring and/or non-deposition (Oertel et al., 1991). The funneling of tidal water creates scouring that deepens and expands the edges of the channel outwards and produces a concave upward-morphology. These forces are responsible for the formation and down-cutting of channels. Large and deep channels are required in order to accommodate large tidal prisms. The channel systems within the study area are very large and, therefore, it is interpreted that the setting had a correspondingly pronounced tidal prism. At a certain point landward, conditions change to hyposynchronous due to friction with the channel margins. As the coastline progrades, the landward end of the tidal network correspondingly begins filling.

Tidal channels are also expressed geologically through lateral migration and accretion of bank attached bars. Tidal flow and sediment supply must be sufficiently high to erode the banks of channels and build point bars for lateral migration/accretion to take place. Rieu et al. (2005) showed, through the use of seismic reflector data from Holocene deposits, that lateral migration and channel infill can occur in tidal channels (Fig 4.9A). Brivio et al. (2016) and D'alpaos et al. (2017) show a modern example of tidal channel meander evolution and multiple cut-off events in the Venice Lagoon, Italy (Fig 4.9B).

Facies Association 3 deposits are interpreted to be tide-dominated, but may have had minor fluvial influence. The fluvial systems that occur at the time of deposition in PSS X and Y were likely small streams that drained off the carbonate highlands, particularly from the Grosmont High to the southwest.

Rieu et al. (2005), using the Zoutkamperlagg Inlet as a model, indicates that small, shallow channels would likely be removed over time while, deep channels would be preserved as isolated/discontinuous deposits in an area experiencing transgressive ravinement. Since both PSS X and Y are interpreted to have been affected by transgressive ravinement, this model provides insight as to why the brackish-water channel (FA3) deposits (especially smaller deposits) appear discontinuous.

The autogenic flooding surfaces in PSS X and Y are interpreted to be related to minor flooding events that may be related to the initiation of another progradational shingle. Parasequence sets X and Y are interpreted to represent roughly similar depositional environments; sheltered shoreface to bay-margins punctuated by brackish-water channels in a brackish-water, low-accommodation setting. Brackish-water channels are interpreted to trend perpendicular to the shoreline, and hence, the shorelines in PSS X and Y are interpreted to be oriented roughly southwest-northeast. The basinward direction for the GPV lies perpendicular to this and thus toward either the northwest or southeast. The best modern example of features described in PSS X and Y may be the tidal flats and tidal channels of the Wadden Sea/German Bight (Fig. 4.10C). However, PSS X and Y are interpreted to have had a lower gradient, so the system would have been much more extensive. Preserved Holocene tidal channels also show similar morphologies (Fig. 4.10B; Reiu et al., 2005).

Transgressive ravinement is interpreted to have occurred at the top of each parasequence set. Transgressive ravinement surfaces and related subsequent flooding surfaces are interpreted to be allogenic, as they can be identified and mapped across the study area. The parasequence sets demarcated by these surfaces can probably be tracked to the west, but the Grosmont High is likely to disrupt deposition. The allogenic surfaces are likely amalgamated or not expressed in areas well removed from the GPV (i.e.: main fairway, north of the Beaverhill Lake Spur).

Well: 1AA/10-21-079-11W4

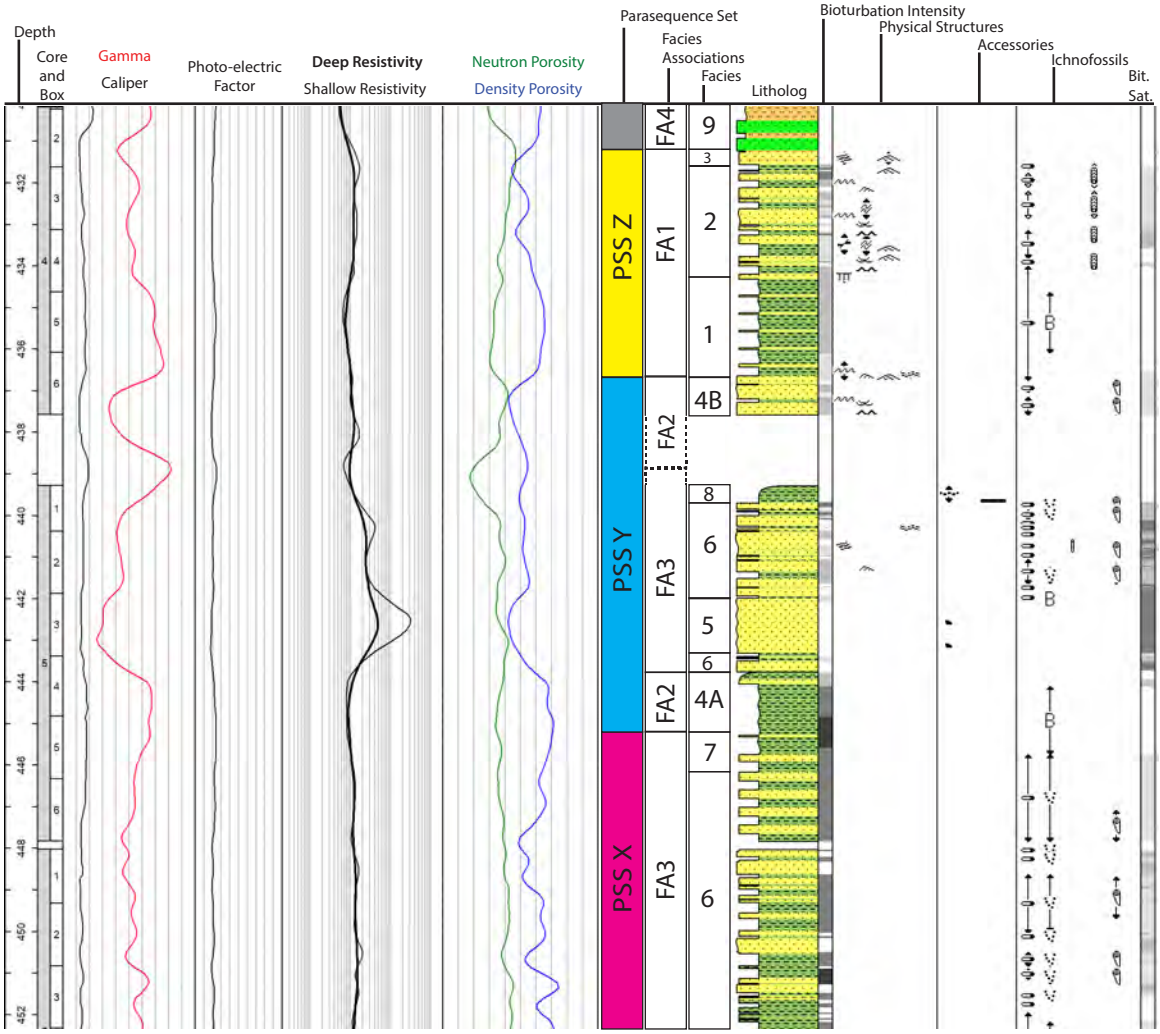

Figure 4.7 – Core description and wireline logs of core 1AA/10-21-079-11W4 displaying a brackish-channel (FA3) deposit with the upper bounding surface terminating at an autogenic surface within PSS Y. The FA3 deposit is overlain by a sheltered shoreface to bay-margin (FA2) deposit. Unfortunately the contact between the FA3 and FA2 deposit occurs in an interval of missing core. The FA3 deposit down cuts into the underlying FA2 deposit within PSS Y. Note FA3 deposits of PSS X are not shown in their entirety.

Well: 1AA/10-21-079-11W4

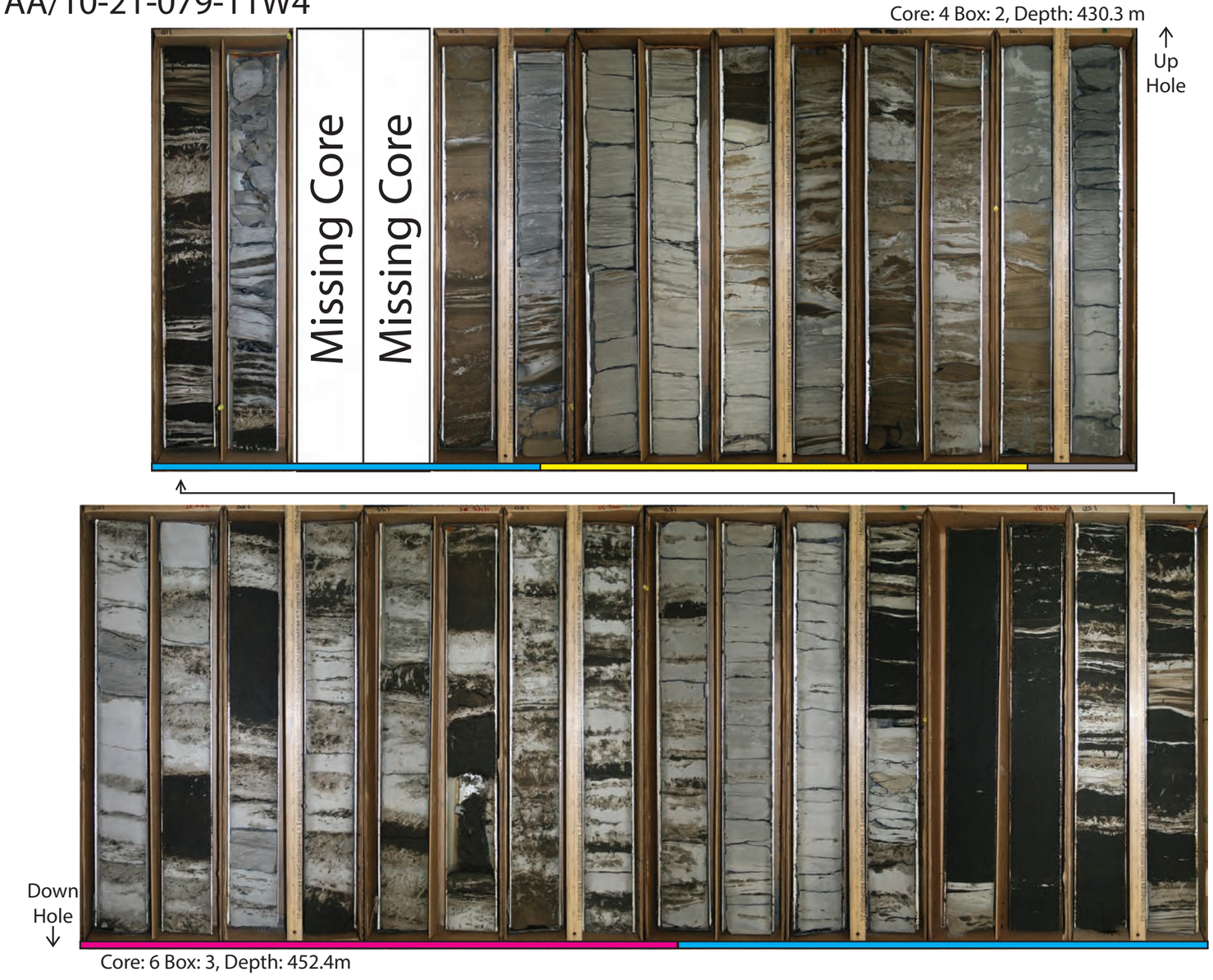

Figure 4.8 – Stitched core photograph displaying a brackish-channel (FA3) deposit with the upper bounding surface terminating at an autogenic surface and overlain by FA2 deposits within PSS Y. The magenta marker denotes PSS X, the cyan marker denotes PSS Y, the yellow marker denotes PSS Z, and the grey marker denotes the Wabiskaw Member. Note FA3 deposits of PSS X are not shown in their entirety.

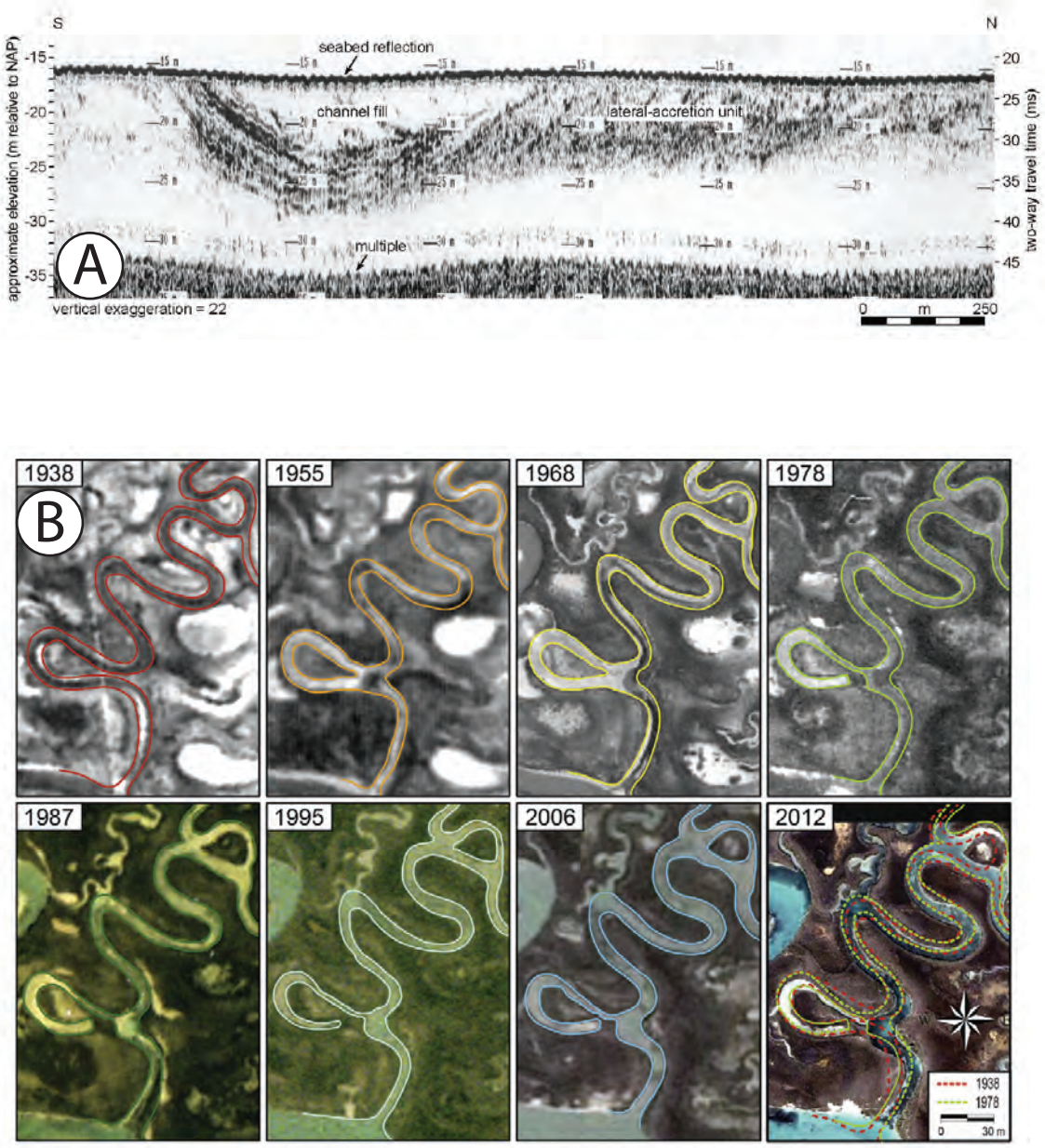

Figure 4.9 – A) Shallow seismic record of preserved Holocene tidal channel, showing lateral accretion and vertical filling off the west coast of the Netherlands (from Rieu et al., 2005). Position of seismic line shown in Fig. 4.10B. B) Temporal evolution of meandering tidal channel, showing multiple partial neck cut offs. Aerial and satellite photos from 1938 to 2012, San Felice salt marsh in the Venice Lagoon, Italy (From D'alpaos et al., 2017).

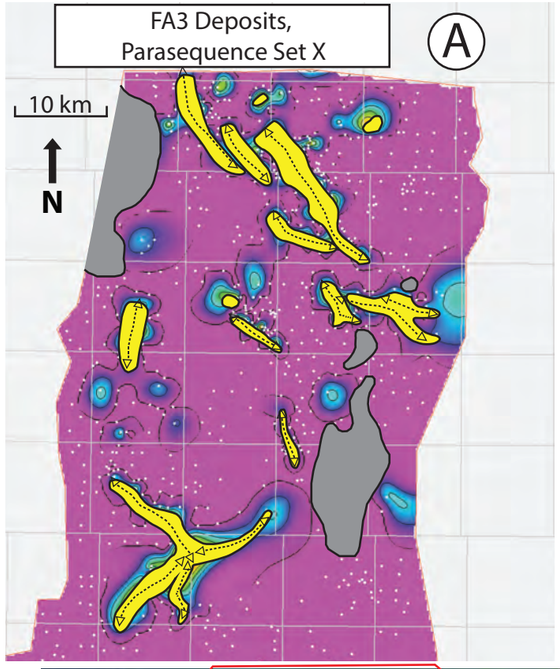

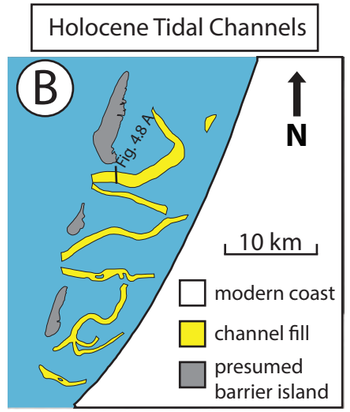

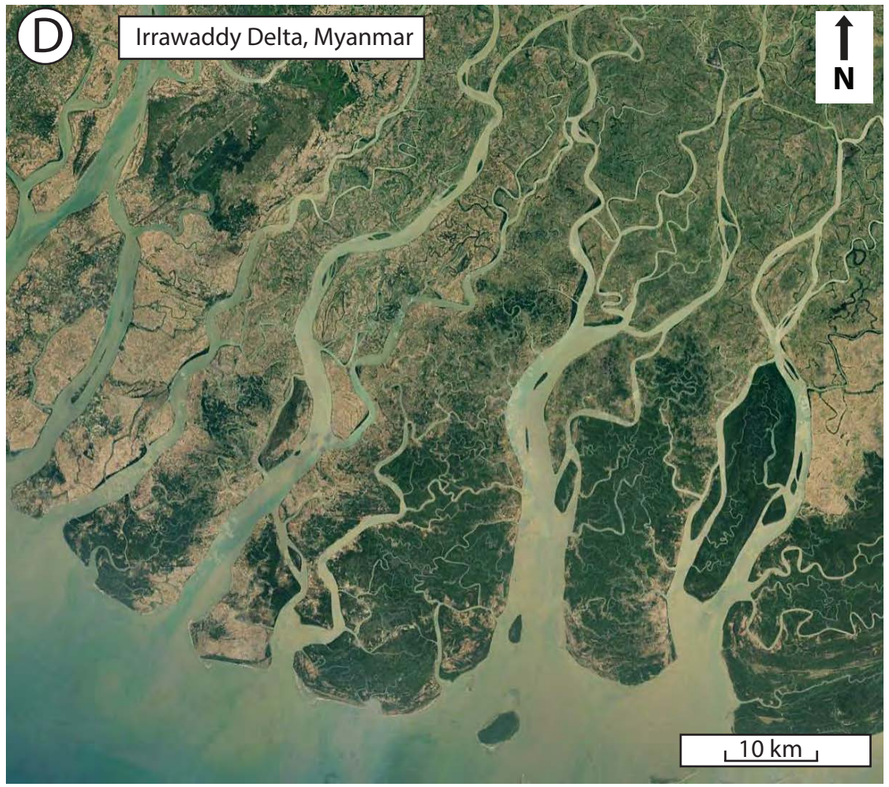

Figure 4.10 - Each figure has been scaled to the same size to compare distributions and morphologies. A) North half of study area, FA3 deposits PSS X (Fig. 4.2). Dashed black lines denote interpreted trends of large tidal channels. B) Preserved Holocene tidal channel fills. The presumed barrier islands have not been mapped, their sizes and extent have been estimated (Modified from Rieu et al., 2005). C) Satellite photo from Google Earth of a portion of the Wadden Sea. Image shows tidal flats with tidal channels oriented perpendicular to the coast. The area in the red polygon displays non-dredged tidal flats punctuated by tidal channels. This area is sheltered from wave energy of the North Sea and contains few, rather small barrier islands. The Elbe Estuary, Germany is in the top right corner of the image. D) Satellite photo from Google Earth of the Irrawaddy Delta, Myanmar, displaying coastline perpendicular channels.

4.2.2 Parasequence Set Z

Parasequence set Z is interpreted to comprise different depositional environments than those found in PSS X and Y. The main difference is the shift from tide-dominated environments to wave-dominated environments, probably as a result of burial of the Beaverhill Lake Spur and more widespread exposure to waves generated in the Boreal Sea lying to the north. As a result of the Beaverhill Lake spur no longer sheltering the area, wave-generated structures (storm and fairweather) dominate the deposits within PSS Z. Due this wave domination, large tidal channels no longer occur as the tidal energies responsible for such structures are no longer dominant. The presence of heterolithic bedding with syneresis cracks suggests that deltaic feeder channels should occur; however, no significant deltaic channels were mapped. These deltaic feeder channels probably fall below the resolution of this study as wave-dominated deltas often have smaller and less abundant channels, or were eroded by transgressive wave ravinement.

Linear thickness trends are observed in FA1 deposits (Fig. 4.5). These trends are interpreted as a prograding, wave-dominated, brackish-water deltas in a low gradient system. There are a lot of variations in geometries of wave-dominated deltaic settings, but in general they tend to be more parallel to the coastline compared to tide and fluvial-dominated deltas (Bhattacharya and Giosan, 2003). Therefore, it is interpreted that these linear trends in FA1 deposits are regionally sub-parallel to the coastline. The seaward direction during Parasequence set Z is interpreted to be towards the northwest.

Facies Association 1 is the most consistently recognizable facies association in the study. Despite this, no up-drift beach ridges, strand plains, or significant feeder channels were observed in the cores. Due to the resolution of this study, no further interpretation can be made on the symmetry of the delta.

An anomalously thick interval of the Wabiskaw Member is interpreted to be responsible for the absence of underlying PSS Z deposits (Township 75, Ranges 9-13W4). Erosion of PSS Z is likely attributed to transgressive ravinement caused by the gradual, but erosive, onlapping of landward-shifted marine deposits of the Wabiskaw Member.

4.2.3 Wabiskaw

The Wabiskaw was not logged in detail; however, there are notable linear trends across the study area apparent during isopach mapping of the Wabiskaw. The thickness trends that run northeast–southwest are interpreted to be related to marine transgression. These trends are consistent with the trends and interpretations made for PSS Z. Therefore, the seaward direction is regarded to be subparallel to the previous interpreted seaward direction – to the northwest.

4.3 Overall Setting

When all the observed trends are overlain on the same map, brackish-water channel (FA3) deposits trend northwest-southeast, and wave-/storm-dominated delta deposits (FA1) and shoreface deposits (FA4) trend southwest-northeast (Fig 4.11). Two overall settings are proposed, termed the ‘consistent model’ and the ‘dynamic model’. The consistent model proposes that the basinward direction was always towards the northwest during the entire depositional history of parasequence sets X, Y, Z in the GPV. The dynamic model proposes that the basinward direction was towards the southeast during the deposition of parasequence sets X and Y and was reoriented 180° towards the northwest during deposition of PSS Z.

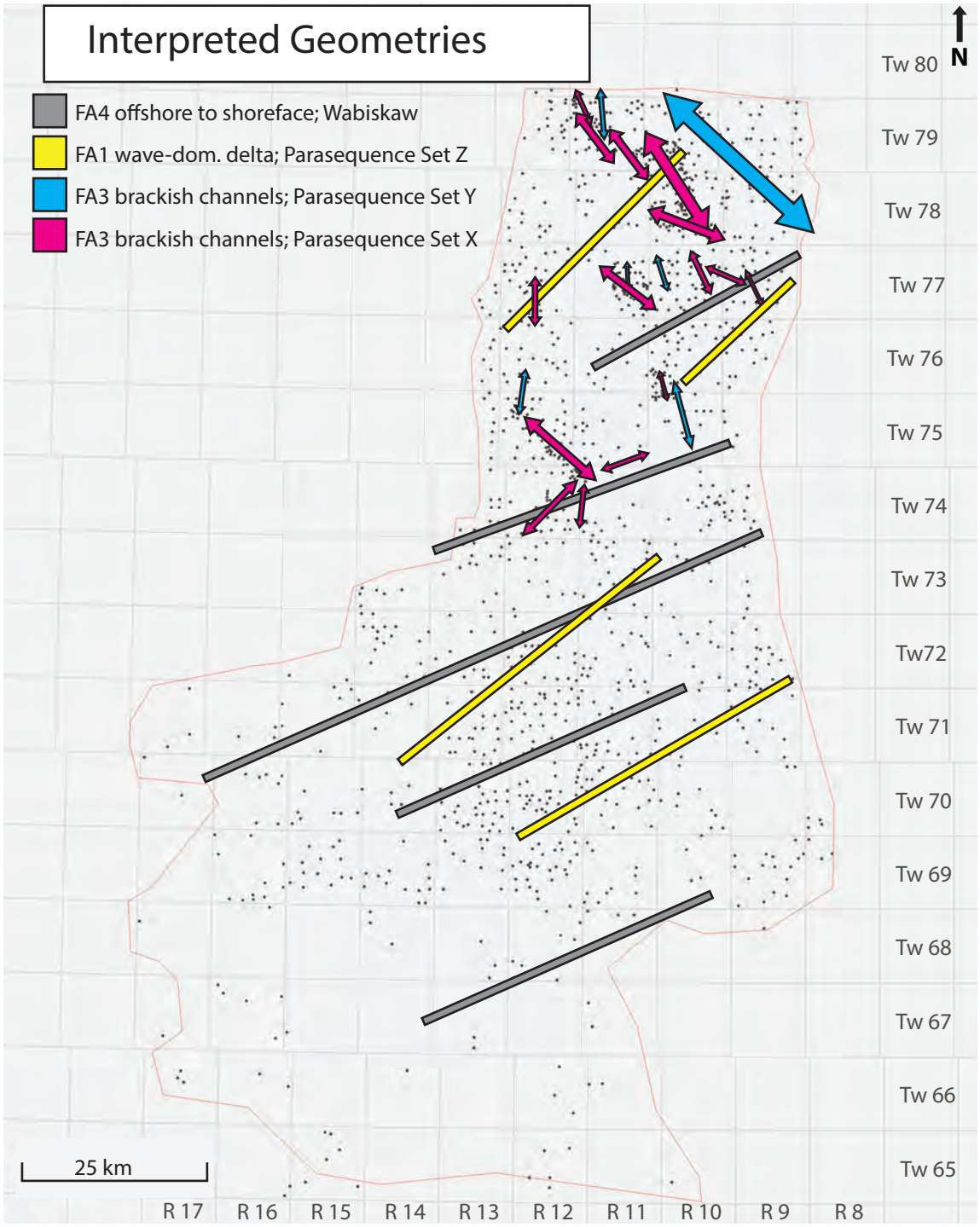

Figure 4.11 - Interpreted trends from figures 4.2, 4.4, 4.5, 4.6. Magenta arrows represent tidal channel trends of PSS X. Cyan arrows are represent tidal channel trends of PSS Y. Yellow bars represent shoreline parallel trends of PSS Z deposits. Grey bars represent shoreline parallel trends of Wabiskaw deposits. In general, tidal channels trend in the northwest – southeast direction in both PSS X and Y. Shoreline parallel features trend southwest – northeast, perpendicular to the tidal channels. The basinward direction is interpreted to be towards the northwest or initially towards the southeast during PSS X and Y then shift towards the northwest during PSS Z.

4.3.1 Consistent Model

Brackish-water channel (FA3) deposits trend northwest-southeast and are interpreted to run perpendicular to the coastline in PSS X and Y. Protected shoreface to bay-margin (FA2) deposits in PSS X and Y display no obvious trends but are interpreted to be perpendicular to the brackish-water channel deposits. PSS X is interpreted to have prograded towards the northwest, where as PSS Y is interpreted to have retrograded along the same trend. Thick deposits in PSS Z are preserved in linear northeast–southwest trends. These trends are interpreted to represent northwest progradation of a wave-/storm-dominated deltaic setting. Wabiskaw deposits show similar trends with the seaward direction interpreted to be towards the northwest. All the environmental interpretations and facies association distributions point to the same conclusion; namely that the seaward direction/direction of progradation is to the northwest and the coastlines trend perpendicular to this (northeast–southwest; Fig. 4.11, 4.12A). It is unknown how far the environments inferred in the GPV extend outside the study area.

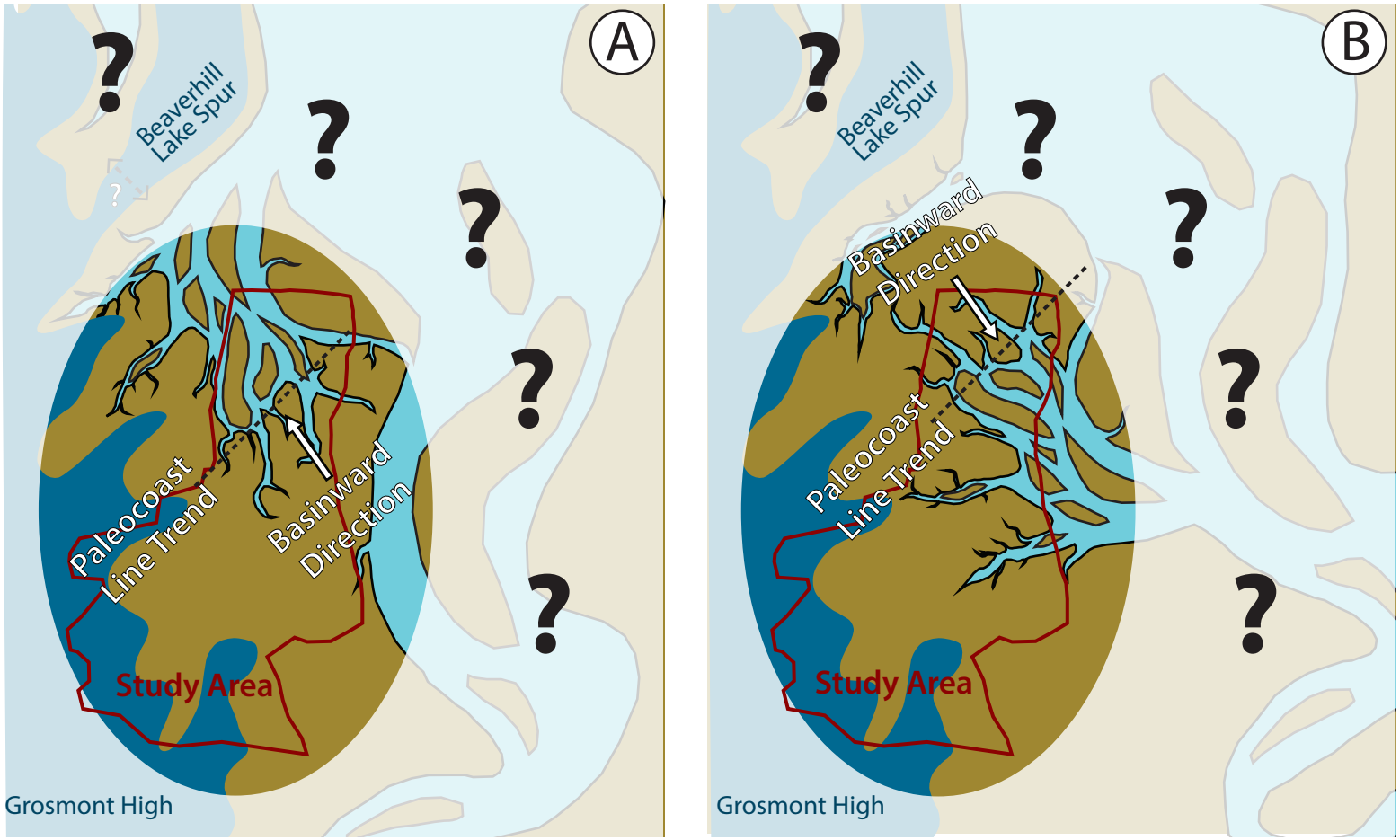

Figure 4.12 – Schematic diagram illustrating the two proposed scenarios of channel orientation and basinward direction in the GPV during deposition of PSS X and Y. Note this figure does not display mapped deposits and is only intended to provide a visual reference. A) Schematic diagram illustrating the consistent model, where the basinward direction was towards the northwest in the study area. White question mark over the Beaverhill Lake Spur may be conduit connecting the Ells Paleovalley with the GPV B) Schematic diagram illustrating the dynamic model, where the basinward direction was towards the southeast in the study area during deposition of PSS X and Y.

4.3.2 Dynamic model

Brackish-water channel (FA3) deposits trend northwest-southeast and are interpreted to run perpendicular to the coastline in PSS X and Y. Protected shoreface to bay-margin (FA2) deposits in PSS X and Y display no obvious trend but are interpreted to be perpendicular to the brackish-water channel deposits. PSS X is interpreted to have prograded towards the southeast, where as PSS Y is interpreted to have retrograded along the same trend. Parasequence sets X and Y are interpreted to be prograding from the Beaverhill Lake spur towards the southeast into a very large restricted bay (Fig. 4.12B). It is also expected that there would be progradation from the Grosmont High in the south west towards the northeast into the bay.

The flooding surface demarcating the base of PSS Z is interpreted to have ultimately drowned the Beaverhill Lake Spur. This would result in a 180° reorientation of the paleoshoreline. Thick deposits in PSS Z are preserved in linear northeast–southwest trends. These trends are interpreted to represent northwest progradation of a wave-/storm-dominated deltaic setting. Wabiskaw deposits show similar trends with the seaward direction interpreted to be towards the northwest.

4.4 Previously Published Stratigraphy

According to Ranger and Pemberton (1997) and Hein et al. (2013), the depositional history of the upper approximately 30 - 50 m of the McMurray are interpreted to represent a 3rd order transgression with 4th order sea level fluctuations. According to the previously proposed stratigraphic frameworks of Ranger and Pemberton (1997) and Hein et al. (2013), facies Association 2 deposits of PSS X were, interpreted to be HST deposits. The deep channels associated with PSS X and Y have been interpreted previously in Ranger and Pemberton (1997) and Hein et al. (2013) as incised valleys (approximately 40 m deep) cut during major sea level fall (Fig. 4.13). If FA3 deposits of PSS X were interpreted in the existing stratigraphic frameworks of Ranger and Pemberton (1997) and Hein et al. (2013), they represent fluvial to estuarine deposits emplaced during an LST and TST cycle. Therefore according to Ranger and Pemberton (1997) and Hein et al. (2013), FA2 deposits of PSS Y would also have to be placed into a younger HST, which was followed by another major sea level fall that led to incision of a second set of 40 m deep incised valleys. According to Ranger and Pemberton (1997), the FA3 deposits of PSS Y would then also be identified as fluvial transitioning into estuarine during another LST and TST. Facies Association 1 deposits of PSS Z would then be interpreted to have been deposited during the following HST, in the frameworks proposed by Ranger and Pemberton (1997) and Hein et al. (2013). Although no thick channelized deposits occur in PSS Z within the GPV, they do occur to the east in the main fairway, and according to Hein et al. (2013), there was another major incisional event wherein incised valley formation was followed by LST-TST infill.

Finally, following drowning of the Grosmont High and transgression by the Boreal Sea, Wabiskaw sedimentation was initiated. Hein et al. (2013) interprets additional incision and fill events in the Wabiskaw. The stratigraphic interpretation of Ranger and Pemberton (1997) and Hein et al. (2013) is plausible, but requires sea level to rise and fall at least three times. Each sea level fall would have produced incisions up to 40 m deep in a stratal stacking package that averages 25 m.

During valley incision there must be a continuous incised conduit through which water and suspended sediment flowed. This conduit would extend from the lowstand delta at the mouth of the incised valley, and continue landward to a point on the continent not affected by sea level change (cf. Van Wagoner et al., 1990; Zaitlin et al.,

1994). Incised valleys and their fills have a high preservation potential in a transgressive setting, due to the creation of new accommodation space (Demarest and Kraft, 1987; Zaitlin et al., 1994). Ranger and Pemberton (1997) and Hein et al. (2013) interpret that the “valley fill” deposits (e.g., FA3) are attributed to transgression and the incised valley would act as a local sediment sink. Consequently, it would be expected that the enclosing valley be filled and preserved along a significant portion of its incisional extent forming a continuous deposit. However, Fig 4.2 and Fig 4.4 show the opposite – these deposits are not continuous. There is no explanation within either Ranger and Pemberton (1997) nor Hein et al. (2013) as to how these deposits would produce such a preservation pattern. Therefore, the interpretation of lowstand incised valleys that have been transgressively filled does not seem plausible within the GPV as these deposits are very discontinuous and isolated.

Dalrymple et al. (1992) proposes a model for tide-dominated estuary preservation, which has fluvial LST deposits at the base that are capped with a transgressive flooding surface. This is, overlain with estuarine tidal-fluvial deposits that transition to tidal meanders as the estuary shifts landward during TST. It is easy to see how Facies 5 could be interpreted as fluvial, especially since it is commonly bitumen saturated, making sedimentary structures extremely difficult to see. However, no evidence of a flooding surface capping Facies 5 was observed in core. Facies 5 and Facies 6 have a gradational contact and there is no evidence of fluvial deposits overlain by estuary deposits in FA3 deposits.

Estuaries typically have widespread coastal plains surrounding the landward portion of the system (Dalrymple et al., 1992). Relative sea level fall would result in valley incision as well as coastal plain development, and it would be expected to result in paleosol development and floral colonisation. Coal beds (>5 cm) are extremely rare and pedogenically altered deposits are also uncommon in the GPV. Although one may argue that these deposits have a low preservation potential and have been eroded, a simpler interpretation would be that there never was widespread paleosol development because there was never significant (+40 m) relative sea level fall to result in significant coastal plain development.

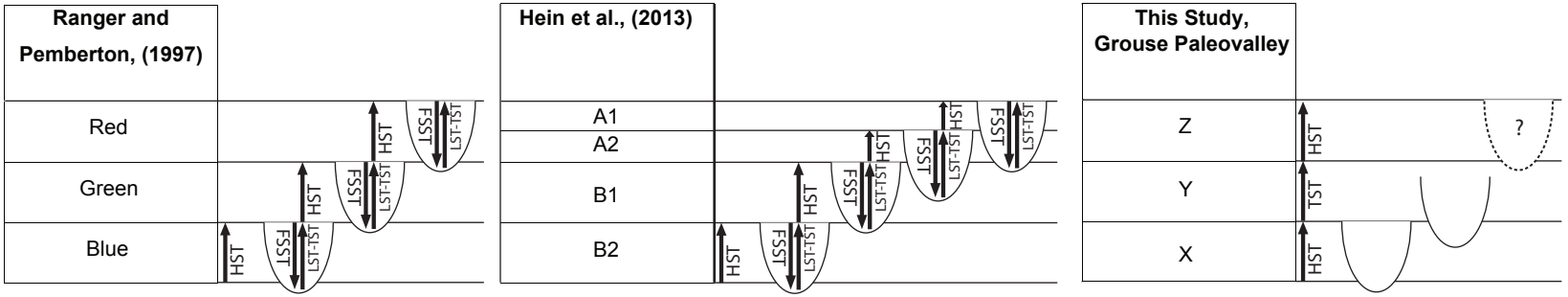

Figure 4.13 – Diagram comparing the stratigraphic models proposed by Ranger and Pemberton, 1997; Hein et al., 2013; and this study. The models of Ranger and Pemberton, 1997 and Hein et al., 2013 propose multiple sea level rises and falls. The model proposed in this study interprets the channels and regional deposits to be syn-depositional. Parasequence Set X and Z are interpreted to be deposited in high stand system tracts, whereas PSS Y is interpreted to be deposited in a transgressive system tract. FA3 deposits may subtend from either allogenic or autogenic surfaces. No FA3 deposits were observed in the PSS Z in the GPV, but may occur outside the study area.

4.5 Proposed Stratigraphic Framework

This study proposes an alternative interpretation. The onset of “upper” McMurray deposition is placed at the basal surface of PSS X, which is consistent with previous interpretations of the McMurray Formation (e.g., Mossop and Flach, 1983; Ranger and Pemberton, 1997; Hein et al., 2013). By the time PSS X deposition began, the majority of the SCU was buried, and sediment deposition was not confined solely to the bottom of the GPV. A 3rd order transgression is responsible for an overall sea level rise. The vertical succession of PSS X, Y, Z, and the overlying Wabiskaw Member show an overall progressive shift to more marine facies (Fig. 3.30). Fourth order relative sea level fluctuations are interpreted to have occurred during deposition of the regional parasequence sets bound by allogenic surfaces within the GPV, and are interpreted as follows. An allogenic transgressive flooding event marks the base of PSS X. The regionally extensive progradational deposits of FA2 and related local deposits of FA3 were accumulated during a period of normal regression during a highstand system tract (Fig 4.13). Sea level is interpreted to have been stable or rising slowly, but more importantly sedimentation rates were able to overcome any slight sea level rises. The end of PSS X is marked by a rapid rise in relative sea level, resulting in an allogenic transgressive ravinement surface. The regionally extensive deposits of FA2 and related local deposits of FA3 in PSS Y accumulated during a period of overall retrogradation within a transgressive system tract, as sedimentation was not able to keep pace with the rate of sea level rise. Parasequence set Y contains transgressive wave ravinement surface near the top of the succession and is capped by a maximum flooding surface. The regional extensive deposits of FA1 within PSS Z were accumulated during a period of normal regression during a highstand system tract, where sedimentation was able to overcome any minor sea level rises. Parasequence set Z is capped by an allogenic ravinement surface related to the transgression of the Wabiskaw Member.

There is no need to extensively lower sea level to facilitate such deposition as brackish-water channels (FA3) were found subtending from autogenic surfaces within parasequences sets. Varying rates of relative sea level rise give way to transgressive and regressive successions. Parasequence set X and Z are deposited during a period of normal regression in highstand conditions, and Parasequence Y is deposited during a

period of retrogradation in transgressive conditions. No deposits in this study are interpreted to occur during falling stage or lowstand system tracts.

4.6 Conclusion

Parasequences set X and Y are interpreted to have been deposited in a prograding sheltered shoreface to bay-margin interspersed with brackish-water channels. Parasequence set Z is interpreted to have been deposited in a in a wave-/storm-dominated deltaic setting. Facies associations that are interpreted to be sub parallel to the coastline have a northeast-southwest orientation, and facies associations that are interpreted to be perpendicular to the coastline trend northwest-southeast. It is concluded that the basinward direction and direction of progradation is either towards the northwest or initially towards the southeast, which then shifts towards the northwest once all relief on the SCU was buried and could no longer impart a control on the paleogeography.

An alternative stratigraphic model is proposed for the regional parasequence sets in the GPV. Normal regressive successions are interpreted to be the progradational highstand system tract deposits of parasequence sets X and Z. The transgressive succession of PSS Y is interpreted to be retrogradational and deposited in a transgressive system tract. This stratigraphic model applies to the study area and potentially the nearby surrounding area.

5 Final Conclusions

The following conclusions for each research objective are summarized as follows.

5.1 Structure of the GPV

Structural maps were created to determine whether there were any structural features affecting the strata in the study area. The structure of the SCU has an overall dip to the southwest but the valleys and ridges that form the GPV are identifiable. The McMurray and Wabiskaw have a dip direction to the southwest (between 229°-214°), which is consistent with the overall dip of the Mannville Group in the area. The McMurray and the Wabiskaw have a fairly consistent dip of 0.076°, also consistent with the overall dip of the Mannville Group in the area. No large faults or karst features were identified.

5.2 Thickness of the GPV

Isopach maps were created between the formation tops to determine how sediment was distributed within the GPV, and provide insight into how the SCU affected accommodation space. Isopach maps of the McMurray-SCU and Wabiskaw-SCU display the ridges and valleys that define the GPV. The Grosmont High demarcates the southern and southwestern edges of the GPV. The main axis of the GPV trends north-northeast. Two secondary conduits occur in the GPV. The Wabiskaw-McMurray isopach maps show little or no influence from the SCU, as it occurs above any Devonian paleo-subcrop, which results in northeast-southwest linear thickness trends.

5.3 Facies and Facies Associations

Eight recurring facies have been identified in the regional parasequence sets of the McMurray Formation, and two facies define from the overlying Wabiskaw Member. The eight McMurray facies combine to form three facies associations in the regional

parasequence sets: wave-/storm-dominated delta (FA1), sheltered shoreface to bay-margin (FA2), and brackish-water channel (FA3). Two working hypotheses of FA3 are presented, mainly related to the degree of fluvial input. The two facies of the Wabiskaw Member forms a single facies association (FA4) and contains marine lower shoreface to upper offshore deposits.

5.4 Regional Parasequence Sets

Three allogenic flooding surfaces are recognized, which define the boundaries of three parasequence sets. These parasequence sets are termed (oldest to youngest) as X, Y, and Z, respectively. Parasequences are demarcated by autogenic flooding surfaces separating shingle-like progradational packages within each parasequence set. Wireline log signatures are defined for each parasequence set. Thickness histograms of FA2 and FA1 show a normal distribution, whereas FA3 deposits display markedly varied thicknesses. These variable thicknesses are attributed to the variations of channel scales that occur in a tidal drainage network.

5.5 Distributions of Facies Associations

Exposure of the SCU within the GPV is most pronounced during deposition of PSS X, with each successive parasequence set being progressively less affected. FA2 deposits in PSS X and Y are regionally extensive (except where eroded), and become difficult to determine on wireline logs towards the Grosmont High in the south. FA3 deposits have a general northwest-southeast trend and are interpreted to be oriented perpendicular to the paleocoastline. The depositional setting of PSS X and Y are interpreted to be similar, as they contain the same facies associations and have similar depositional architectures. Parasequence sets X and Y are interpreted to be deposited in a prograding, sheltered shoreface to bay-margin, punctuated with brackish-water channels in a low gradient and accommodation setting. Parasequence sets X and Y are interpreted to have been sheltered from significant wave energies by the Beaverhill Lake Spur.

The Beaverhill Lake Spur is thought to have been drowned over during the deposition of PSS Z, and was no longer able to protect the GPV from strong wave energies. Parasequence set Z is, correspondingly, dominated by regionally extensive FA1 deposits. The lack of FA3 brackish-water channel deposits is interpreted to be due to the domination of wave energies at that time. The depositional environment of PSS Z is interpreted as a prograding, wave-/storm-dominated delta in a low accommodation setting. Linear thickness trends of FA1 trend southwest-northeast and are interpreted to have been subparallel to the paleocoastline. The Wabiskaw Member also has northeast-southwest linear thickness trends attributed to marine transgression.

The distribution of facies associations within each parasequence all show similar trends. That coastline parallel facies associations trend northeast-southwest and coastline perpendicular facies trend northwest-southeast. Two models are proposed regarding the basinward direction. One model proposes that the basinward direction and progradation direction has been towards the northwest in the GPV. The second model proposes that during the deposition of PSS X and Y, the Devonian highlands resulted in a very large sheltered bay, and progradation trended away from these highs. This resulted in progradation towards the southeast away from the Beaverhill Lake Spur in the north. During deposition of PSS Z, sea level drowned the Beaverhill Lake Spur resulting in a reorientation of the paleoshoreline, changing the direction of progradation to the northwest.

5.6 Stratigraphic Framework

An alternative stratigraphic framework is proposed for the regional parasequence sets of the McMurray Formation in the GPV. The proposed model proposes that the successions only varies with respect to the rate at which relative sea level rose coupled with sediment supply. In the proposed stratigraphic framework, the stacked parasequence sets, indicate an overall relative sea level rise. Periods of stable or slow sea level rise resulted in normal (progradational) regression that resulted in progradational parasequence sets X and Z. Periods of rapid sea level rise led to discrete allogenic ravinement and/or flooding surface and the retrogradation succession of PSS Y. Brackish-water channels (FA3) deposits are regarded to be genetically linked to the

parasequences sets and do not require any base level falls during deposition. This stratigraphic model is simpler in that is does not require large and frequent changes in sea level than do those previously proposed.

References

Alam, M.M., Crook K.A.W., and Taylor, G. 1985. Fluvial herring-bone cross-stratification in a modern tributary mouth bar, Coonamble, N.S. Wales, Australia. Sedimentology, v. 32, p. 235 - 244.

Alberta Energy Regulatory. 2003A. Report 2003-A. Athabasca Wabiskaw-McMurray Regional Geological Study. Alberta Energy Utility Board: Annual Report.

Alberta Energy Regulatory. 2003B. Decision 2003-023: Chard Area and Leismer Field, Athabasca Oil Sands Area. Alberta Energy Utility Board, Decision.

Alberta Energy Regulator. 2015. ST-98-2015: Alberta's energy reserves 2014 and supply/demand outlook 2015-2024

Alexander, C.R., DeMaster, D.J., and Nittrouer, C. A. 1991. Sediment accumulation in a modern epicontinental-shelf setting: the Yellow Sea. Marine Geology, v. 98(1), p. 51-72.

Ashley, G.M., and Zeff, M.L. 1988. Tidal channel classification for a low-mesotidal salt marsh. Marine Geology, v. 82(1-2), p. 17-32.

Athabasca Oil Corporation (2017) AER Leismer Update 10935. Alberta Energy Regulator, Directive 054, 2017 Annual Performance Presentation.

Barnes, R.S.K. 1989. What, is anything, is a brackish-water fauna?. Royal Society of Edinburgh, Transactions, Earth Science, v.80, p. 235–240.

Barwis, J.H. 1978. Sedimentology of some South Carolina tidal-creek point bars, and a comparison with their fluvial counterparts. In: Fluvial Sedimentology. A.D. Miall (ed.). Canadian Society of Petroleum Geologists, Memoir, v. 5, p. 129–160.

Barwis, J.H., and Makurath, J. H. 1978. Recognition of ancient tidal inlet sequences: an example from the Upper Silurian Keyser Limestone in Virginia. Sedimentology, v. 25(1), p. 61-82.

Belknap, D.F., and Kraft J.C. 1985. Influence of antecedent geology on stratigraphic preservation potential and evolution of Delaware's barrier systems. Marine Geology, v. 63(1-4), p. 235-262.

Benyon, C., Leier, A., Leckie, D.A., Webb, A., Hubbard, S. M., Gehrels, G. 2014. Provenance of the Cretaceous Athabasca Oil Sands, Canada: implications for continental-scale sediment transport. Journal of Sedimentary Research, v. 84.2, p. 136-143.

Beynon, B.M., Pemberton, S.G., Bell, D.A. and Logan, C.A. 1988. Environmental implications of ichnofossils from the Lower Cretaceous Grand Rapids Formation, Cold Lake Oil Sands Deposit. In: Sequences, Stratigraphy, Sedimentology: Surface and Subsurface. D.P. James and D.A. Leckie (eds.). Canadian Society of Petroleum Geologists, v. 15, p. 275-290.

Bhattacharya, J.P., and Giosan, L. 2003. Wave-influenced deltas: Geomorphological implications for facies reconstruction. Sedimentology, v. 50(1), p. 187-210.

Bhattacharya, J.P., and MacEachern, J.A., 2009. Hyperpycnal rivers and prodeltaic shelves in the Cretaceous Seaway of North America. Journal of Sedimentary Research, v.79, p. 184-209.

Blum, M., Pecha, M. 2014. Mid-Cretaceous to Paleocene North American drainage reorganization from detrital zircons. Geology, v. 74, p. 607-610.

Brivio, L., Ghinassi, M., D'Alpaos, A., Finotello, A., Fontana, A., Roner, M., & Howes, N. 2016. Aggradation and lateral migration shaping geometry of a tidal point bar: an example from salt marshes of the Northern Venice Lagoon (Italy). Sedimentary Geology, v. 343, p. 141-155.

Broughton, P.L. 2013. Devonian salt dissolution-collapse breccias flooring the Cretaceous Athabasca oilsands deposit and development of the lower McMurray formation sinkholes, northern Alberta Basin, Western Canada. Sedimentary Geology, v. 283, p. 57-82.

Broughton, Paul L., 2013, Depositional setting and oil sands reservoir characterization of giant longitudinal sandbars at Ells River: Marginal marine facies of the

McMurray formation, northern Alberta Basin, Canada, in: F. J. Hein, D. Leckie, S. Larter, and J. R. Suter, eds., Heavy-oil and oil-sand petroleum systems in Alberta and beyond: AAPG Studies in Geology 64, p. 313–357.

Burst, J.F. 1965. Subaqueously formed shrinkage cracks in clays. Journal of Sedimentary Petrology, v. 35, p. 348-353.

Carrigy, M.A., 1959. Geology of the McMurray Formation, Part 3: General Geology of the McMurray Area. Research Council of Alberta, Geological Division, p. 130.

Carrigy, M.A., 1963. Paleocurrent directions from the McMurray Formation. Research Council of Alberta, p. 389–395.

Carrigy, M.A. 1971. Deltaic sedimentation in Athabasca Tar Sands. Bulletin American Association of Petroleum Geology, v. 55, p. 1155-1169.

Catuneanu, O. 2006. Principles of sequence stratigraphy. Elsevier. 386 p.

Cleveringa, J., and Oost, A.P. 1999. The fractal geometry of tidal-channel systems in the Dutch Wadden Sea. Geologie en Mijnbouw, v. 78(1), p. 21-30.

Cloyd, K.C., Demicco, R.V., and Spencer, R.J. 1990. Tidal channel, levee, and crevasse-splay deposits from a Cambrian tidal channel system: a new mechanism to produce shallowing-upward sequences. Journal of Sedimentary Research, v. 60(1) p. 73-83.

D'Alpaos, A., Ghinassi, M., Finotello, A., Brivio, L., Bellucci, L.G., and Marani, M. 2017. Tidal meander migration and dynamics: A case study from the Venice Lagoon. Marine and Petroleum Geology v. 87, p. 80-90.

Dalrymple, R.W., Makino, Y., and Zaitlin, B. A. 1991. Temporal and spatial patterns of rhythmite deposition on mud flats in the macrotidal Cobequid Bay-Salmon River estuary, Bay of Fundy, Canada. In: Clastic Tidal Sedimentology. D.G Smith, G.E. Reinson, B.A. Zaitlin, and R.A. Rahmani (eds.) Canadian society of Petroleum Geologists. Memoir 16. p. 137-160.

Dalrymple, R.W., Zaitlin, B.A., and Boyd, R. 1992. Estuarine facies models: conceptual basis and stratigraphic implications: perspective. Journal of Sedimentary Petrology, v. 62(6), p. 1130-1146.

Dalrymple, R.W., and Choi, K. 2007. Morphologic and facies trends through the fluvial–marine transition in tide-dominated depositional systems: a schematic framework for environmental and sequence-stratigraphic interpretation. Earth-Science Reviews, v. 81(3), p. 135-174.

Dashtgard, S.E., Venditti, J.G., Hill, P.R., Sisulak, C.F., Johnson, S M., and La Croix, A. D. 2012. Sedimentation across the tidal–fluvial transition in the Lower Fraser River, Canada. SEPM, The Sedimentary Record, v. 10(4), p. 4-9.

Demarest, J.M., and Kraft, J.C., 1987, Stratigraphic record of quaternary sea levels: implications for more ancient strata. In: Sea-level fluctuations and coastal evolution. D. Nummedal, O.H, Piikey, and J.D. Howard (eds.). SEPM Special Publication 41, p. 223-239.

Dott, R.H., and Bourgeois, J., 1982. Hummocky stratification: Significance of its variable bedding sequences. Geological Society of America Bulletin, v.93, p. 663-680.

Ekdale, A.A., Bromley, R.G., Pemberton, S.G., 1984. Ichnology: Trace Fossils in Sedimentology and Stratigraphy. Society of Economic Paleontologists and Mineralogists: Short Course, 15. 317 p.

Ekdale, A.A., 1985. Paleoecology of the marine endobenthos: Palaeogeography, Palaeoclimatology, Palaeoecology, v. 50, p. 63–81.

Fenies, H., and Faugères, J.C. 1998. Facies and geometry of tidal channel-fill deposits (Arcachon Lagoon, SW France). Marine Geology, v. 150, p. 131-148.

Flach, P.D., and Mossop, G.D., 1985. Depositional environments of Lower Cretaceous McMurray Formation, Athabasca oilsands, Alberta. American Association of Petroleum Geologists Bulletin, v.69, p. 1195–1207.

Gingras, M.K., Pemberton, S.G., Saunders, T. and Clifton, H.E., 1999. The ichnology of modern and Pleistocene brackish-water deposits at Willapa Bay, Washington; variability in estuarine settings. Palaios, v. 14(4), pp.352-374.

Gingras, M.K., Räsänen, M., and Ranzi, A. 2002. The significance of bioturbated inclined heterolithic stratification in the southern part of the Miocene Solimoes Formation, Rio Acre, Amazonia Brazil. Palaios, v. 17(6), p. 591-601.

Gingras, M.K., MacEachern, J A., and Dashtgard, S.E. 2011. Process ichnology and the elucidation of physico-chemical stress. Sedimentary Geology. v. 237, p. 115-134.

Gingras, M.K. and MacEachern, J.A., 2012. Tidal ichnology of shallow-water clastic settings. In Principles of Tidal Sedimentology (pp. 57-77). Springer Netherlands.

Gingras, M.K., MacEachern, J A., and Dashtgard, S.E. 2012. The potential of trace fossils as tidal indicators in bays and estuaries. Sedimentary Geology, v. 279, p. 97-106.

Gingras, M.K., MacEachern, J.A., Dashtgard, S.E., Ranger, M.J., Pemberton, S.G. 2016. Significance of trace fossils in the McMurray Formation, Alberta, Canada. Bulletin of Canadian Petroleum Geology, v. 64 (2), p. 233-250.

Ginsberg, S.S. and Perillo, G.M.E. 2004. Characteristics of tidal channels in a mesotidal estuary of Argentina. Journal of Coastal Research, v. 20(2), p. 489-497.

Harms, J.C., 1969. Hydraulic significance of some sand ripples. Geological Society of American Bulletin, v. 80, p. 363-396.

Harms, J.C., Southard, J.B., and Walker, R.G. 1982. Fluvial deposits and facies models. In: structures and sequences in clastic rocks. SEPM Special Publication. p. (5)1-26.

Hauck, T.E., Peterson, J.T., Hathway, B., Grobe, M., and MacCormack, K. 2017. New insights from regional-scale mapping and modelling of the Paleozoic succession in northeast Alberta: Paleogeography, evaporite dissolution, and

controls on Cretaceous depositional patterns on the sub-Cretaceous unconformity. Bulletin of Canadian Petroleum Geology, v. 65(1), p. 87-114.

Hayes, B.J.R., Christopher, J.E., Rosenthal, L., Los, G., McKercher, B., Minken, D., Tremblay, Y.M. and Fennell, J. 1994. Cretaceous Mannville Group of the Western Canadian Sedimentary Basin. In: Geological Atlas of the Western Canada sedimentary Basin, Chapter 19. G. Mossop and I. Shetsen (compilers). Canadian Society of Petroleum Geologists and the Alberta Research Council. Calgary, Alberta, Canada. p. 317-334.

Hein, F.J., Cotterill, D.K., and Berhane, H. 2000. An atlas of lithofacies of the McMuray Formation Athabasca oilsands deposit, northeastern Alberta; surface and subsurface. Alberta Energy and Utilities Board, Alberta Geogical Survey, Earth Science Report 2000-07. p. 1-217.

Hein, F.J., Dolby G., and Fairgrieve B., 2013, A regional geologic framework for the Athabasca oil sands, northeastern Alberta, Canada, in: Heavy-oil and oil-sand petroleum systems in Alberta and beyond. F. J. Hein, D. Leckie, S. Larter S, and J.R. Suter (eds.). AAPG Studies in Geology 64, p. 207 – 250.

Hijma, M.P., Van der Spek, A.J.F., and Van Heteren, S. 2010. Development of a mid-Holocene estuarine basin, Rhine–Meuse mouth area, offshore The Netherlands. Marine geology, v. 271(3), p. 198-211.

Horton, R.E. 1945. Erosional development of streams and their drainage basins; hydrophysical approach to quantitative morphology. Geological society of America bulletin, v. 56(3), p. 275-370.

Howard, J.D., C.A. Elders and J.F. Heinbokel. 1975. Estuaries of the Georgia Coast, U.S.A.: Sedimentology and biology V. Animal-sediment relationships in estuarine point bar deposits, Ogeechee River - Ossabaw Sound, Georgia. Senckenbergiana maritima, 7: 18 p. 1-204

Hubbard, S.M., Smith, D.G., Nielsen, H., Leckie, D.A., Fustic, M., Spencer, R.J., and Bloom, L. 2011. Seismic geomorphology and sedimentology of a tidally influenced river deposit, Lower Cretaceous Athabasca oilsands, Alberta, Canada. AAPG Bulletin, v. 95, p. 1123-1145.

Hughes, Z.J., FitzGerald, D.M., Wilson, C.A., Pennings, S.C., Więski, K., and Mahadevan, A. 2009. Rapid headward erosion of marsh creeks in response to relative sea level rise. Geophysical Research Letters, v. 36(3) p. 1-5

Hughes, Z.J. 2012. Tidal channels on tidal flats and marshes. In: Principles of Tidal Sedimentology. R.A. Davis, and R.W. Dalrymple (eds.). Springer Netherlands, p. 269-300.

Jackson, R.G. II. 1976. Depositional model of point bars in the lower Wabash River. Journal of Sedimentary Petrology. v. 46(3), p. 579-594.

Jeletzky, J.A. 1971. Marine Cretaceous Biotic Provinces and Paleogeography of Western and Arctic Canada: illustrated by a detailed study of ammonites. Geological Survey of Canada Paper, v. 70, p. 1-92.

Johnson, S.M., and Dashtgard, S.E. 2014. Inclined heterolithic stratification in a mixed tidal–fluvial channel: Differentiating tidal versus fluvial controls on sedimentation. Sedimentary Geology, v. 301, p. 41-53.

Komar, P.D., 1974. Oscillatory ripple marks and the evaluation of ancient wave conditions and environments, Journal of Sedimentary Research, v. 44, p. 169-180.

La Croix, A.D., Dashtgard, S.E., 2015. A synthesis of depositional trends in intertidal and upper subtidal sediments across the tidal-fluvial-transition in the Fraser River, Canada. Journal of Sedimentary Research 85, 683-698.

La Croix, A.D., Dashtgard, S.E., Gingras, M.K., Hauck, T.E., & MacEachern, J.A. 2015. Bioturbation trends across the freshwater to brackish-water transition in rivers: refinement of the brackish-water ichnological model. Palaeogeography, Palaeoclimatology, Palaeoecology, v. 440, p. 66-77.

MacEachern, J.A., Pemberton, S.G., 1992. Ichnological aspects of Cretaceous shoreface successions and shoreface variability in the Western Interior Seaway of North America. In:Applications of Ichnology to Petroleum Exploration, a coreworkshop. Pemberton, S.G. (Ed.), Society of Economic Paleontologists and Mineralogists: core workshop, 17, pp. 57–84.

MacEachern, J.A., Bann, K.L., Bhattacharya, J P., & Howell Jr, C. D. 2005. Ichnology of deltas: organism responses to the dynamic interplay of rivers, waves, storms, and tides. In: River Deltas – Concepts, Models, and Examples. L. Giosan, and J.P. Bhattacharya (eds.). SEPM Special Publication no. 83, p. 49-85

MacEachern, J.A., Bann, K L., Pemberton, S.G., and Gingras, M. K. 2007. The ichnofacies paradigm: high-resolution paleoenvironmental interpretation of the rock record. SEPM short course, v. 52, p. 27 - 64.

MacEachern, J.A., and Gingras, M.K. 2007. Recognition of brackish-water trace fossil suites in the Cretaceous Western Interior Seaway of Alberta, Canada. in: Sediment–Organism Interactions: A Multifaceted Ichnology. R.G. Bromley, L.A. Buatois, M.G. Mangano, J.F. Genise, and R.N. Melchor (eds.). SEPM, Special Publication, v. 88, p. 149–194.

MacEachern, J.A. and Bann, K.L., 2008. The role of ichnology in refining shallow marine facies models. Recent Advances in Models of siliciclastic shallow-marine stratigraphy: SEPM, Special Publication, v. 90, p.73-116.

MacKay, D.A., and Dalrymple, R.W. 2011. Dynamic mud deposition in a tidal environment: the record of fluid-mud deposition in the Cretaceous Bluesky Formation, Alberta, Canada. Journal of Sedimentary Research, v. 81(12), p. 901-920.

Marani, M., Lanzoni, S., Zandolin, D., Seminara, G., Rinaldo, A. 2002. Tidal meanders. Water Resources Research. v. 38 (11)

Moser, S.M., and Macintosh, D.J. 2001. Diurnal and lunar patterns of larval recruitment of Brachyura into a mangrove estuary system in Ranong Province, Thailand. Marine Biology, v. 138(4), p. 827-841.

Mossop, G.D. and Flach, P.D., 1983. Deep channel sedimentation in the Lower Cretaceous McMurray Formation, Athabasca Oilsands, Alberta. Sedimentology, v. 30(4), p. 493-509.

Miller, M.C., and Komar, P.D., 1980. A field investigation of the relationship between oscillation ripple spacing and the near-bottom water orbital motions. Journal of Sedimentary Petrology, v.50, p. 183-191.

Musial, G., Reynaud, J.Y., Gingras, M.K., Féniès, H., Labourdette, R., and Parize, O. 2012. Subsurface and outcrop characterization of large tidally influenced point bars of the Cretaceous McMurray Formation (Alberta, Canada). Sedimentary Geology, v. 279, p. 156-172.

Muto, T., Steel, R.J., AND Swenson, J.B. 2007. Autostratigraphy: a framework norm for genetic stratigraphy. Journal of Sedimentary Research, v. 77(1), p. 2-12.

Odin, G.S. and Matter, A., 1981. De glauconiarum origine. Sedimentology, v. 28(5), p. 611-641.

Oertel, G.F., Henry, V.J., and Foyle, A.M. 1991. Implications of tide-dominated lagoonal processes on the preservation of buried channels on a sediment-starved continental shelf. In: Shelf sand and sandstone bodies: geometry, facies and sequence stratigraphy. J.P. Swift, G.F. Oertel, R.W. Tillman, and J.A. Thorne (eds.) The International Association of Sedimentologists. p. 377-393.

Oldale, H.S. and Munday R.J. 1994. Devonian Beaverhill Lake Group of the Western Canadian Sedimentary Basin, in: Geological Atlas of the Western Canada Sedimentary Basin. G.D. Mossop and I. Shetsen (comp.). Canadian Society of Petroleum Geologists and Alberta Research Council, p. 149-163.

Pearson, N.J., and Gingras, M.K. 2006. An ichnological and sedimentological facies model for muddy point-bar deposits. Journal of Sedimentary Research, v. 76(5), p. 771-782.

Pemberton, S.G., Flach, P.D., and Mossop, G.D. 1982. Trace fossils from the Athabasca oil sands, Alberta, Canada. Science, v. 217(4562), p. 825-827.

Pemberton, S.G., and Wightman, D.M., 1992, Ichnological characteristics of brackish water deposits: Examples of the Mannville Group of Alberta. In: Applications of ichnology to petroleum exploration - A core workshop:. S.G. Pemberton (ed.).

Society of Economic Paleontologists and Mineralogists, Core Workshop no. 17, p. 141-67.

Ranger, M.J. and Pemberton, S.G. 1992. The sedimentology and ichnology of estuarine point bars in the McMurray Formation of the Athabasca oil sands deposits, north-eastern Alberta, Canada. In: Applications of ichnology to petroleum exploration - A core workshop. S.G. Pemberton (ed.). Society of Economic Paleontologists and Mineralogists, Core Workshop no. 17, p. 401-421.

Ranger, M.J. and Pemberton, S.G. 1997. Elements of a stratigraphic framework for the McMurray Formation in the south Athabasca area, Alberta. Canadian Society of Petroleum Geologists, Memoir, p. 263 – 291.

Rahnama, F., Marsh, R.A, and Philp L. 2013. The Alberta Oilsands: Reserves and long-term supply outlook. In: Heavy-oil and oil-sand petroleum systems in Alberta and beyond. F.J. Hein, D. Leckie, S. Larter, and J.R. Suter, (eds.). AAPG Studies in Geology v. 64, p. 133 – 144.

Reineck, H. E., and Wunderlich, F. 1968. Classification and origin of flaser and lenticular bedding. Sedimentology, v. 11(1-2), p. 99-104.

Reineck, H.E., and Singh, I.B. 1980. Tidal flats. In: Depositional Sedimentary Environments. Springer Berlin Heidelberg. p. 430-456.

Rhoads, D.C., McCall, P.L., and Yingst, J.Y., 1978, Disturbance and production on the estuarine seafloor: American Scientist, v. 66, p. 592–597.

Rieu, R., Van Heteren, S., Van Der Spek, A.J., and De Boer, P. L. 2005. Development and preservation of a mid-Holocene tidal-channel network offshore the western Netherlands. Journal of Sedimentary Research, v. 75(3), p. 409 - 419.

Santos Jr, A.E.D.A., and Rossetti, D.D.F. 2006. Depositional model of the Ipixuna Formation (Late Cretaceous-? Early Tertiary), Rio Capim area, northern Brazil. Latin American journal of sedimentology and basin analysis, v. 13(2), p. 101-117.

Shchepetkina, A., Gingras, M.K., & Pemberton, S.G. 2016. Sedimentology and ichnology of the fluvial reach to inner estuary of the Ogeechee River estuary, Georgia, USA. Sedimentary Geology, v. 342, p. 202-217.

Sisulak, C.F., and Dashtgard, S.E. 2012. Seasonal controls on the development and character of inclined heterolithic stratification in a tide-influenced, fluvially dominated channel: Fraser River, Canada. Journal of Sedimentary Research, 82v. (4), p. 244-257.

Smith. D.G. 1988. Modern point bar deposits analogous to Athabasca oil sands, Alberta, Canada. In: Tide-Influenced Sedimentary Environments and Facies. P. L. deBoer, A. Van Gelder, S.D. Nio (eds.). Boston, Reidel Publ. Co. p. 416 – 432.

Smith, D.G., Hubbard, S.M., Leckie, D.A., and Fustic, M. 2009. Counter point bar deposits: lithofacies and reservoir significance in the meandering modern Peace River and ancient McMurray Formation, Alberta, Canada. Sedimentology, v. 56(6), p. 1655-1669.

Smith, N.D. 1997. Flume experiments on the durability of mud clasts. Journal of Sedimentary Research, v. 42(2), p. 378-383.

Stonecipher, S.A. Genetic characteristic of glauconite and siderite: implications for the origin of ambiguous isolated marine sandbodies. In: Isolated shallow marine sand bodies: sequences stratigraphic analysis and sedimentological interpretation. K.M. Bergman and J.W. Snedden (eds.) SEPM special publication no. 64, p. 191-204.

Switzer, S.B., Holland, W.G., Christie, D.S., Graf, G.C., Hedinger, A.S., McAuley, R.J., Wierzbicki, R.A., and Packard, J.J. 1994. Devonian Woodbend-Winterburn Strata of the Western Canada Sedimentary Basin, in: Geological Atlas of the Western Canada Sedimentary Basin .G.D. Mossop and I. Shetsen (comp.). Canadian Society of Petroleum Geologists and Alberta Research Council. p. 165-202.

Terwindt, J.H.J. 1988. Palaeo-tidal reconstructions of inshore tidal depositional environments. In: Tide-Influenced Sedimentary Environments and Facies. P. L. deBoer, A. Van Gelder, S.D. Nio (eds.). Boston, Reidel Publ. Co. p. 233-263.

Thomas, R.G., Smith, D.G., Wood, J.M., Visser, J., Calverley-Range, E.A., Koster, E.H., 1987.Inclined heterolithic stratification — terminology, description, interpretation and significance. Sedimentary Geology. v. 53, p. 123–179.

Van Wagoner, J.C., Mitchum, R. M., Campion, K.M., and Rahmanian, V.D. 1990. Siliciclastic sequence stratigraphy in well logs, cores, and outcrops: concepts for high-resolution correlation of time and facies. AAPG Methods in Exploration Series v. 7, p. 1-55.

Visser, M.J. (980. Neap-spring cycles reflected in Holocene subtidal large-scale bedform deposits: a preliminary note. Geology, v. 8(11), p. 543-546

Weimer, R.J., Howard, J.D., and Lindsay, D. R. 1982. Tidal flats and associated tidal channels. In: Sandstone Depositional Environments. P.A. Scholle and D. Spearing (eds.). American Association of Petroleum Geologists, Memoir, 31, p. 191-245.

Whitlatch, R.B., and Zajac, R.N., 1985. Biotic interactions among estuarine infaunal opportunistic species: Marine Ecology Progress Series 21, p. 299-311.

Wood, J.M., Thomas, R.G., and Visser, J. 1988. Fluvial processes and vertebrate taphonomy: the upper cretaceous Judith River formation, south-central dinosaur Provincial Park, Alberta, Canada. Palaeogeography, Palaeoclimatology, Palaeoecology, v. 66(1-2), p. 127-143.

Yale, D.P., Mayer, T., Wang, J. 2010. Geomechanics of oil sands under injection. 44th US Rock Mechanics Symposium and 5th US-Canada Rock Mechanics Symposium. American Rock Mechanics Association Symposium, 23-30 June, Salt Lake City, Utah.

Yang, B.C., Dalrymple, R.W. and Chun, S.S., 2005. Sedimentation on a wave-dominated, open-coast tidal flat, south-western Korea: summer tidal flat–winter shoreface. Sedimentology, v. 52(2), pp.235-252.

Zaitlin, B.A., Dalrymple R.W., Boyd, R. 1994. The stratigraphic organization of incised-valley systems associated with relative sea-level change. In: Incised-valley

Systems: Origin and Sedimentary Sequences R.W. Dalrymple, R. Boyd, B.A. Zaitlin. SEPM Special Publication No. 51. p. 45-60.

Appendix A. AppleCore Legend